Spring 2017

Deposition Patterns and Rates of Mining-Contaminated Sediment within a Sedimentation Basin System, S.E. Missouri

Joshua Carl Voss
Missouri State University - Springfield, Voss123@live.missouristate.edu

DEPOSITION PATTERNS AND RATES OF MINING-CONTAMINATED SEDIMENT WITHIN A SEDIMENTATION BASIN SYSTEM, BIG RIVER, S.E. MISSOURI

A Masters Thesis

Presented to

The Graduate College of

Missouri State University

In Partial Fulfillment

Of the Requirements for the Degree

Master of Science, Geospatial Sciences in Geography, Geology, and Planning

By

Josh C. Voss

May 2017

DEPOSITION PATTERNS AND RATES OF MINING-CONTAMINATED SEDIMENT WITHIN A SEDIMENTATION BASIN SYSTEM, BIG RIVER, S.E. MISSOURI

Geography, Geology, and Planning

Missouri State University, May 2017

Master of Science

Josh C. Voss

ABSTRACT

Flooding events exert a dominant control over the deposition and formation of floodplains. The rate at which floodplains form depends on flood magnitude, frequency, and duration, and associated sediment transport capacity and supply. While it is known that sediment in the Big River is contaminated from historical mining, little is known about the patterns and rates of deposition on floodplains, especially those that have been modified for remediation purposes. The goal of this study was to evaluate the influence of flood characteristics and topography on contemporary deposition patterns and rates in a sedimentation basin system located within a floodplain along the Big River. The basin system was constructed in April 2015 with the purpose of trapping contaminated sediment and reducing downstream lead (Pb) loads. The duration the basin was inundated and cumulative flood peak had the strongest influence on the amount of sediment deposited. A majority of the sediment was deposited close to channel margins near the inlet and chute where flow velocities are reduced in the upper basin. Deposition rates in the upper basin averaged 10.3 cm/yr, which is 10 times greater than average pre-construction floodplain deposition rates. Sediment deposited in the basin system is highly contaminated with average concentrations of 1,142 ppm Pb and 1,223 ppm Zn, with both coarse (2-16 mm) and fine (<2 mm) sediment containing high (>1,000 ppm) concentrations of Pb and Zn.

KEYWORDS: floods, deposition rates, sedimentation basin, historical mining, Big River

This abstract is approved as to form and content

_____

Dr. Robert Pavlowsky
Chairperson, Advisory Committee
Missouri State University

DEPOSITION PATTERNS AND RATES OF MINING-CONTAMINATED SEDIMENT WITHIN A SEDIMENTATION BASIN SYSTEM, BIG RIVER, S.E. MISSOURI

By

Josh C. Voss

A Masters Thesis
Submitted to the Graduate College
Of Missouri State University
In Partial Fulfillment of the Requirements
For the Degree of Master of Science, Geospatial Sciences in Geography, Geology, and Planning

May 2017

Approved:

_____
Robert Pavlowsky, PhD

_____
Toby Dogwiler, PhD

_____
Matthew Pierson, PhD

_____
Julie Masterson, PhD: Dean, Graduate College

ACKNOWLEDGEMENTS

There were a number of people involved in this research project, and I would like to thank all of them for their help. First, I would like to thank my committee members Drs. Robert Pavlowsky, Matthew Pierson, and Toby Dogwiler for support and guidance on this project. I would like to especially thank my thesis advisor, Dr. Robert Pavlowsky, for his endless mentoring and guidance over the past two years. I would also like to thank Marc Owen for his extensive help, support, inputs, and patience throughout this project.

A special thanks to all of the Ozarks Environmental and Water Resources Institute (OEWRI) graduate assistants for helping me complete field work and providing encouragement and support along the way. In addition, this project would not have been possible without funding from United States Environmental Protection Agency (U.S. EPA) Region 7 grant number 97751001 entitled "Big River Riffle-Basin Structure Monitoring Project" awarded to Robert Pavlowsky and Matthew Pierson. I would also like to thank Missouri State University Graduate College and OEWRI for partial funding of research and travel to conferences.

Finally, a huge thank you to all of my family and friends that have supported me through this process. I could not have completed this project without the support and encouragement of the people closest to me. Without all of these helping hands, this research would never have been possible.

TABLE OF CONTENTS

Chapter 1 - Introduction....1
- Floodplain Landforms and Features....2
- Flood Factors....7
- Floodplain Formation Processes....8
- Floodplain Deposition Rates....13
- Sediment-Metal Contamination....16
- Contaminated Floodplains from Historical Mining....17
- Big River Mining Contamination....19
- Purpose and Objectives....23
- Hypotheses....24
- Benefits....25

Chapter 2 – Study Area....26
- Regional Location....26
- Study Site Characteristics....28
- Geology and Soils....30
- Climate and Hydrology....33
- Mining History....34

Chapter 3 - Methods....36
- Field Sampling....36
- Laboratory Preparation and Analysis....43
- Geospatial and Statistical Analysis....45

Chapter 4 – Results and Discussion....52
- Sedimentation Basin Form....52
- Flood Analysis....57
- Repeat Topographic Surveys using RTK....62
- Sediment Trap Monitoring using Concrete Blocks....68
- Sediment Size and Contamination....73
- Flood Influence on Sediment Deposition....92
- Longitudinal Basin Trends....99
- Study Period Deposition Rates....110
- Basin Mitigation Effectiveness....115

Chapter 5 – Summary and Conclusions....117
- Key Findings....118
- Future Work....120

References....122

Appendices....131

Appendix A. Photo Log 131
Appendix B. Sediment Sample Grain Size Distribution 140
Appendix C. Sediment Sample Geochemistry 145

LIST OF TABLES

Table 1. General floodplain characteristics....3

Table 2. Examples of short-term (top) and long-term (bottom) floodplain deposition rates....14

Table 3. Description of tailings piles, after Newfields (2007) in Pavlowsky et al. (2010)....20

Table 4. Soil series present at BRLRS site (USDA, 1981)....31

Table 5. Monument locations....38

Table 6. Summary of field visits and work completed....40

Table 7. Flooding events at the BRLRS site from May 1, 2015 to December 1, 2016....61

Table 8. Sampling block deposition....71

Table 9. Grain-size data from sampling block sediment samples....75

Table 10. Sampling block Pb concentrations....85

Table 11. Sampling block Zn concentrations....87

Table 12. Storage of Pb in sediment 2-16 mm and <2 mm....89

Table 13. Storage of Zn in sediment 2-16 mm and <2 mm....90

Table 14. Estimated sediment storage during the study period using flood characteristics....98

Table 15. Sediment data of samples collected throughout basin system....101

Table 16. Summary of sediment storage in basin system....108

Table 17. Deposition rates for areas of the upper basin....110

Table 18. Long-term deposition rates at the BRLRS site....113

LIST OF FIGURES

Figure 1. Floodplain landforms 4

Figure 2. Diagram of a large, sinuous river floodplain, showing the different types of floodplain landforms and deposits (Dunne and Alto, 2013) 6

Figure 3. Floodplain formation 9

Figure 4. Big River tailings piles. Tailings piles have been showed to contaminate the Big River and Flat River with heavy metals 19

Figure 5. Big River watershed and tailings piles 27

Figure 6. BRLRS site construction plans (Designed by Joseph Asher Leff, 2014) 29

Figure 7. Soil series at BRLRS site 32

Figure 8. Locations of sampling blocks in upper basin 37

Figure 9. Sampling block 7 and post (12/14/15) 37

Figure 10. Monument 2 (top) and monument 3 (bottom) (1/22/16) 39

Figure 11. Splay deposits on sampling block with sand and fine gravel deposited over a layer of fine sand mixed with leaf litter (1/22/16) 41

Figure 12. Location of basinwide samples 42

Figure 13. Steps used to analyze repeat topographic surveys 46

Figure 14. Rating curve for basin elevation related to gage stage 51

Figure 15. BRLRS site pre-construction (November 2013) (top) and post-construction (October 2015) (bottom) (Google Earth Pro, 2016) 53

Figure 16. Sedimentation basin system features 54

Figure 17. Longitudinal survey points (top) and longitudinal profiles (bottom) of the Big River and basin system 56

Figure 18. Flood RI of Irondale, Richwoods, and Byrnesville USGS gaging stations 58

Figure 19. Flood RI for Desloge gage (Flood record May 13, 2015 – Present) 59

Figure 20. Stage height (top) and discharge (bottom) at the Desloge gage from May 13, 2015 to December 1, 2016 60

Figure 21. Changes in erosion and deposition from September 2015 to November 2016 63

Figure 22. Coarse chute and splay deposits near inlet and chute (9/17/15)..... 64

Figure 23. Fine-grained overbank deposits west of splay deposits (12/14/15)..... 64

Figure 24. Bank erosion along bank of upper basin (12/14/15)..... 65

Figure 25. Changes in erosion and deposition from December 2015 to January 2016..... 66

Figure 26. Location of sampling blocks (top) and average depth of sediment on sampling blocks in upper basin (bottom). 70

Figure 27. Frequency distribution of sampling block sediment depths..... 72

Figure 28. Location of sampling blocks (top) and average percent >2 mm on sampling blocks in upper basin (bottom). 74

Figure 29. Relationship between distance from the inlet and percent sediment <2 mm ... 77

Figure 30. Distribution of Pb concentrations 79

Figure 31. Distribution of Zn concentrations..... 79

Figure 32. Average concentrations of Pb (top) and Zn (bottom) in block samples collected each sampling period with ± one standard deviation. 81

Figure 33. Average concentrations of Ca (top) and Pb/Zn ratios (bottom) of block samples collected each sampling period with ± one standard deviation 82

Figure 34. Location of sampling blocks (top) and average Pb concentration of sampling block deposits in the upper basin (bottom). 84

Figure 35. Location of sampling blocks (top) and average Zn concentration of sampling block deposits in the upper basin (bottom). 86

Figure 36. Relationship between concentrations of Pb (top) and Zn (bottom) in sediment 2-16 mm and <2 mm. 91

Figure 37. Relationship between peak gage height and average sediment depth 93

Figure 38. Relationship between cumulative peak gage height and average sediment depth 93

Figure 39. Relationship between number of flood events and average sediment depth ... 94

Figure 40. Relationship between days basin was inundated and average sediment depth 95

Figure 41. Relationship between cumulative peak gage stage at Desloge and days the basin was inundated. 96

Figure 42. Depth of sediment throughout the entire basin system since construction 100

Figure 43. Relationship between inlet distance and depth (top), texture (middle), and Pb concentrations (bottom) 102

Figure 44. Concentrations of Pb in samples collected throughout the basin system 104

Figure 45. Concentrations of Zn in samples collected throughout the basin system 105

Figure 46. Basin system sediment storage areas 107

Figure 47. Erosion and deposition in high and low deposition areas 111

Figure 48. Location of cores collected in 2014 114

CHAPTER 1 – INTRODUCTION

Floodplains are generally defined as low-relief sedimentary surfaces adjacent to the active channel that are constructed by the effects of floods of varying magnitudes and their associated geomorphological processes (Nardi et al., 2006; Wohl, 2014). Geomorphologists have traditionally referred to floodplains as geomorphic surfaces that are flooded at least once every two years, with the assumption that these landforms are composed largely of fluvial sediments deposited under the current flow regime (Dunne and Alto, 2013; Wohl, 2014). The morphology of a floodplain reflects the history of both erosion and deposition processes, although most floodplains are depositional features that store large quantities of sediment over various lengths of time (Wohl, 2014).

Floodplains serve many ecological and hydrological functions including floodwater storage, sediment storage, biological cycling, and transitional aquatic and terrestrial habitats (Nardi et al., 2006; Schenk and Hupp, 2010). Floodplains also play an important role as a storage site for contaminated sediment for periods of 10-100 years or more (Lecce and Pavlowsky, 1997). The storage of these sediments represents a conveyance loss that will reduce the contaminant flux through the river system (Walling et al., 2003). As a result, floodplains can contribute to the improvement of water and sediment quality in downstream segments (Olde Venterink et al., 2006). The effectiveness of floodplain functions is often affected by upstream changes in sediment supply due to increased discharge from mining or land use changes, sediment capture by dams, or from rivers being disconnected hydrologically by constructed levees and

drainage systems that protect infrastructure from flooding (Bridge, 2003; Schenk and Hupp, 2010).

The purpose of this study is to evaluate the effects of floodplain topography and flood event characteristics on contemporary deposition patterns and rates in a sedimentation basin system designed to trap mining-contaminated sediment for waste disposal and reduce exposure downstream. The basin system was designed by the U.S. Army Corps of Engineers and constructed within a floodplain on the inside of a large valley bend of the Big River below Desloge, Missouri. This basin system represents the first remediation structure of this design to be used to mitigate contaminated sediment in the region, and to the best of our knowledge, the USA as a whole.

Floodplain Landforms and Features

Floodplains consist of various landforms that form diverse and complex systems which respond to watershed changes heterogeneously and in space and time (Table 1; Figure 1). These landforms vary with elevation and will have different flood frequencies (Bridge, 2003). Floodplain landforms at lower elevations will have a higher flood frequency than those at higher elevations (Lecce and Pavlowsky, 2001). As flood frequency increases, there is an increase in available sediment, thus lower elevation floodplain landforms will be able to accumulate more sediment (Howard 1996; Ciszewski and Malik, 2004; Owen et al., 2011). Further, floodplain landforms closer to sediment sources such as chutes will receive more sediment over time compared to areas farther away (Howard, 1996; Ciszwski and Malik, 2004; Wohl, 2014).

Table 1. General floodplain characteristics.

Landform	Relative Elevation	Flood Frequency	Depositional Capability	Erosional Capability	Sediment Size
Bench	Low/Moderate	Moderate	Moderate/High	Moderate	Clay to Sand
Chute	Low/Moderate	Moderate	Low	High	Silt to Gravel
Splay	Low/Moderate	Moderate	Moderate/High	Low	Silt to Gravel
Backswamp	Low/Moderate	Moderate	Moderate/High	Low	Clay to Silt
Levee	Moderate	Moderate	Moderate/High	Low	Clay to Sand
Floodplain	Moderate	Low/Moderate	Moderate	Low	Clay to Sand
Terrace	High	Low	Low	Low	Clay to Silt

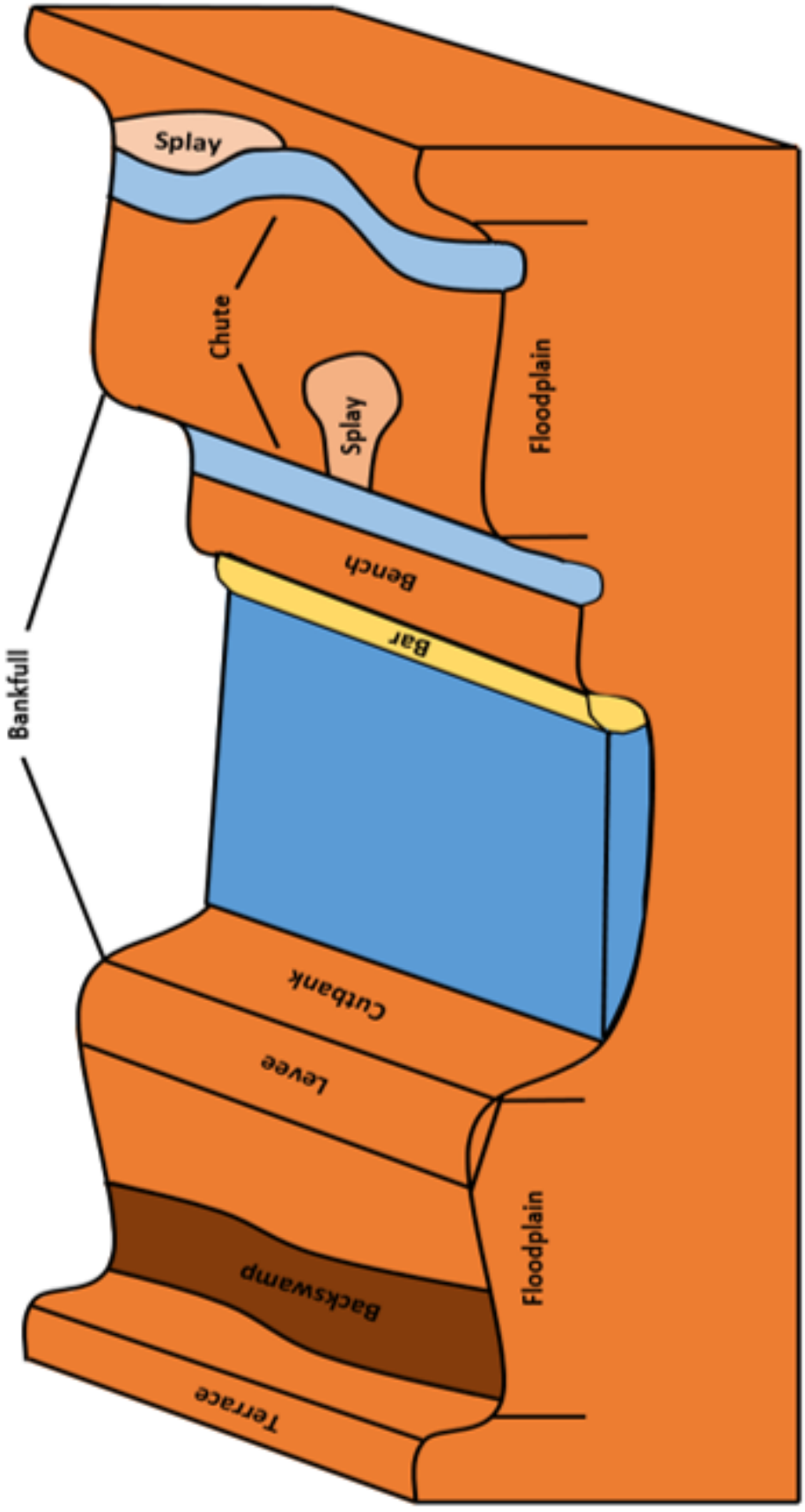

Figure 1. Floodplain landforms.

There are several features typically associated with a floodplain (Table 1; Figure 1). A bench is defined as an alluvial feature similar to a floodplain, but has a lower elevation (Owen et al., 2011; Huggins, 2016). The bench will be flooded more frequently than a floodplain and as a result will have a greater amount of contaminated sediment deposited during flooding events (Howard, 1996; Lecce and Pavlowsky, 2001). However, sediment deposition is not solely based on elevation. It is also important to consider hydraulic variables. If a floodplain landform such as a backswamp has poor drainage during flooding events, water can pool in depressions, allowing suspended sediment to be deposited at relatively higher rates than surrounding floodplain areas (Table 1; Figure 1**)**. These backswamps can act as an important areas for fine-grained floodplain deposition (Howard, 1996; Hupp et al. 2015; Huggins, 2016).

On the other hand, if the floodplain is well-drained, secondary channels or chutes can begin to form on the floodplain and concentrated floodwater flows that promote scouring or deposition of coarser sediment (Table 1; Figure 1). Thus, chutes will typically have higher flow velocities than backswamps during floods and will typically deposit less fine grained sediment and scour existing deposits. Chutes can develop on floodplains where water leaves the channel with sufficient depth and velocity to retain enough momentum to scour floodplain sediment (Figure 2) (Harrison et al., 2015). McGowen and Garner (1970) interpreted that chutes develop on the inside of bends of streams during extreme floods when the thalweg shifts from the outside bank toward the inside bank and extends over the upstream part of the inside bank, scouring the channel through which bedload is transported during extreme floods. The development of chutes is

sensitive to floodplain topography and the density of floodplain vegetation, which affects the rate at which floodwaters reduce velocity (Harrison et al., 2015).

Splay deposits are often associated with chutes. Splay deposits are generally fan-shaped sand deposits, although Kruit (1955) also observed elongated, linear splays, whose sedimentary features are determined by the flow and magnitude of a flood (Figure 1 and 2) (Elliott, 1974; Charlton, 2008). These deposits can be found at the end of chutes or also at levee breaches where sediment-laden water escapes the channel and flows across the floodplain (Charlton, 2008). The initial higher flow velocity is sometimes able to transport coarser sediment into backswamp areas with sediment size decreasing with increasing distance from the channel as flow velocities drop (Wohl, 2014). As a result, chutes and levee breaches can aid in sediment transport across the floodplain, increasing sedimentation at a greater distance from the channel (Howard, 1996). Together, hydraulic and topological differences can create significant spatial variation in sedimentation patterns and associated contaminant concentrations across a floodplain (Lecce and Pavlowsky, 2004).

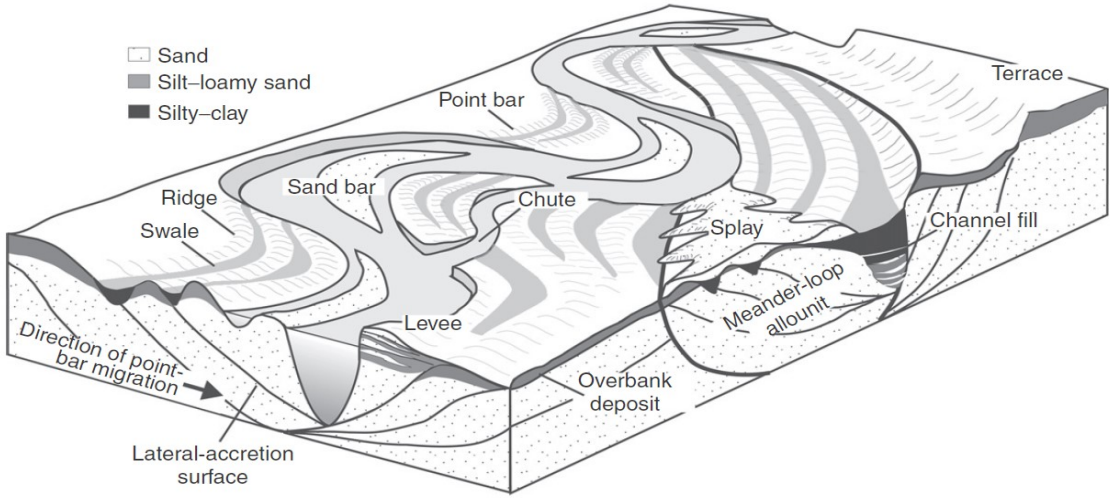

Figure 2. Diagram of a large, sinuous river floodplain, showing the different types of floodplain landforms and deposits (Dunne and Alto, 2013).

Flood Factors

Flood events exert a dominant control over the formation of floodplains (Benedetti, 2003). This action of flowing water, mediates geomorphic processes that transfer sediment and develop floodplains (Curtis et al., 2013; Hupp et al., 2015). In general, flood events occur when relatively high flows exceed the bankfull capacity of a channel (Charlton, 2008). Wolman and Leopold (1957) defined bankfull discharge as the stage just before flow begins to overtop the banks of the channel. Numerous studies have indicated that bankfull discharge recurs approximately every one to two years in natural streams (Wolman and Leopold, 1957; Leopold et al., 1964; Castro and Jackson, 2001). This discharge transports the majority of suspended sediment in many rivers (Simon et al., 2004). As a result bankfull discharge has been interpreted as the most important flow magnitude for controlling channel processes and form (Wolman and Miller, 1960; Dunne and Leopold, 1978).

Flood events of different sizes are defined in terms of high water levels or discharges that exceed certain arbitrary limits (Charlton, 2008). The height of the water level in a river is referred to as its stage. For a given river, there is a relationship between the size of a flood and the frequency in which it occurs. The larger the flood, the less often it can be expected to occur. Therefore, floods are defined in terms of their magnitude (size) and frequency (how often a flood of a certain size can be expected to occur) (Charlton, 2008). In the past it was generally believed that rare extreme events are the most important in the development of landforms, such as floodplains (Asselman and Middelkoop, 1998). However, Wolman and Miller (1960) stated that a more accurate sense of overall effectiveness of geomorphic processes should not only include rare

extreme events, but also events of moderate intensity that occur more frequently. Though, overall it has been difficult to reach a consensus on the role of flood intensity on floodplain evolution and landscape modification (Lecce et al., 2004).

Floodplain Formation Processes

Floodplains are typically formed by the deposition of fine overbank deposits over coarser channel deposits (Figure 3) (Day et al., 2008). Hupp et al. (2015) stated that fine overbank deposition is the primary process by which most floodplains develop. However, the situation is more complicated and varies greatly among different river system environments (Wohl, 2014). Floodplains in low-energy rivers or watersheds affected by accelerated soil erosion are primarily developed from the deposition of fine overbank deposits (Lecce and Pavlowsky, 2004; Piegay et al., 2008; Dunne and Alto, 2013). In these systems, the storage of overbank sediment represents a significant component of fluvial sediment budgets (Lecce and Pavlowsky, 2004). Whereas coarser channel deposition is more typical in piedmont and intramontane actively shifting rivers (Piegay et al, 2008; Dunne and Alto, 2013).

The rate and pattern at which floodplains form depend on a number of variables including magnitude, frequency and duration of inundation, sediment load, and floodplain topography and roughness (Benedetti, 2003; Baborowski et al., 2007; Curtis et al., 2013). Generally, an increase in any of those variables could increase sedimentation rates on floodplains to store sediment for long periods of time compared to in-channel sand and gravel deposits (Asselman and Middelkoop, 1998; Lecce and Pavlowsky, 2001; Curtis et al., 2013). However, storage time is also related to the rate of lateral channel

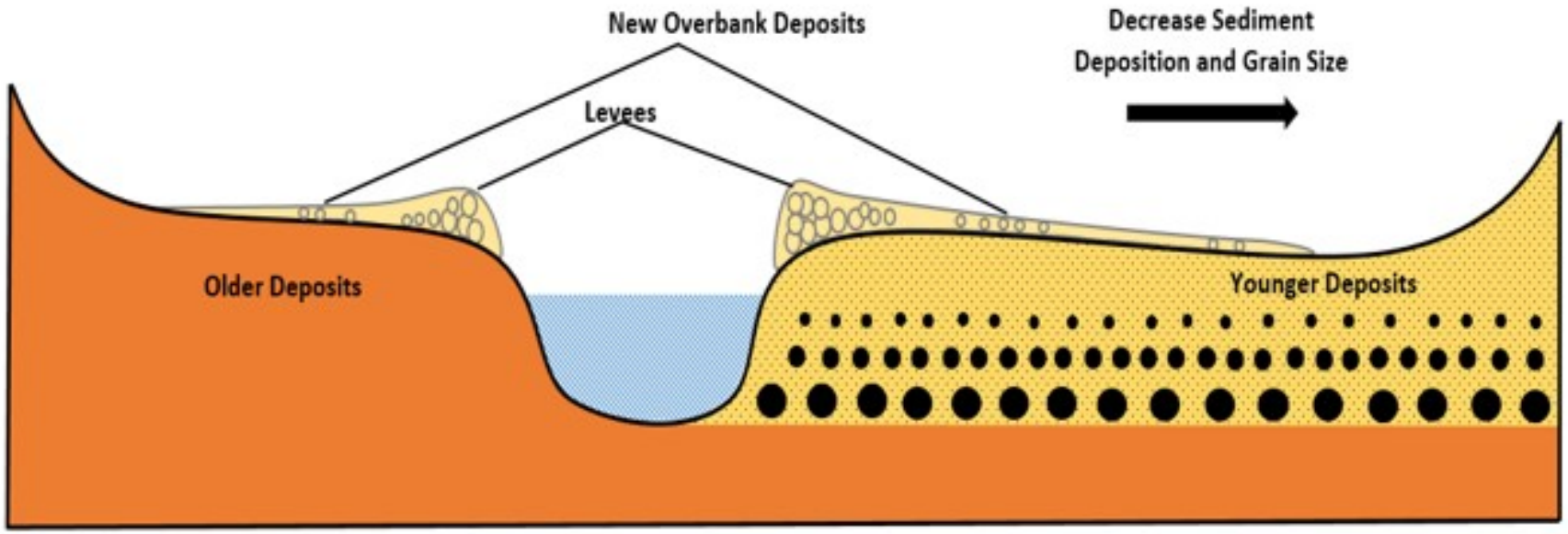

Figure 3. Floodplain formation.

migration and bank erosion which act to release sediment from floodplain storage back to the stream (Macklin et al., 2006; Martin, 2015).

Coarser channel deposits, or lateral accretion deposits, are created by progressive erosion of the cut bank along the outside of the meander bend and deposition of the opposite point bar that causes the channel to migrate across the valley (Figure 2 and 3) (Wolman and Leopold, 1957; Nanson and Croke, 1992). The relatively high shear stress along the outer margins of the meander bend can erode the bank through fluid shear or they can erode the pool or the foot of the bank, leaving the bank too steep to be stable (Dunne and Alto, 2013). Deposition of point bars is related to the helicoidal flow associated with the bend of the channel and are made up of coarse-grained sands and gravels, often showing a fining upward sequence (Wolman and Leopold, 1957; Nanson and Croke, 1992). The helicoidal flow is described as the rotational component of flowing water in a meander that develops as the result of greater hydraulic resistance along the channel margins than in the center of the channel. This flow creates alterations in the location of the greatest flow velocity that results in differences in boundary erosion, sediment transport, and sediment deposition (Wohl, 2014).

Typically, deposition of point bars and erosion of the cut bank tend to be greatest just downstream of the meander apex (Wolman and Leopold, 1957; Dunne and Alto, 2013). If point bars are sufficiently developed, they may intensify the flow along the outer margins of the bend and accelerate bank erosion and bend growth. Point bars may be incorporated into the floodplain as the channel migrates away from the inside bank, lowering the shear stress and sediment transport across the point bar which allows the

growth of vegetation and accumulation of finer suspended sediment to form new floodplains (Dunne and Alto, 2013).

Finer overbank deposits, or vertical accretion deposits, are created when the channel flow exceeds the bankfull capacity and the water and sediment spills out across the floodplain, thus increasing bank height (Figure 3) (Zwolinski, 1992; Miller 1997). When channel flow exceeds bankfull capacity, the difference between flow velocities in the channel and over the floodplain produces eddies, which transfer sediment and energy from the deeper and faster flow in the channel to the shallower and slower flow over the floodplain. Sediment can also be transferred to the floodplain by convection which occurs where there is a component of flow perpendicular to the channel. Convective sediment transport across the floodplain tends to be most effective on sinuous rivers, as they induce flows responsible for sediment deposition on the inside banks of channel bends (Ciszewski and Grygar, 2016). Generally, vertical accretion deposits are finer than lateral accretion deposits and tend to distribute sediment into floodplain depressions and reduce the effect of both positive and negative topographic features (Lecce and Pavlowsky, 2001; Dunne and Alto, 2013). These deposits are typically most abundant in the middle and lower reaches of rivers because of decreasing river slope, slow lateral channel migration, high frequency and magnitude of floods, and human activity (Zwolinski, 1992).

Floodplain vertical accretion deposits occur in six general phases during flooding events as described by Zwolinski (1992). The six phases that occur are: (1) rising of water stage and bank modification; (2) floodplain inundation and initial deposition; (3) flood peak and widespread transport and deposition; (4) falling of water stages and high

intensity deposition; (5) cessation of overbank flow and final deposition; and (6) post-flood transformation of overbank forms and deposits. These phases occur during a flood with a single peak for lowland meandering rivers in temperate climates (Zwolinski, 1992).

The first phase involves the increase in the volume of water in the channel and associated erosion to accommodate the extra water. The erosional process prepares the channel for the increase flow of flood waters and transport alluvial material from the channel onto the floodplain. In the second phase, the channel exceeds bankfull and water spills across the floodplain. During this phase erosion occurs in breaches, crevasses, and chutes, while re-deposition of previously stored sediment occurs within chutes and terrace channels. Phase three is divided into two sub-phases. The first sub-phase involves the adjustments of the overbank flow pattern to the floodplain morphology. During this time transport processes are dominant. The second sub-phase occurs as the flood peaks and transport over the whole floodplain remains dominant, especially along terrace channels and chutes. These conditions favor the transport of the largest quantities of sediment to the farthest parts of the floodplains. Sediment deposition tends to decrease in quantity and in grain-size with increasing distance from the channel since flow velocities decrease with distance from the channel, depositing coarser sediment near the channel and finer sediment in vertical layers further away from the channel (Zwolinski, 1992).

Phase four involves the dissipation in energy, fall in floodwaters, and changes in overbank flow pattern. Also, the quantity of sediment delivered from the channel is decreased and erosion is minimal. The reduction in sediment transport rate is accompanied by the highest intensity of deposition of all floodplain features, particularly

within crevasse splays, terrace channels, chutes, oxbow-lakes, and swamps. Sediment deposition ceases with time during the fifth phase, however deposition is still rather intensive at the start of the phase. If floodwater returning to the channel has sufficient energy to erode, previously deposited sediment may be modified or eroded. During the six and final phase, only stagnant water in floodplain depressions remains and recent deposits are disturbed by wind, animals, and vegetation growth. Overall, the formation of floodplains by vertical accretion deposits operates as a process of cyclic erosion and sedimentation with human disturbance becoming an important factor (Zwolinski, 1992).

Floodplain Deposition Rates

Typically, overbank deposition rates are no more than a few centimeters per year and tend to decrease across the floodplain with distance from the channel as function of roughness and decreasing suspended sediment concentration (Piegay et al., 2008; Wohl, 2014). However, due to fluctuations in fluvial processes and flood characteristics that control the amount of sediment transported and deposited, patterns of floodplain sedimentation, and consequently associated contaminants, are highly variable (Dennis et al, 2009; Sear et al., 2010). Also, complex topography and variable geometry of floodplains may contribute to irregular rates and patterns of sediment deposition that result from the combination of diffusion, convection, and variations in the time and depth of inundation (Lecce and Pavlowsky, 2004).

A wide range of deposition rates have been documented for numerous floodplains in the United States (Kleiss, 1996**;** Curtis et al., 2013; Hupp et al., 2015) and in Europe (Walling and He, 1997**;** Hensel et al., 1999; Jeffries et al., 2003) (Table 2). Piegay et al.

Table 2. Examples of short-term (top) and long-term (bottom) floodplain deposition rates.

Short-term

Location	River	Method	Record	Rate(s)	Reference
Eastern, TN	Hatchie River	Clay pads	2002-2005	0.39 cm/yr	Pierce and King (2008)
Northern, MO	Missouri River	Clay pads	1995-1998	1.00 cm/yr	Hiemann and Roell (2000)
Northern, NC	Roanoke River	Clay pads	2003-2005	0.03-0.59 cm/yr	Hupp et al. (2015)
Devon, UK	Lower River Culm	Artificial mats	1982-1984	0.05 cm/yr	Lambert and Walling (1987)
Central, CA	Lower Consumnes River	Repetitive surveys	1999-2000	10.0 cm/yr	Florsheim and Mount (2002)

Long-term

Location	River	Method	Record	Rate(s)	Reference
Southwest, MO	James River	Cs 137 dating and Historical mining tracers	1850-2009	0.46 cm/yr	Owen et al. (2011)
Wisconsin and Minnesota	Upper Mississippi River	Repetitive Surveys and Cs 137 dating	1964-2003	1.08 cm/yr	Benedetti (2003)
North Carolina	Gold Hill mining district	Historical mining tracers	1842-2007	0.9 cm/yr	Lecce and Pavlowsky (2014)
Upper Mississippi Valley	Blue River	Historical mining tracers	1920-1997	0.19-1.29 cm/yr	Lecce and Pavlowsky (2001)

(2008) estimated a range of floodplain deposition rates along the Ain River that varied between 0.65 and 2.4 cm/yr over a period of 10 to 40 years. Owen et al. (2011) estimated floodplain deposition rates along the James River from 1850 to 2009 to average 0.46 cm/yr. Both of these rates are generally greater than most lowland floodplains of Coastal Plain rivers in the United States where rates tend to range between 0.15 to 0.54 cm/yr (Hupp, 2000) and also along the lower Rhine River where rates range from 0.2 to 15 mm/yr (Middlekoop, 2002). The high rate of deposition documented by Florsheim and Mount (2002) for the floodplain of the Lower Consumnes River can be explained by intentional levee breaches created in an attempt to restore floodplain topography by increasing connectivity between the channel and floodplain.

Other studies have described similar attempts to increase connectivity between channels and floodplains in attempt to improve flood control and floodplain biodiversity (Acreman et al., 2003; Baptist et al., 2004). Acreman et al. (2003) did so by removing embankments that separated the channel from its floodplain and reduced the width and bankfull depth of an incised channel to its pre-engineered dimensions. While Baptist et al. (2004) lowered floodplains and created secondary channels. In both cases, modifications made to floodplains increased connectivity by creating preferential pathways for flood waters and associated sediment to be transported. Thus, increasing floodplain deposition rates by delivering sediment from the channel to interior floodplain areas.

Deposition rates on floodplains can be measured using a variety of methods that cover a range of times scales. Historical deposition rates estimate long-term sediment deposition that occurs over 10 to 100s of years. While contemporary deposition rates aim

to estimate the sediment deposited during a single flooding event or over the course of a few years (Asselman and Middelkoop, 1998). Deposition rates are mainly estimated using sediment traps (Lambert and Walling, 1987; Baborowski et al., 2007; Curtis et al., 2013; Hung et al., 2013), repetitive topographical surveys (Hooke, 1995; Gomez et al., 1995), artificial markers (Kleiss, 1996; Hupp, 2000), dendrochronology (Hupp, 2000; Piégay et al., 2008), radionuclide dating (He and Walling, 1996), analyses of conveyance losses (Walling and Bradley, 1989), and tracer studies (Lecce and Pavlowsky, 2001; Ciszewksi et al., 2012; Lecce and Pavlowsky, 2014).

Among these methods, only sediment traps, repetitive topographical surveys, and analyses of conveyance losses estimate sediment deposited during a single flood event (Asselman and Middlekoop, 1998). Sediment traps may be the most efficient and convenient due to their simple design, low cost, easy field application, and inexpensive laboratory analysis (Hung et al., 2013). In general, sediment traps are installed prior to flood events and are retrieved for analysis after the event. Recently, more attention has been paid to contemporary sedimentation rates due to the increasing awareness of suspended sediment in the transport of contaminants and the potential significance of floodplains to act as a sink for contaminants (Walling and Bradley, 1989).

Sediment-Metal Contamination

In order to better understand the effects of historical mining on a fluvial system, it is important to know the characteristics associated with contaminated sediment. Mining-contaminated sediment is produced as a result of heavy metal mining which aims to extract the ore in rocks, such as lead and zinc, for economical purposes. This is

accomplished by crushing and grinding rock which separates the ore. Ore processing is completed using dry processes such as gravitational separation or wet processes such as wet washing or flotation separation (Smith and Schumacher, 1993). Both of these processes produce large volumes of metalliferous waste across a range of particle sizes including waste rock, tailings, and ultrafine (rock flour) particles (Macklin et al., 2006; Hill, 2016). Generally, the finest particle fractions tend to contain the highest residual metal concentrations, however, all particles sizes tend to contain residual heavy metal concentrations (Smith and Schumacher, 1993; Pavlowsky et al., 2010).

During most historical mining operations there were few regulations that governed the disposal of mining waste. As a result, waste was carelessly released to the surrounding landscapes. It was not until after World War II that mining wastes were confined to on-site tailing piles or impoundments (Smith and Schumacher, 1993). These mining wastes often severely contaminated river systems over long distances >100 km due to erosion, runoff, and retention pond and dam failure. (Meneau, 1997; Macklin et al., 2006). Macklin et al. (2006) provides a summary of recent studies on the dispersion of heavy metal contaminated sediment in rivers affected by mining activities. One example is a case study on a tailings dam failure in Aznalcolar, Spain that dumped high concentrations of lead (Pb), zinc (Zn), copper (Cu), and arsenic (As) into the river and contaminated several hundred kilometers of the river.

Contaminated Floodplains from Historical Mining

It is generally recognized that floodplains in historically mined river systems can function as a semi-permanent sink for metal-contaminated sediment where it can remain

stored for hundreds or even thousands of years (Lambert and Walling, 1987; Lecce and Pavlowsky, 1997; Dennis et al., 2009). Numerous studies have shown that floodplains in mined river systems can act as long-term sinks for large quantities of heavy metal contaminated sediment (e.g., Marron, 1992; Lecce and Pavlowsky, 1997; Macklin et al., 2006; Lecce and Pavlowsky, 2014). Marron (1992) suggested that approximately 30-45% of contaminated sediment entering the Belle Fourche river system is stored in floodplains. Dennis et al (2009) estimated 35% of the total metal production in the Swale catchment is stored in the floodplains. Indicating the Swale floodplain is likely to represent the single largest storage of metal-contaminated sediment. While Forstner and Salomons (2010) suggested that large reservoirs such as floodplains trap between 25-30% of the sediment. All these studies show a significant storage of contaminated sediment in floodplains.

However, floodplains are not necessarily a permanent storage for metal-contaminated sediment. Instead, contaminated sediment can be re-worked and redistributed back into the fluvial system by bank erosion and channel migration (Walling et al., 2003; Dennis et al., 2009). Phillips et al. (2007) found that 30 to 40% of alluvium remobilized from the floodplain within a century of deposition in the Waipaoa River in New Zealand. Once remobilized, sediment is transported downstream to potentially become stored in new floodplain deposits (Nanson and Croke, 1992). As a result, metal-contaminated sediment can continue to cause present and future environmental problems long after mining operations have ceased (Dennis et al., 2009).

Big River Mining Contamination

Historical mining in the Old Lead Belt, a sub-district of the larger Southeast Missouri Lead Mining District, created a serious contamination problem within the Big River watershed (Smith and Schumacher, 1993; Meneau, 1997). During a period of mining from 1869 through 1972, the Old Lead Belt was a national leader in Pb and Zn ore production (Smith and Schumacher, 1993; Pavlowsky et al., 2010; Martin et al., 2016). Through the milling process, large volumes of metalliferous waste were produced and stored into large piles or stored in retention ponds on or near floodplains in Leadwood, Desloge, Park Hills, Flat River, and Bonne Terre, Missouri (Figure 4; Table 3).

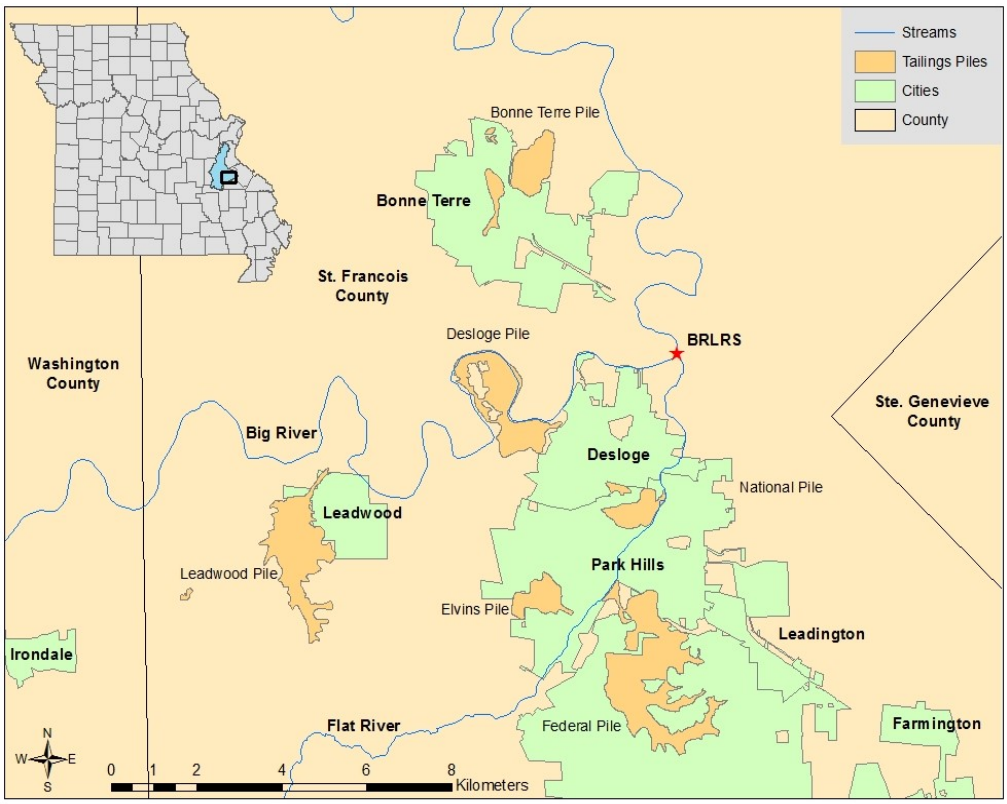

Figure 4. Big River tailing piles. Tailing piles have been showed to contaminate the Big River and Flat River with heavy metals.

Table 3. Description of tailings piles, after Newfields (2007) in Pavlowsky et al. (2010).

Tailings Pile	Area (km^2)	Volume (m^3)	Avg. Pb (ppm)	Avg. Zn (ppm)	Pb/Zn (ratio)
Leadwood	2.3	3,896,000	2,382	4,961	0.5
Desloge	1.5	4,966,000	2,105	1,243	1.7
Federal	4.7	3,979,000	885	293	3.0
Elvins	0.6	7,946,000	4,440	5,541	0.8
National	0.6	4,890,000	3,661	417	8.8
Bonne Terre	1.4	4,355,000	2,495	457	5.5

These mining waste are generally referred to as tailings, which are made of sand and fine gravel-sized particles of crushed rock and ore that contain high concentrations of residual metals. Tailings released from mills can be classified into three different types based on particle size. They are classified as chat (4-16 mm), fine tailings (0.06-0.20 mm), and slimes (>32 um) (Gale et al., 2004; Pavlowsky et al., 2010). These mining wastes contain high concentrations of heavy metals including Pb and Zn (Smith and Schumacher, 1993). Large quantities of heavy metal-rich sediment entered local streams through erosion, runoff, and retention pond and dam failure. Since then, fluvial processes have reworked contaminated sediment and distributed it downstream (Meneau, 1997). As a result, over 170 km of floodplain and channel sediment along with Big River have accumulated toxic levels of both Pb and Zn (Pavlowsky et al., 2010).

Mining sediment released from tailing piles contributing to Big River contamination at Bonne Terre, Desloge, National, Elvins, Federal and Leadwood piles (Figure 4; Table 3). In compliance with the Comprehensive Environmental Response

Compensation Liability Act ("Superfund"), the six major tailing piles have been stabilized to limit the risk of contamination. However, contaminated sediment within floodplain deposits present a significant non-point source for heavy metal contamination for the Big River watershed (Mosby et al., 2009; Pavlowsky et al., 2010). Pavlowsky et al., (2010) found that floodplain material tended to have higher Pb concentrations than in channel sediments. Also, Huggins (2016) found that surface soil deposits along the Big River are highly contaminated with >1,000 ppm Pb from historical mining activity, with low floodplain soils such as benches containing the highest Pb concentrations. Thus, floodplain soil weathering and bank erosion represent significant Pb sources to the Big River that can create future contamination problems.

Besides floodplains, there are still large quantities of contaminated sediment stored in channel and bar deposits that provide a potential source of contamination to downstream segments along Big River. Removal of Pb-contaminated sediment from the channel creates an opportunity to decrease transport of contaminated sediment downstream and mitigate long-term contamination risks along the Big River (Owen et al., 2012). There are many strategies to remediate sediment contaminated from historical mining operations, however it is often difficult to remediate this contamination (Macklin et al., 2006).

The most commonly used remediation strategies involve capping the contaminated sediment with a thick layer of clean sediment, phytoremediation, soil washing and leaching by chemical extractants, and direct removal by dredging (Mulligan et al., 2001; Wang et al., 2004; Peng et al., 2009). However, dredging and capping are some of the oldest and most available remediation strategies (Forstner and Salomons,

2010). Generally, dredging can be very effective in cleaning up heavily contaminated sediment, although it can cause adverse environmental threats by resuspension of contaminated sediment. Also, the treatment of the dredged sediment is usually very costly. As an alternative, dredged sediment is commonly capped following disposal (Wang et al., 2004).

In response to the concerns over the fate of contaminated sediment in Big River, in-channel dredging was implemented for the Big River that removed Pb contaminated sediment from an impoundment above a low water crossing in 2009-10 with some success (Owen et al., 2012). To expand on the earlier project, the Big River Lead Remediation Structure (BRLRS) Project was implemented in the spring of 2015 by the Environmental Protection Agency and the U.S. Army Corps of Engineers. The goal of the BRLRS project was to create a system of managed sedimentation areas where mining-contaminated sediment would be deposited during flooding events and later be removed by dredging for land disposal. The project site is located along the Big River below the town of Desloge in St. Francois County, Missouri where the channel bends to the north immediately below the confluence of the Flat River (Figure 4). The site includes a Newberry-type rocked riffle below the confluence of the Flat River and an off-line sedimentation basin system within a floodplain area. These structures are designed to collect channel bed-load sediment and trap finer-grained suspended sediment that will eventually be dredged and taken to repositories off-site. Photographs of the remediation structures can be found in Appendix A.

In addition to remediation projects, extensive studies have been carried out on the contamination of the Big River to assess soil, water, and ecosystem quality (Smith and

Schumacher, 1993; Meneau, 1997; Gale et al., 2002; Pavlowsky et al., 2010; Young, 2011; Huggins 2016; Hill, 2016). While these studies offer detailed information related to mining contamination across the watershed, less is known about the current sedimentation patterns and rates across Ozark floodplains and the amount of sediment moved by flooding events (Owen et al., 2012). Further, even less is known about the flood variables that influence the rates and patterns of contemporary sediment deposition across disturbed floodplains modified for remediation purposes and how they might differ from natural floodplains

Purpose and Objectives

The purpose of this study is to evaluate the effects of floodplain topography and flood event characteristics on contemporary deposition rates and patterns in a sedimentation basin system designed to trap mining-contaminated sediment for waste disposal and reduce exposure downstream. This system represents the first remediation structure of this design to be used to mitigate contaminated sediment in the region, and to the best of our knowledge, the USA as a whole. To accomplish this study, it was necessary to assess the influence of flood characteristics and floodplain topography on sediment deposition and grain size distribution throughout the sedimentation basin system. It was also be necessary to assess the trapping efficiency and storage of contaminated sediment in the basin for remediation purposes. This was accomplished through the following objectives:

1) Quantify contemporary deposition rates of the sedimentation basin. This was accomplished by setting sediment traps throughout upper basin and also by completing repetitive topographical surveys throughout basin following flooding

events using a real-time kinematic (RTK) GPS. Sediment traps and repetitive surveys also aided in assessing how floodplain topography affects sedimentation;

2) Identify important flood characteristics that control sedimentation patterns and rates within the sedimentation basin. Understanding the important variables of floods allowed for a better overall understanding of floodplain sedimentation along with how they influence deposition rates and storage within the basin. This was accomplished by linking a USGS gage record to the basin flood stage;

3) Quantify grain size distribution across the sedimentation basin. Grain size patterns can provide insight into the distribution and storage of sediment transported downstream;

4) Quantify Pb, Zn, and Ca concentrations in recently deposited sediment throughout the sedimentation basin. This allowed for the examination of contamination patterns across the basin as well as aid in quantifying the storage of contaminated sediment. It also helped evaluate trends in gravel sediment contamination. Geochemical analysis was accomplished through sampling sediment recently deposited by flooding events; and

5) Determine the effectiveness of the basin system at trapping contaminated sediment and reducing downstream Pb loads. This was accomplished by quantifying the amount and rate of contaminated sediment storage within the basin and comparing to previously published channel sediment-Pb storage estimates.

Hypotheses

In developing this study and examining the background literature within this field, there are four guiding relationships that were expected to surface:

1) Contemporary sedimentation rates for the sedimentation basin would be greater than that of a natural floodplain due to a lowered bank and increased connectivity with channel (Florsheim and Mount, 2002; Acreman et al., 2003; Baptist et al., 2004).

2) Flood characteristics of magnitude, frequency, and duration of flooding events would have a strong influence on sediment deposition due to various transport capacities and sediment supplies. Larger flood peaks and longer flood durations typically result in higher sedimentation rates (Asselman and Middelkoop, 1998; Lecce and Pavlowsky, 2001; Curtis et al., 2013; Hupp et al., 2015).

3) Sediment deposition rates would decrease with distance from the channel due to flood regime and sedimentation controls (Zwolinski, 1992; Piegay et al., 2008; Wohl, 2014).

4) Concentrations of Pb and Zn would be higher in sediment samples consisting of sediment being <2 mm due to the tendency of finer tailings to have the highest concentrations of heavy metals (Horowitz, 1991; Smith and Schumacher, 1993; Pavlowsky et al., 2010). These samples would be deposited in areas of the basin that experience lower sedimentation rates.

Benefits

This thesis will provide valuable insight into the influences of floodplain topography and various flood characteristics on the patterns and rates of sediment deposition within a sedimentation basin as compared to a natural floodplain. It is also the first known off-line sedimentation basin system created to manage long-term sediment contamination for rivers affected by mining. There remains a gap in knowledge in examining the influence of flood characteristics on contemporary floodplain sedimentation rates, even more so for disturbed floodplains modified for remediation purposes (Owen et al., 2012). The results of this thesis will improve our understanding of how sediment transport and deposition is influenced by floodplain morphology and variable flood characteristics in Ozark river systems. It will also allow for the assessment of the sedimentation basin system for remediation purposes, which will help manage mining contamination and lower the health risk of aquatic and human life by improving water and soil quality. This is a main concern for environmental managers and geomorphologists who are working to remediate contamination in floodplain areas affected by historical mining operations or who are studying the effects of flood characteristics on contemporary floodplain sedimentation rates.

CHAPTER 2 – STUDY AREA

Regional Location

The Big River is located in southeastern Missouri within the Upper Mississippi River basin (Figure 5). It is the southernmost river in the Upper Mississippi River Basin with headwaters originating in the St. Francois Mountains at 530 meters above sea level where it flows north for 222 km until it reaches the Meramec River, a tributary of the Mississippi River at 125 meters above sea level (Meneau, 1997). The Big River watershed (2,500 km^2) drains Jefferson, Washington, Franklin, St. Francois, Ste. Genevieve, and Iron counties. Most of the mining operations located in the Old Lead Belt are drained by the Big River watershed (Smith and Schumacher, 1993; Meneau, 1997). The release of mining waste from these areas have contaminated channel and floodplain sediments with toxic levels of metals from Leadwood to its confluence with the Meramec River (Roberts et al., 2009).

In 1992, the Old Lead Belt was added to the U.S. Environmental Protection Agency's Superfund National Priorities List for Pb contamination (Gale et al., 2002; Martin et al., 2016). In 1994, Doe Run Company agreed to remediate the Desloge tailing and remediation work began in 1995 (Gale et al., 2004). All major tailings piles in St. Francois County have been stabilized or are undergoing construction for stabilization by capping the mine waste, excluding the east Bonne Terre tailings pile which is currently being used as an on-site soil repository for Pb-contaminated soils. The channel reach of interest for this study is at the BRLRS site located at the confluence with the Flat River, its largest tributary (Figure 5).

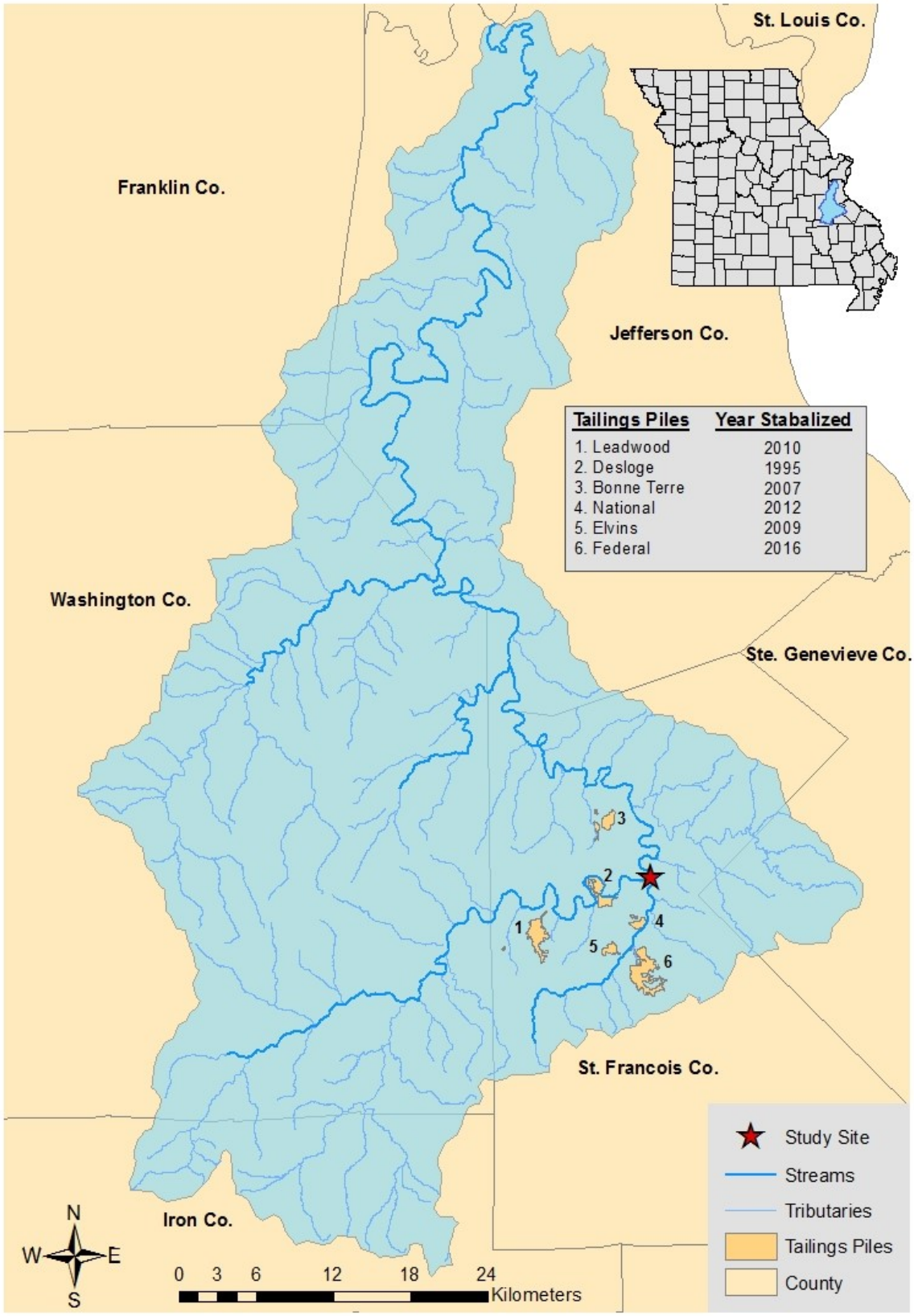

Figure 5. Big River watershed and tailings piles.

Study Site Characteristics

The BRLRS site is located in St. Francois County, MO, near of the town of Desloge, MO. The structures are located within the floodplain along the inside of a large valley bend near the confluence of the Big River and the Flat River (Figures 5 and 6). Prior to construction of remediation structures, human activities modified the natural planform of the floodplain through soil mining excavation as well as fill upon which built a levee and road across the property. A dirt and gravel road runs parallel to the Big River and along the top of the levee that is about two meters higher than the adjacent floodplain. Land use was estimated using aerial photography to be 49 % forest, 48 % grass, and 3% road.

Due to the unique location, BRLRS receives inputs of contaminated sediment from both the Big River, including Leadwood and Desloge tailings piles, and the Flat River, including Elvins, Federal, and National tailings piles. The main remediation structures include: (1) upper sedimentation basin built along the inside of a large valley bend to pond water and capture contaminated suspended sediment and finer bed sediment during inundation, including an inlet from main channel; (2) lower sedimentation basin to pond flood water and dissipate flood energy, including an outlet structure and flood water spillway; and (3) Newberry-type rocked riffle downstream of the Flat River confluence that is designed to locally raise the base-level in the channel, decrease channel slope, and trap contaminated sediment behind it (Figure 6). This study focuses on the sedimentation basin system located within a moderately wide valley (370 m) which was constructed within the exiting floodplain and situated within areas previously disturbed by soil mining. Photographs of the sedimentation basin system can be found in Appendix A.

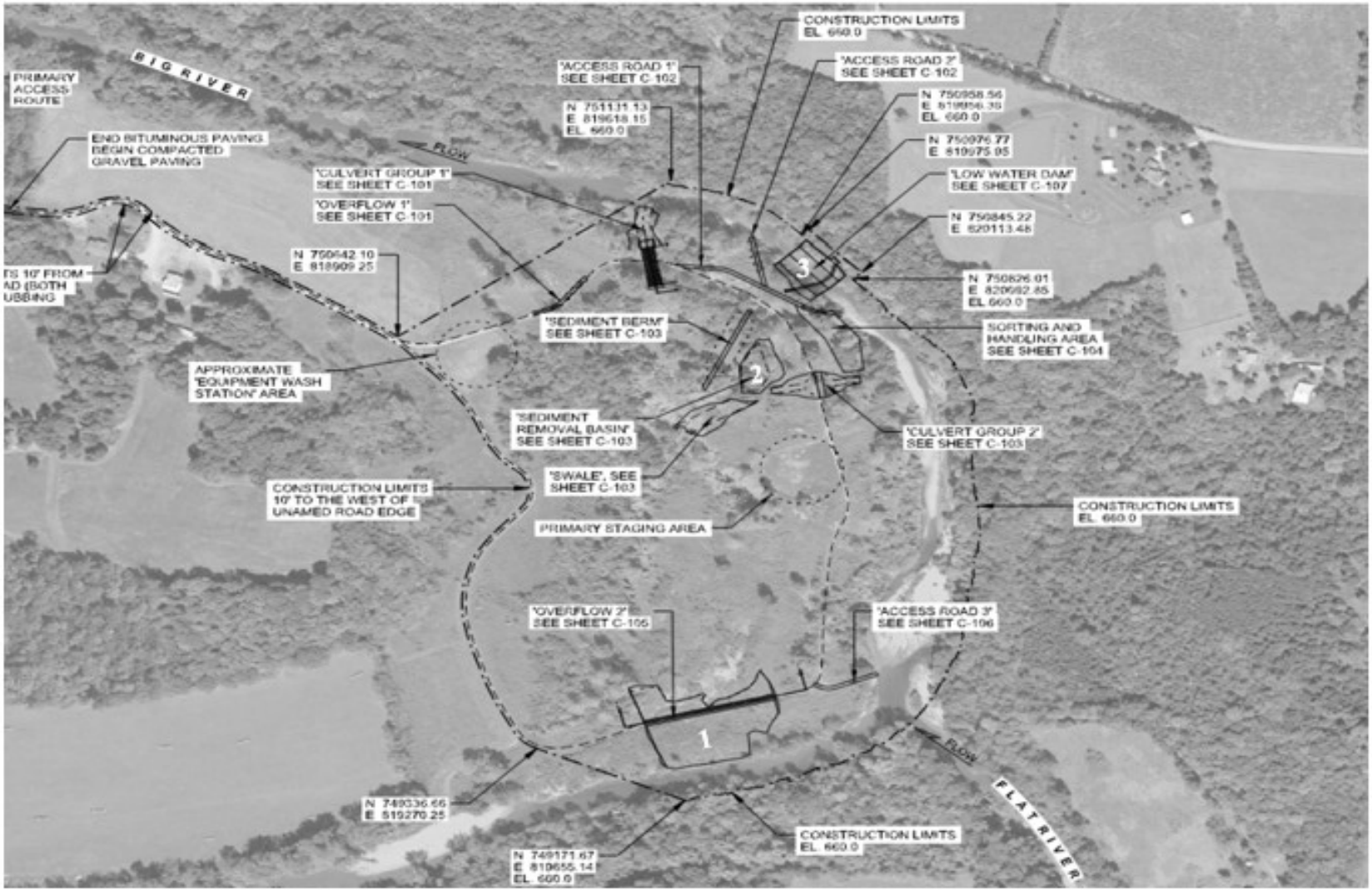

Figure 6. BRLRS site construction plans (Designed by Joseph Asher Leff, 2014).

Geology and Soils

The major geologic unit at the BRLRS site is the Bonne Terre formation. The Bonne Terre formation is 375-400 foot thick Cambrian rock composed of mostly dolomite ($CaMg(CO_3)_2$). As a result of hydrothermal mineralization, significant amounts of galena (Pb-sulfide), sphalerite (Zn-sulfide), pyrite (Fe-sulfide), and various copper sulfides crystalized within this formation (Gregg and Shelton, 1989; Smith and Schumacher, 1993). Thus, this is a key formation for mining activity. Another important formation in mining activity is called the Potosi formation, which lies above the Bonne Terre formation stratigraphically. The Potosi formation is also Cambrian and predominately dolomite, and is approximately 200 feet thick. However, the total production from this formation was relatively low (Smith and Schumacher, 1993).

Upland soil series at the study site include the Crider silt loam, Caneyville silt loam, and Gasconade silty clay loam (Table 4; Figure 7). These soils commonly are adjacent to one another and are formed in pleistocence glacial loess overlying clayey residuum (USDA, 1981). Higher terraces include the Horsecreek silt loam soil series that are only occasionally flooded during larger floods (Table 4: Figure 7). These soils are composed of material eroded from loess, residuum, and bedrock (USDA, 1981; USDA, 2002).

The primary floodplain soil series is the Haymond silt loam that is frequently flooded for short durations (Table 4; Figure 7). These soils formed from silty alluvium washed from nearby loess covered uplands and are generally found on nearly level floodplains in areas that meander and have relatively narrow valleys (USDA, 1981). Typically, the surface layer of Haymond soils is composed of dark brown silt loam about

10 inches thick with a moderate medium granular structure. Below the surface layer is 76 inches of brown silt loam and brown loam with weak fine granular structures that is stratified with lenses of pale brown fine sandy loam. The particle-sizes found in soil below the surface layer range from 10-18% clay, 1-20% very fine sand, and 0-14% fine and coarse sand (USDA, 1981). Wilbur soils are similar to Haymond soils and are often found on adjacent floodplains, however, Wilbur soils are not found at the BRLRS site.

Table 4. Soil series present at BRLRS site (USDA, 1981).

Series Name	Landform	Slope	Flood Frequency	Drainage
Crider Silt Loam	Uplands	5-9%	Never	Well
Caneyville Silt Loam	Upland-Slopes	14-20%	Never	Well
Gasconade Rock Outcrop	Upland-Slopes	9-35%	Never	Very Well
Horsecreek Silt Loam	Terrace	0-2%	Occasionally	Well
Haymond Silt Loam	Floodplain	0-2%	Frequently	Well

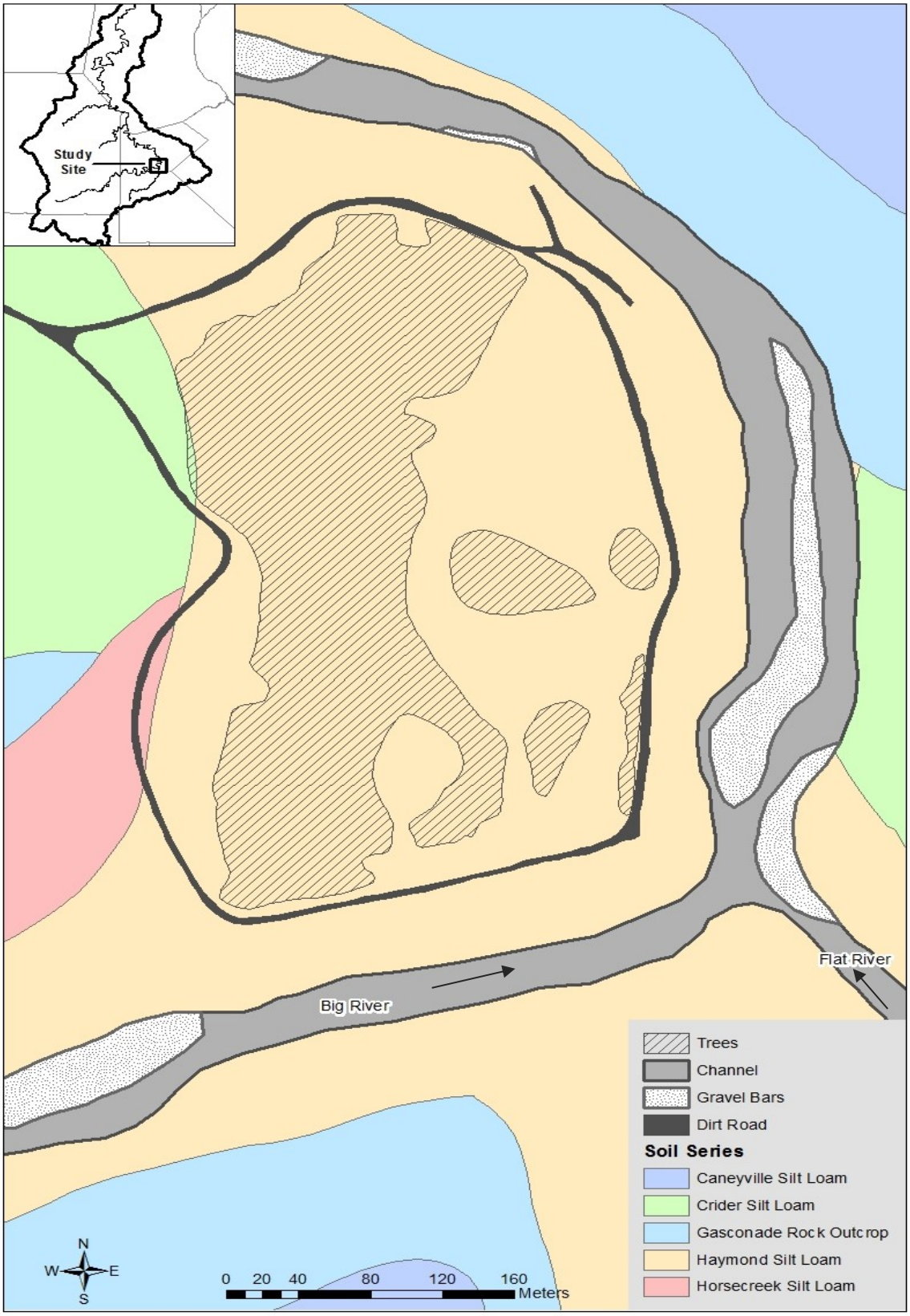

Figure 7. Soils series at BRLRS site.

Climate and Hydrology

The Ozark Plateau lies within a region with a humid continental climate. The average annual temperature is about 55 ˚F with ranges from an average temperature of 32 ˚F in the winter to 77 ˚F in the summer (USDA, 1981; Pavlowsky et al., 2010). Average annual precipitation for the region is about 100 cm with rainfall accounting for approximately 75% of the annual total (Smith and Schumacher, 1993; Meneau 1997). During the spring, the area receives the highest amount of precipitation as warm, humid air moves north from the Gulf of Mexico. This period of increased precipitation usually occurs from March to June, with May tending to be the wettest month (Adamski et al., 1995; Meneau, 1997). There are five active U.S. Geological Survey (USGS) gaging stations along the Big River that measure discharge and flood stage and are located at the following locations in order from upstream to downstream:

(1) Big River at Irondale, MO (07017200), draining 453 km^2 with a mean flow of 5.2 m^3/s since 1965;

(2) Big River below Desloge, MO (07017260), draining about 685 km^2 with a mean flow of 11.8 m^3/s since 1988;

(3) Big River below Bonne Terre, MO (07007610), draining about 1,060 km^2 with a mean flow of 17.8 m^3/s since 2012;

(4) Big River near Richwoods, MO (07018100), draining about 1,904 km^2 with an average flow rate of 20 m^3/s since 1942.

(5) Big River at Byrnesville, MO (07018500), draining 2,375 km^2 with a mean flow of 25 m^3/s since 1921.

Although the Irondale, Richwoods, and Byrnesville gages have the three longest records, they are located the furthest away from the BRLRS site. On the other hand, the Desloge and Bonne Terre gages have a limited record over a relatively short period, but

they are located 1 km upstream and 23 km downstream of the site, respectively. Thus, their records are more likely to represent the current flood regime at the BRLRS site.

Mining History

Lead was first discovered west of St. Francois County by French settlers around 1700 (Rafferty, 1980; Smith and Schumacher, 1993). Soon after, small scale mining operations began mining activity in shallow open-pit mines that mined large galena crystals (Smith and Schumacher, 1993). In the mid-1860s, mining operations quickly expanded due to technological advances such as dynamite blasting and the diamond drill, the latter which allowed miners to explore several hundred feet deeper (Rafferty, 1980). During the late 1800s and early 1900s as many as 15 companies had mining operations in the Old Lead Belt (Smith and Schumacher, 1993). Mining activity in the Old Lead Belt peaked in 1942 and continued until 1972 as mining operations were gradually shut down due to a depletion of ore deposits and increase production from the Viburnum Trend or New Lead Belt (Smith and Schumacher, 1993; Pavlowsky et al., 2010).

Mining operations used either mechanical or chemical separators to processes lead ore. Both of these processes produced large volumes of mining waste referred to as tailings that contain varying quantities of trace elements (Smith and Schumacher, 1993; Pavlowsky et al., 2010). As technology advanced, more efficient chemical separators were used that produced finer-grained tailings. It is estimated that 250 million tons of tailings were produced in the Old Lead Belt (Smith and Schumacher, 1993). These tailings were stored directly on the land and cover roughly 12.1 km^2 (Table 3). Coarse

tailings were placed in piles, while fine tailings were transported as a slurry to impoundments such as slurry ponds (Smith and Schumacher, 1993).

Few environmental regulations existed or were enforced between 1850 and 1940. As a result, mining waste stored in tailings piles or impoundments were often discharged directly to surrounding streams. It was not until after World War II that environmental restrictions were put in place stop the release of mining waste into streams (Gale et al., 2004; Pavlowsky et al., 2010). Since 1992, remediation efforts have stabilized six major tailings piles in the Big River watershed. However, mining wastes with high concentrations of heavy metals have been and still are being introduced to the Big River due to weathering and erosion of channel and floodplain deposits (Smith and Schumacher, 1993; Pavlowsky et al., 2010). According to Pavlowsky et al., (2010) approximately 86,800,000 m^3 of contaminated floodplain material is stored along the main stem of the Big River, which represents a significant portion of the estimated 91,500,000 m^3 of contaminated material for the entire river system. Additionally, Hill (2016) recently estimated 170,000 m^3 of sediment is stored in channel bed and bar deposits in the Flat River. Both of these studies indicate the magnitude of contamination in the Big River watershed that poses long-term contamination risks.

CHAPTER 3 – METHODS

This study utilizes sediment traps and repetitive topographical surveys to estimate contemporary sedimentation rates and storage, GIS to examine spatial distribution of sedimentation, and statistical analysis to examine trends in sedimentation and contamination. Field sampling and laboratory methods allow for sedimentation and geochemical analysis (Lecce and Pavlowsky, 2001), while GIS analysis allows spatial trends and relationships to be studied and mapped efficiently (Kooistra et al., 2001).

Field Sampling

This study uses concrete patio blocks (16 in x 16 in) as sediment traps. These patio blocks will be referred to as sampling blocks. A network of 25 (16 in x 16 in) sampling blocks were set even to the elevation of the present upper basin floor to monitor sedimentation rates and patterns (Figure 8 and 9). These blocks (1) provide a stable surface to measure and collect sediment; (2) are easy to find with a tile probe in case of burial; (3) can easily be adjusted to ground-level after each flood event; and (4) reduce obstacle effects on local flows and sediment transport.

The block surface provided a stable reference point to measure overlying sediment deposits after inundation from flooding events. Metal posts were placed 30 cm north (direction opposite of the channel) to help relocate blocks after deposition and vegetation growth (Figure 9). During each sampling event, sediment depth was measured at five points on the block, at the four corners and middle of the block, to the nearest millimeter using a folding ruler. The top surface of the block was cleared and reset to the new ground elevation after each sampling event. Sedimentation rates in the

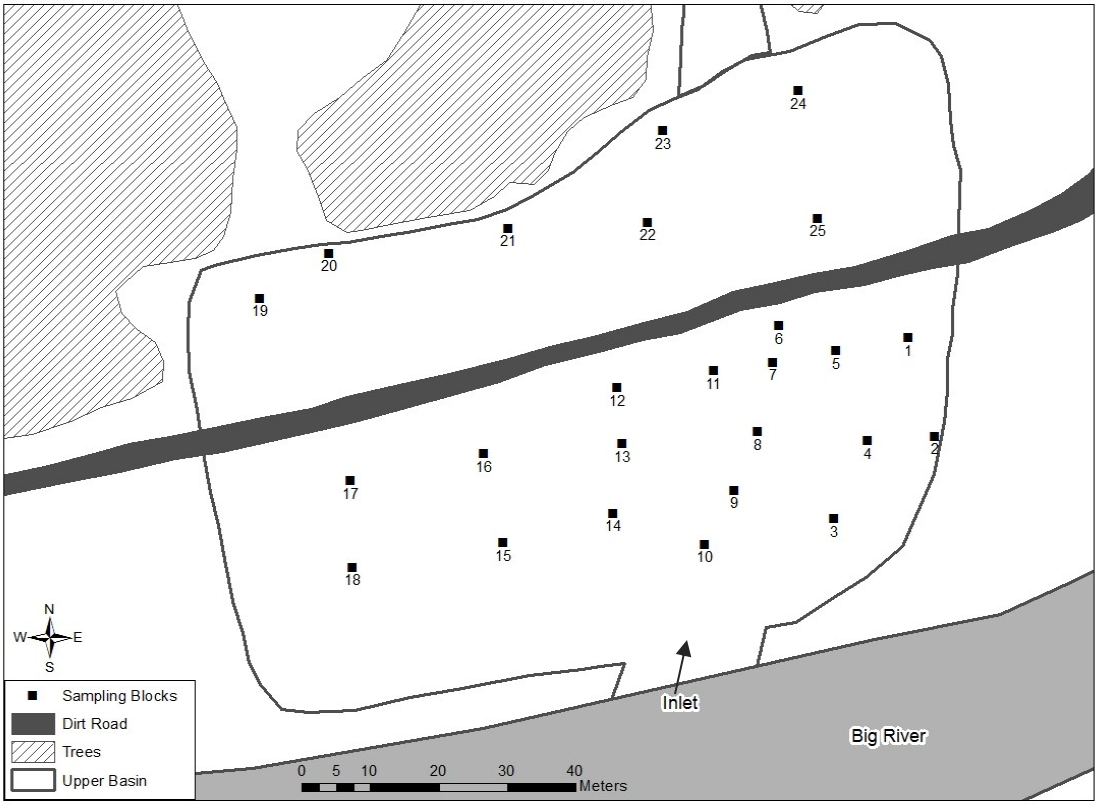

Figure 8. Locations of sampling blocks in upper basin.

Figure 9. Sampling block 7 and post (12/14/15).

upper basin were calculated by dividing the average depth of sediment on the blocks by the number of days sampling blocks were set out of a year.

In addition to sampling blocks, high-density topographical surveys of the upper basin floor were collected after flooding event(s) using a high-resolution Topcon HiPER Lite+ RTK (Real-time Kinematic) global positioning system (GPS). The RTK GPS has a post-processed differential correction of 1 to 5 cm for elevation. The upper basin was surveyed using numerous east-west transects, at key breaks in slope, and around important features of the excavated area in order to obtain a detailed map of basin topography and to measure sediment deposition and storage. The entire basin system was also surveyed following the same procedure used for the upper basin but transects were spaced 25 m apart. In order to provide stable reference points and ensure accuracy and precision of GPS points collected during surveys, three permanent elevation monuments were installed throughout the study area (Table 5; Figure 10). The location of the monuments were recorded during each survey, using the first recorded locations of the three monuments to correct for any error between monument locations of any following surveys.

Table 5. Monument locations.

ID	Northing (m)	Easting (m)	Elevation (m)	Description
Mon 1	228,827.944	249,928.769	202.452	Concrete with rebar
Mon 2	228,478.220	249,932.820	204.285	Concrete with rebar
Mon 3	228,337.057	249,634.626	203.244	Concrete with rebar

Figure 10. Monument 2 (top) and monument 3 (bottom) (1/22/16).

Sediment samples were collected for analysis from each block using a trowel. Samples were placed in 1-quart plastic freezer bags and labeled according to date of collection and site location. Over the course of a year, sediment deposited on sampling blocks was collected five times and generated 143 individual samples for geochemical and physical analysis (Table 6). Occasionally, more than one sample type was collected from a single block during a sampling event where obvious stratigraphic differences were observed within sample deposits (Figure 11). Over the course the study, two of the 25 blocks were lost due to burial, transport, or mowing, one only being sampled twice (Block 4) and the other being sampled three times (Block 1). Leaving a total of 23 blocks that were sampled over the entire study period.

Table 6. Summary of field visits and work completed.

Field Visit	Date	Work Completed
1	8/4/2015	Set Blocks and Sampled Upper Basin
2	9/17/2015	Sampled and Surveyed Upper Basin
3	12/14/2015	Sampled and Surveyed Upper Basin
4	1/21/2016	Sampled and Surveyed Upper Basin
5	7/8/2016	Sampled and Surveyed Upper Basin
6	8/3/2016	Surveyed Basin System
7	11/22/2016	Sampled Basin System and Surveyed Upper Basin

Figure 11. Splay deposits on sampling block with sand and fine gravel deposited over a layer of fine sand mixed with leaf litter (1/22/16).

In addition to repeat sampling and surveying of the upper basin, sediment depths were measured, sampled, and located at 22 sites throughout the entire basin system to evaluate broader sedimentation trends (Figure 12). At each site, depth of sediment deposition since construction (April 2015) was measured from obvious stratigraphic differences between floodplain soil and recent sediment deposits to the nearest centimeter using a folding ruler. Sediment samples were placed in 1-quart plastic freezer bags and labeled according to date of collection and site location. A total of 22 samples were collected for geochemical and textural analysis. Of those 22 samples collected, 9 were from the upper basin, 5 were from the well-drained flood way, 4 were from the hillslope left of the well-drained flood way, 2 were from the lower basin, and 2 were from the poorly-drained flood way (Figure 12).

Figure 12. Location of basinwide samples.

Laboratory Preparation and Analysis

Laboratory methods involved the preparation, physical analysis, and geochemical analysis of sediment samples and followed the Environmental Protection Agency (EPA) approved Quality Assurance Project Plan (QAPP) for this study (Pavlowsky and Owen, 2016). After field collection, sediment samples were brought to the Ozarks Environmental and Water Resources Institutes (OEWRI) laboratory following approved chain-of-custody procedures (OEWRI, 2006). Sample preparation and analysis was performed following similar procedures done by Lecce and Pavlowsky (2014). Sediment samples were first placed in oven to dry at 60 degrees Celsius. Once dry, samples were disaggregated and sieved through a stack of 16 mm, 8 mm, 4 mm, and 2 mm sieves to separate sediment into individual fractions. Grain size distribution of all samples can be found in Appendix B.

It is important to know the distribution of these fractions to evaluate the effects of selective transport and fluvial sorting on the deposition of sediment within the basin. Sediment <2 mm was placed into a small lead-free plastic bag necessary for use of the X-ray fluorescence (XRF) instrument according to the EPA XRF analysis protocol (EPA, 2007). The <2 mm fraction was chosen over the <63 mm fraction since in mined-watersheds, like the Big River watershed, sand-sized ore particles and Fe-Mn coatings on sand grains may contain significant amounts of heavy metals (Horowitz, 1991). Also, the <2 mm fraction is more representative of sediment deposited in the upper basin due to the inputs of bed and suspended sediment.

To account for variations of heavy metals between different fraction sizes, 12 samples that contained significant amounts (40 to 90%) of coarse material (2-16 mm)

were selected in order to determine the heavy metals in these fractions. To analyze this fraction, 1 tablespoon of sediment was taken from each sample. That sediment was then powdered using a ball mill and placed into a small lead-free plastic bag necessary for use of the XRF instrument.

Geochemical procedures are aimed to evaluate the mining and background or natural source fingerprints in river sediments (Horowitz, 1991). High Pb and Zn concentrations of river sediments from the Big River tend to be positively related to the degree of mining influence (Smith and Schumacher, 1993). Geochemical analysis was completed using a handheld X-MET3000TX+ XRF and followed the methodology for undertaking semi-quantitative investigations provided by EPA Method 6200 (EPA, 2007). Serval other studies have used a similar method to determine concentration levels of contaminated sediment in the Big River (MDNR, 2001, 2003, 2007; Roberts et al., 2009; Pavlowsky et al., 2010; Huggins, 2016). In this study, a XRF was used determine the concentrations of Pb, Zn, and Ca in parts per million (ppm). The elements with the highest analytical resolution on the XRF include, Pb, Zn, Cu, Ti, Fe, Se, and Ca. Standard checks and duplicated analyses were run every 10 to 20 samples depending on the total number of samples. Additionally, quality assurance and quality control (QA/QC) was completed for XRF data of each sample. Geochemistry for all samples can be found in Appendix C.

Assessment of accuracy is important to ensure laboratory instruments are creating results that are reliable and reflect true values. Accuracy calculations for XRF analysis completed by analyzing a known standard and assessing the difference between the true value and measured valued. For this study, a US Geological Survey (USGS) standard

(Jasperoid, GRX-1) was analyzed with a known Pb concentration of 856 ppm. By comparing the measured value from the XRF to the known standard, accuracy can be quantified (EPA, 2007). Of the 165 sediment samples, the accuracy for Pb was -1.20%, for Zn was -3.46%, and for Ca was -2.08%. Precision is another important measure for laboratory instruments since is assesses the consistency of the results that enable the identification of error within the system. Precision calculations for XRF analysis were completed by running duplicate samples to compare the results of the same sample (EPA, 2007). Of the 165 sediment samples, the precision for Pb was -3.44%, for Zn was -5.51%, and for Ca was -7.25%.

Geospatial and Statistical Analysis

A geospatial database and GIS were used to organize and analyze field and laboratory data. The geospatial database is composed of several sources of spatial data readily available through OEWRI Ozarks GIS database and data collected in the field using survey equipment. A 1-meter LiDAR-derived digital elevation model (DEM) was downloaded from Missouri Spatial Data Information Service (MSDIS).

Repeat Topographic Surveys using RTK. A series of surveys were completed throughout the upper basin using an RTK global positioning system (GPS). A RTK GPS offers an efficient way of providing near-instantaneous positions that has been widely adopted as an engineering surveying tool (Featherstone and Stewart, 2001). A total of 5 surveys were completed over the course of the study, typically following one or multiple flooding events (Table 6). The GPS data from repeat surveys were imported into ArcMap 10.2.2 from Excel spreadsheets (Figure 13). Each individual survey was used to create a

triangular irregular network (TIN) which was then converted into rasters using the "TIN to Raster" tool. Using the "Raster Calculator" tool, the elevations of two raster files were subtracted from each other to calculate the depth of sediment deposited during particular flooding events. This was completed using the first and last survey to calculate depth of sediment accumulated over the course of the entire study, and also using surveys in-between to calculate depth of sediment accumulated from particular flooding events (Figure 13). To estimate the volume of sediment stored, the average sediment depth deposited between surveying events was multiplied by the area all surveys covered. This data was mapped to enhance visualization of deposition quantities and patterns and how they vary over time.

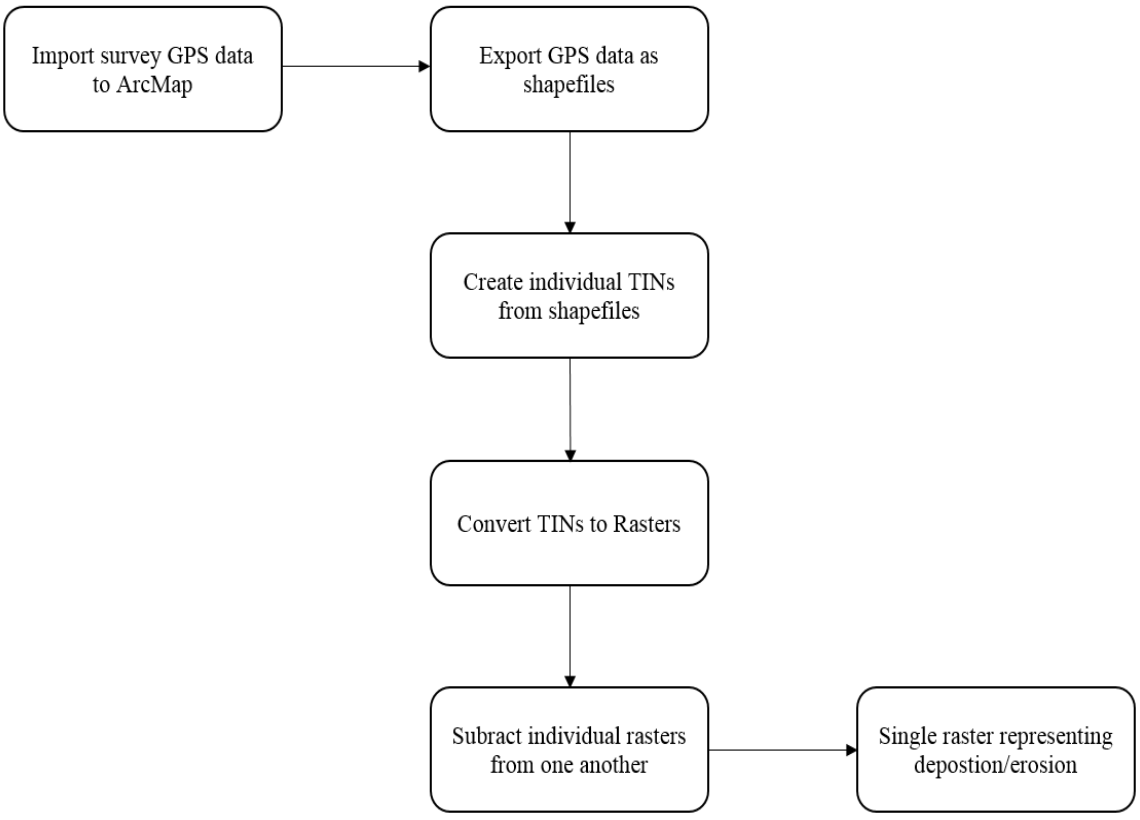

Figure 13. Steps used to analyze repeat topographic surveys.

Study Period Deposition Rates. Sediment deposition measured from repeat surveys was used to estimate deposition rates for the upper basin. The average depth of sediment deposited was determined by the average difference in elevations between the first (September 17, 2015) and last (November 22, 2016) survey. That average depth estimated the amount of sediment that has accumulated over that time. To estimate deposition rates during the study period, the average depth was multiplied by the total number of days between surveys out of a year (365.25 days).

Historical Deposition Rates. Identification of ^{137}Cs in floodplain deposits can be used to document sedimentation since the mid-1950s (Owen et al., 2011). Nuclear weapon testing beginning in the mid-1950s emitted radioactive the carbon isotope ^{137}Cs into the atmosphere that was spread throughout the world as fallout (Walling et al., 1992). As a result, the presence of ^{137}Cs in sediments provides a marker in the sedimentation record (Faulkner and McIntyre, 1996). The maximum fallout of ^{137}Cs occurred in 1963 and can be used to estimate the landform surface at that time (Walling and He, 1994). Five pre-construction cores were collected throughout the natural floodplain at the BRLRS site in 2014. Those cores were analyzed for peaks of ^{137}Cs in 10 cm sections. The depth between the upper and lower boundary depths of a core section where ^{137}Cs peaked was used as the post-1963 depth.

Lead and Zinc Storage. The Pb and Zn concentrations found in both fine (<2 mm) and coarse sediment (2-16 mm) collected from sampling blocks and depth of sediment deposited were used to determine the differences in mass of Pb and Zn stored in fine and coarse sediment. To calculate storage for a particular block, the mass of sediment stored on a block for both sediment fraction sizes was first estimated by

multiplying the volume of sediment by the fraction of the sample 2-16 mm or <2 mm. That product is then multiplied by a bulk density to produce the mass of sediment stored by each size fraction and can be determined by:

$$M_{sediment} = (V \times F)*(B)$$

Where $M_{sediment}$ is the mass of sediment (g), V is the volume of sediment stored on a block (cm^3), F is the fraction 2-16 mm or <2 mm (0-1), and B is the bulk density (g/cm^3). The volume of sediment stored on a block was calculated by multiplying the area of the block (cm^2) by the average sediment depth (cm) measured for a particular block. The bulk density of floodplain soils at the study site range from 1.3 to 1.5 g/cm^3 (USDA, 2000). Therefore, an average bulk density of 1.4 g/cm^3 was assumed for sediment <2 mm since these deposits are similar to those of floodplain deposits. Bunte and Abt (2001) found that the bulk density of gravel in gravel-bed rivers ranged between 1.7 and 2.6 g/cm^3 and averaged 2.1 g/cm^3. A bulk density of 2.1 g/cm^3 was used for sediment 2-16 mm since those sample are a mixture of sand and gravel.

To calculate the storage of Pb mass in each size fraction by sampling block area, the mass of sediment stored is multiplied by the Pb concentration in the 2-16 mm sediment or <2 mm sediment. The product is then divided by 1,000,000 to convert to grams and can be determined by:

$$M_{Pb} = (M_{sediment} \times C_{Pb}) / 1{,}000{,}000$$

Where M_{Pb} is the mass of Pb (g), $M_{sediment}$ is the mass of coarse or fine sediment (g), and C_{Pb} is the Pb concentration (ppm) of the coarse or fine sediment. The same calculation was done to estimate Zn storage, but used the Zn concentrations. The percent of Pb and Zn in the two fraction sizes was calculated to help assess the importance of coarse

grained sediment to the overall storage. To calculate this, the mass of Pb stored in each fraction was divided by the total mass stored and then multiplied by 100.

Flood Analysis. Recurrence intervals (RI) of local flooding events were calculated to better understand the frequency of overbank events that promote deposition. This was accomplished through the quantification of flows from USGS gage data. Annual peak discharges from 1980 to present were collected from three USGS gaging station on the Big River (Irondale, Richwoods, and Byrnesville). The Desloge gaging station was not included due to a limited record of less than 10 years, which is the minimum number of years required for this type of analysis (Weaver et al., 2009).

The gage data was then analyzed in PeakFQ, which is a program created by the USGS to perform statistical flood-frequency analysis of annual-maximum peak flows. This program uses gaging records to estimate the probability and discharges of different magnitude floods (Flynn et al., 2006). Probabilities generated by PeakFQ were converted to RI of 1.05, 1.25, 1.5, 2, 2.33, 5, and 10 years for each gaging station (RI = 1/probability of flood). Estimated peak discharges for each RI were then graphed by the drainage area of each gage, showing a relationship between flood magnitudes of each RI as gage drainage area increased. Linear regression was used to model this relationship by fitting a linear regression equation to the observed gage data. Linear regression equations were used to estimate the peak discharges that related to the RI for the Desloge gage, given the drainage area of the gage. The estimated RI for the Desloge gage were then graphed by the estimated peak discharge and exponential regression was used to model the relationship between peak discharge and RI of the Desloge gage. That regression

equation was used to estimate the RI of each flooding event at the Desloge gage over the study period using its recorded peak discharge.

Basin Elevation Control. Known elevations of particular features in the upper basin, recorded by the RTK and cross-section transects, were used to determine the relationship between the gage stage at the Desloge gage and the water surface height at the basin inlet. The low flow water line recorded on August 5, 2015 was 200.6 m above sea level (asl) and the thalweg was 199.5 m asl, resulting in a water depth of 1.13 m. During this time, the gage stage was 1.08 m (3.55 ft). On September 17, 2015 the water depth was measured to be 0.93 m while the gage stage was at 0.95 (3.11 ft). Therefore, a one-to-one relationship to road crest elevation (199.5 m to 202.2 m asl) is assumed. The thalweg depth is approximately equal to gage stage at the inlet during low flow conditions.

However, there is a slightly different relationship during peak flood stages. The peak flood stage on August 15, 2016 was 6.76 m (22.18 ft). This flood event almost topped the highest road at 204.8 m asl (5.27 m above channel bed) as indicated by stranded large woody debris along the high road. A similar relationship is also found for the peak flood stage on December 26, 2015. Therefore, a curvilinear line is used between road crest (202.2 m asl) to high road top (204.8 m asl) to match the peak discharge with the gage stage at 6.76 m (22.18 ft). A polynomial rating curve can then be used to predict inlet elevations from gage stage and can be determined by:

$$I_{elevation} = -0.0866(gs)^2 + 1.4142(gs) + 199.19 \quad (r^2 = 0.997)$$

Where $I_{elevation}$ is the basin inlet elevation (m asl) and gs is the gage stage (m) at a particular time (Figure 14). The one-to-one relationship suggests that when the gage stage

reaches 1.7 m (5.5 ft), the depth of water in the channel at the basin inlet reaches the point where water starts to enter the upper basin. Then when the gage stage reaches approximately 2.6 m (8.5 ft) it is at the point where water overtops the low road and enters the basin system. Using this relationship, the Desloge gage record was analyzed for gage stages of 2.6 m (8.5 ft) or greater to determine the frequency, duration, and magnitude of each flooding event. This provided a flood record for the study site that included: (1) peak gage stage, (2) peak discharge, and (3) number of days each flooding event inundated the basin over the course of the study. This data, along with the sedimentation record from the sampling blocks and RTK surveys, were used to analyze the quantities, rates, and patterns of sedimentation for individual flooding events.

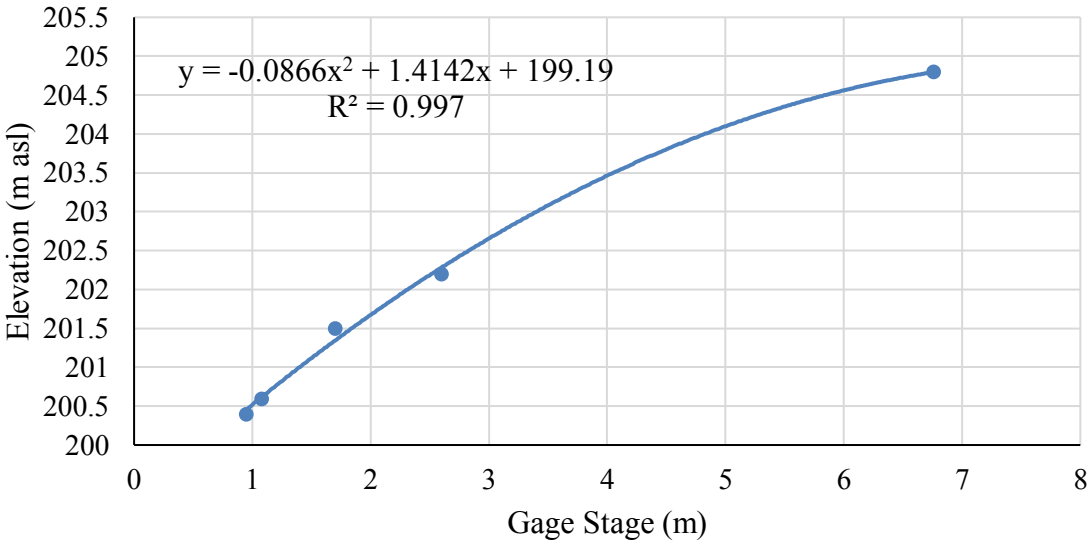

Figure. 14. Rating curve for basin elevations related to gage stage.

CHAPTER 4 – RESULTS

Sedimentation Basin Form

Basin Features and Topography. Basin features were mapped following the construction of remediation structures using aerial photographs and repeat surveys (Figure 15). The entire sedimentation basin system consists of: (1) primary inlet; (2) upper sedimentation basin; (3) well-drained flood way, (4) lower sedimentation basin; (5) secondary inlet; (6) poorly-drained flood way; (7) primary outlet; and (8) spillway (Figure 16). The upper inlet was created by removing portions of the bank so that bank height was the same as bar height. The inlet allows sediment-laden water to enter the basin system during high flow conditions. The upper sedimentation basin was constructed within the pre-existing floodplain by lowering the floodplain surface to be lower than that of the road that cuts across the upper basin. This road was designed to be overtopped at 202.1 m asl and slopes upward at each end to intercept the natural ground surface. Additionally, the upper basin surface was graded so that area south of the road dips towards the Big River and the area north of the road dips towards the lower basin.

A hillslope along the east outer margins of the basin system aids in confining and directing the flow of water and associated sediment through the upper basin, towards the lower basin and outlet. While area along the west margins gradually slopes upward until it intercepts the dirt road and is dominated by forest and grass. The lower basin helps dissipate flood energy by ponding water that flows through the well-drained flood way from the upper basin and water that flows directly from the Big River through a set of culverts. The lower basin also collects any fine-grained sediment still in suspension. A set

Figure 15. BRLRS site pre-construction (November 2013) (top) and post-construction (October 2015) (bottom) (Google Earth Pro, 2016).

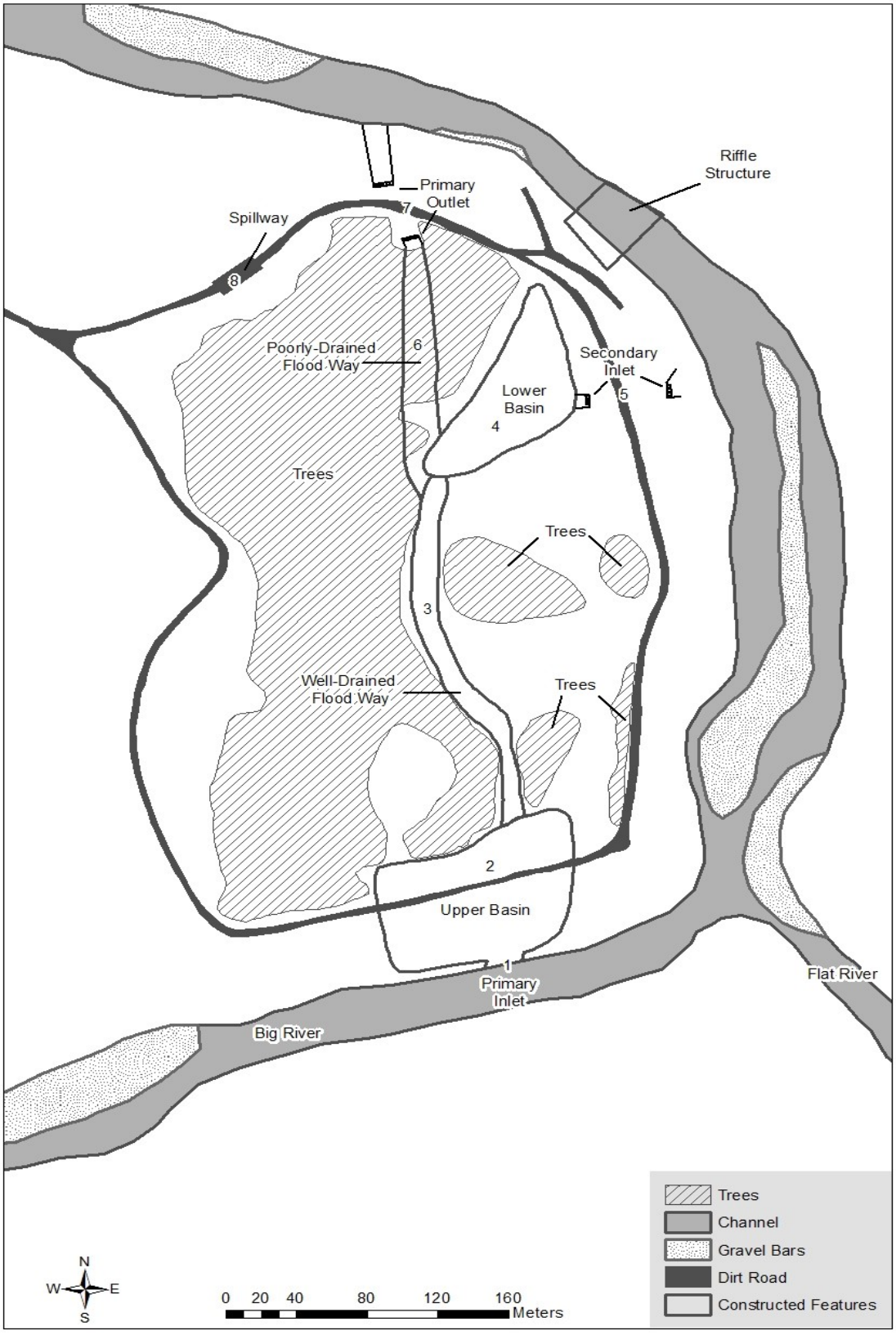

Figure 16. Sedimentation basin system features.

of culverts were placed within the lower basin to act as an inlet during the rising limb of floods and an outlet during the falling limb of floods. Located north of the lower basin is a poorly-drained flood way that acts as an outlet for flood waters through a set of culverts and over a spillway. The spillway was designed to be overtopped at 202.4 m asl and slopes upward at each end to intercept the natural ground surface.

Overall, the longitudinal profile of the basin system is steeper than that off the Big River (Figure 17). Through the basin system, there generally is an upward slope from the primary inlet to the well-drained flood way. The slope through the well-drained flood slopes downward and is relatively steep until it reaches the poorly-drained flood way where the slope tends to vary up to the primary outlet. The relatively steeper slope of the basin system creates favorable conditions to initiate "cut-off" processes for chutes by increasing flow velocities and transport capacities.

Basin Changes since Construction. Since construction, the thalweg of Big River has shifted to the left and has directed both erosive forces and sediment load toward the basin system. In addition to the shift of the thalweg, flood events have also modified the topography of the basin. A chute has developed within the upper basin where water enters the inlet. Further, the inlet and bank along the upper basin has experienced significant erosion, mainly during the first 6 months after construction as the thalweg has shifted to the left. This has caused the banks to recede and increased the width and depth of the inlet. Changes in slope and increased flow velocities from the upper to the lower basin has caused a headcut to form in the well-drained flood way. Additionally, large magnitude floods have caused the low point of the downstream road, which acts a spillway, to wash out. This may have been enhanced due to woody debris blocking the

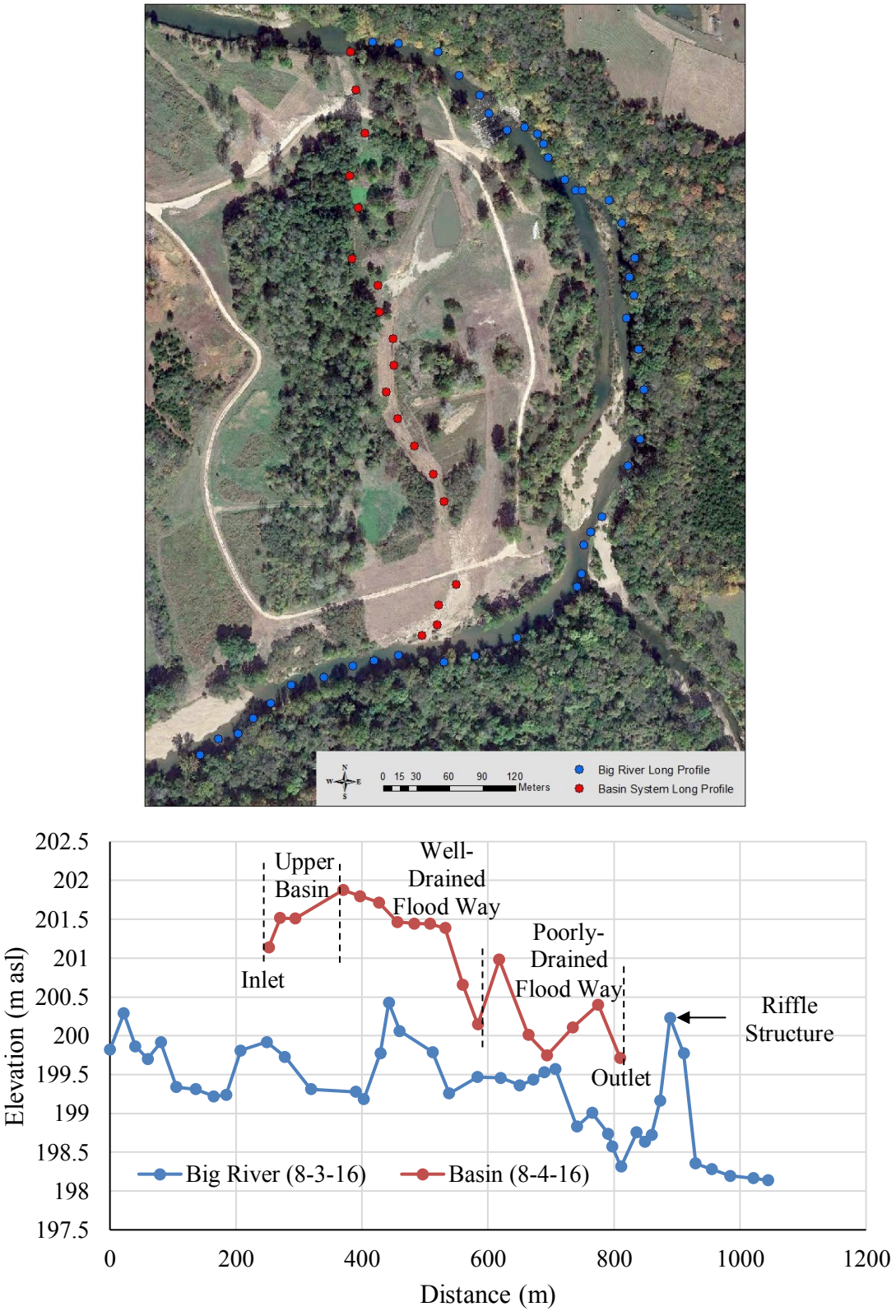

Figure 17. Longitudinal survey points (top) and longitudinal profiles (bottom) of the Big River and basin system.

outlet culverts and preventing water to flow out through the culverts. To prevent the road from continuing to wash out, woody debris was removed from the culverts and a concrete spillway was created over the road in November of 2016. Photographs of the entire basin system along with major changes that have occurred can be found in Appendix A.

Flood Analysis

Basin Flood Frequency Analysis. Flood frequency analysis of the Irondale, Richwoods, and Byrnesville gages was used to estimate peak discharge of flood recurrence intervals (RI) for the Desloge gage (Figure 18). Flood RI trends of the Irondale, Richwoods, and Byrnesville gages display a fairly linear trend with increasing drainage area. The peak discharges calculated for flood RI of the Desloge gage was used to estimate the RI of individual flooding events that occurred during the study period (Figure 19).

Flooding events during the study period were considered to occur when the stage of the Desloge gage reached 2.6 m (8.5 ft) or 64.0 m^3/s (2,260 ft^3/s). At this point, water is able to enter the basin system by overtopping the road in the upper basin. However, water first enters the basin through the inlet when the stage reaches approximately 1.7 m (5.5 ft) or 15.5 m^3/s (548 ft^3/s). These discharges are associated with flooding events with less than the 1 year RI. Typical bankfull discharge at reaches that have not been altered is reached when the stage reaches approximately 3.5 m (11.5 ft) or 137.6 m^3/s (4,860 ft^3/s) and a RI of 1 year.

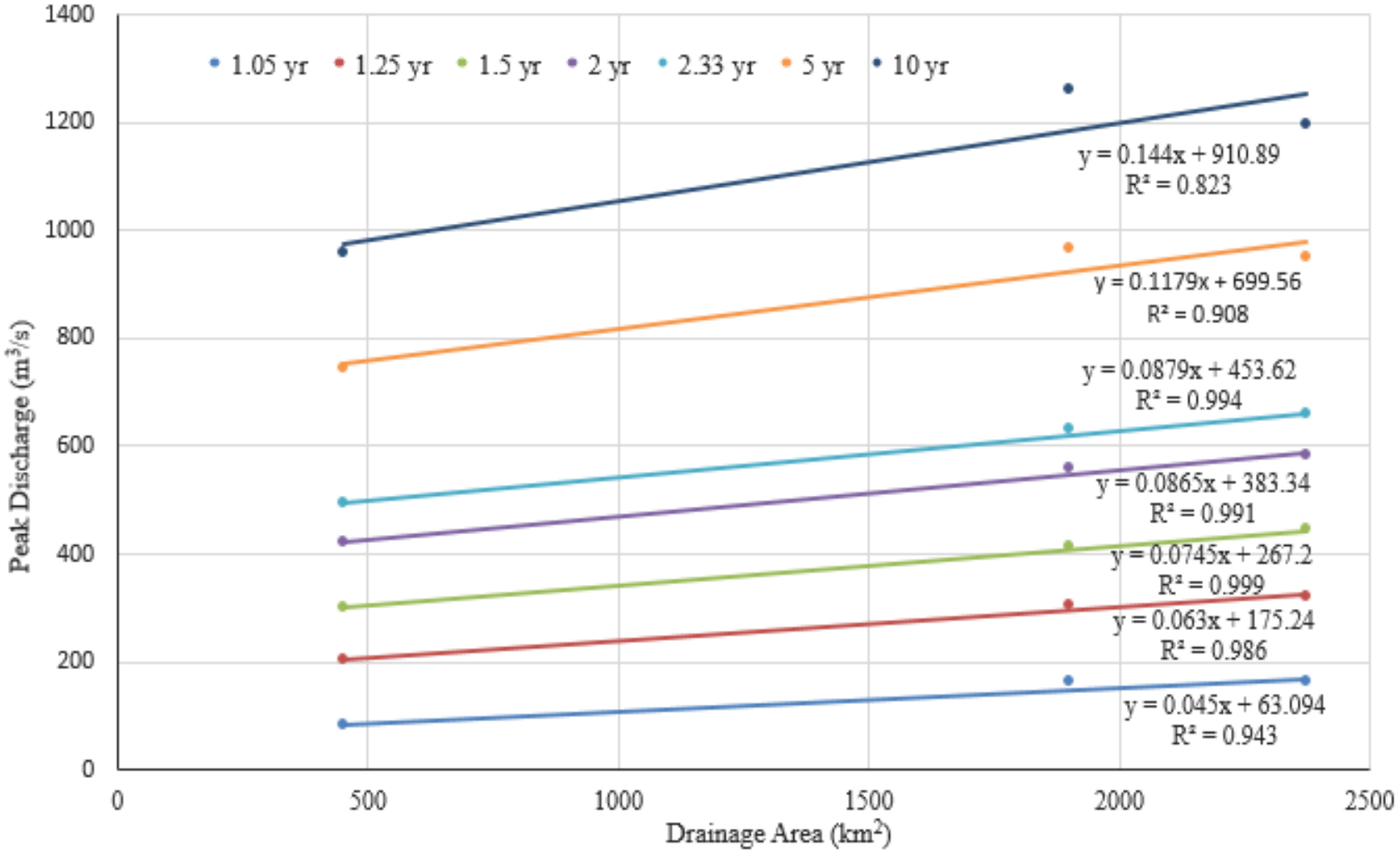

Figure 18. Flood RI of Irondale, Richwoods, and Byrnesville USGS gaging stations.

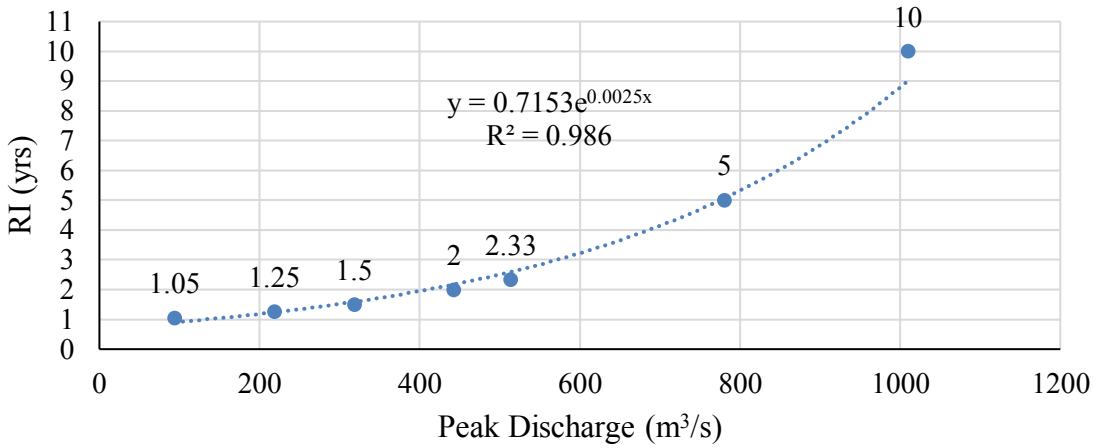

Figure 19. Flood RI for Desloge gage (Flood record May 13, 2015 – Present).

Study Period Flood Record. The Desloge gage record shows that from May 13, 2015 to December 1, 2016 there were 15 flooding events that were able to enter the basin system by overtopping the road in the upper basin (Figure 20; Table 7). The magnitude, frequency, and duration of flooding events varied between flooding events and sampling events (Figure 20; Table 7). The peak gage stage of all flooding events ranged from 2.63 m (8.63 ft) to 7.24 m (23.76 ft) with an average peak stage of 4.4 m (14.3 ft). Peak discharges associated with gage stages ranged from 68.0 m^3/s (2,400 ft^3/s) to 685.3 m^3/s (24,200 ft^3/s) with an average peak discharge of 209.5 m^3/s (7,397 ft^3/s). The two largest magnitude floods occurred in December and August with peak gage stages of 7.24 m (23.76 ft) and 6.76 m (22.18 ft), respectively. While the two smallest magnitude floods occurred in November and July with peak gage stages of 2.63 m (8.63 ft) and 3.12 m (10.24 ft), respectively. The range in flood magnitudes transport varying quantities of sediment that can only be transported to certain areas of the basin.

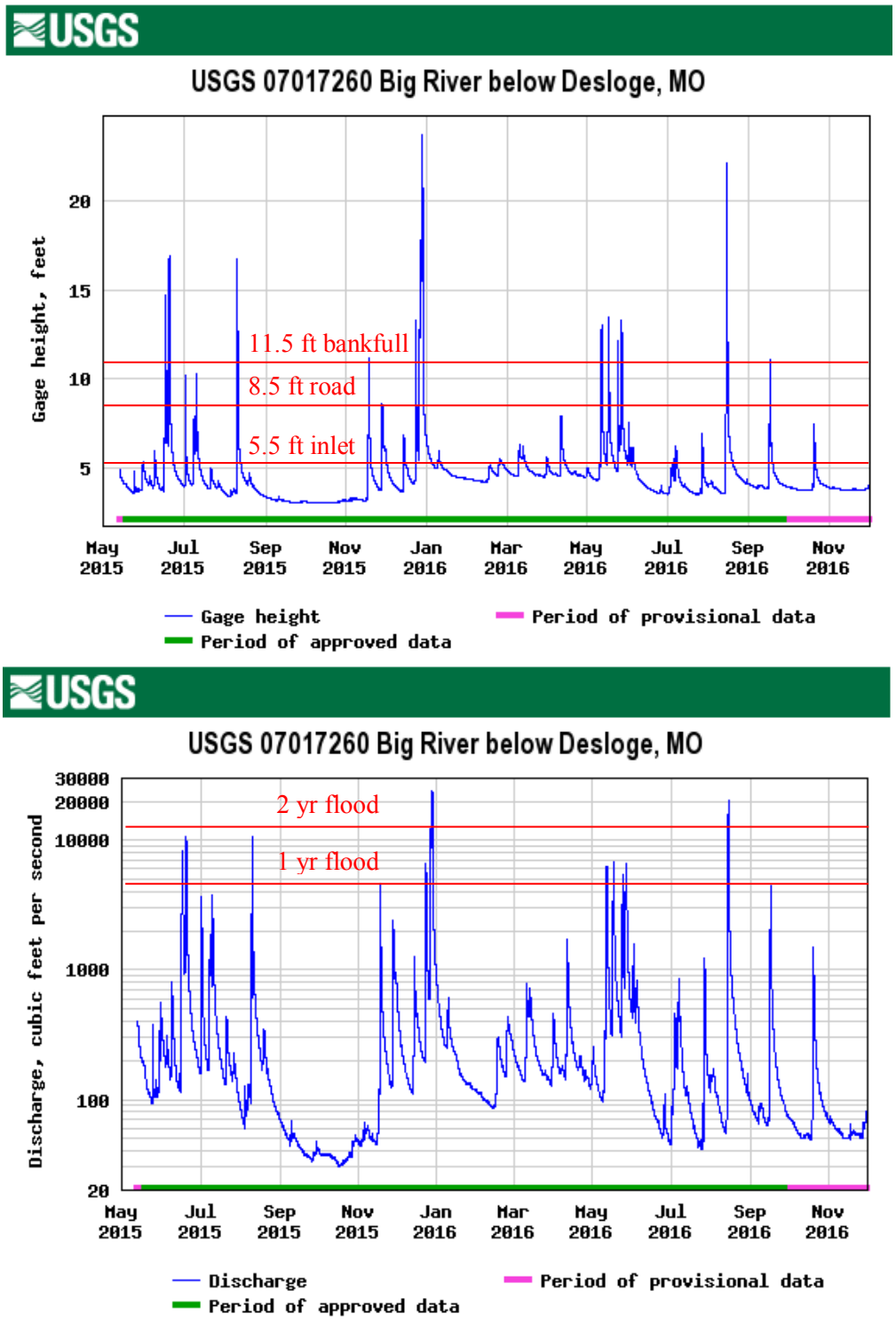

Figure 20. Stage height (top) and discharge (bottom) at the Desloge gage from May 13, 2015 to December 1, 2016 (NWIS, 2016).

Table 7. Flooding events at BRLRS site from May 1, 2015 to December 1, 2016.

Flooding Event	Date	Peak Gage Stage (m)	Peak Discharge (m^3/s)	Inundation (days)	RI (years)
1	6/16/2015	4.49	231.9	1.5	1.28
2	6/19/2015	5.15	305.8	1.75	1.54
3	7/2/2015	3.12	104.5	0.4	0.93
4	7/10/2015	3.13	105.9	0.75	0.93
5	8/10/2015	5.11	300.2	0.75	1.52
6	11/18/2015	3.40	128.6	0.5	0.99
7	11/28/2015	2.63	68.0	0.4	0.85
8	12/23/2015	4.04	186.3	1	1.14
9	12/26/2015	7.24	685.3	3.5	3.97
10	5/11/2016	3.96	177.8	1.5	1.12
11	5/17/2016	4.10	191.1	1.3	1.15
12	5/24/2016	3.71	155.2	0.6	1.05
13	5/26/2016	4.06	187.2	2	1.15
14	8/15/2016	6.76	580.5	1.6	3.05
15	9/17/2016	3.39	127.1	0.4	0.98

The RI of the 15 flooding events that occurred during the study period ranged from less than 1 to 4 years. There were multiple <1.5 year floods that occurred over the course of a year and half. It is expected that only up to two events of this magnitude would occur during a given year. Additionally, two flooding events with RI of 3 and 4 years occurred within 9 months of one another. Since an average year would bring 1-3 overbank floods into the basin, having 15 flooding events suggests that flood frequency over the past year has been higher than normal. It is uncertain whether this trend of increased frequency of flooding events will continue or return to the expected flood frequency. However, National Oceanic and Atmospheric Administration (NOAA) and

others predict a trend in increased intense rainfall events in the Ozark region (Kennedy, 2014; Mallakpour and Villarini, 2015). If these prediction hold true, it is likely that flooding events could continue to occur more frequently and at larger magnitudes.

Repeat Topographic Surveys using RTK

Sediment Deposition and Erosion. Post-construction sedimentation was monitored throughout the upper basin using repeat topographical surveys. Over the course of the study, the upper basin was surveyed 5 times. All surveys covered an area of approximately 7,100 m^2. Sediment accumulation in this area between the first (Sept. 17, 2015) and last (Nov. 22, 2016) survey ranged from -140.2 to 87.8 cm with an average of 12.2 cm (Figure 21). A majority of the upper basin experienced sediment deposition. The largest amounts of sediment deposition occurred near the primary inlet and along the outside of the chute that formed a relative coarse-grained splay deposit composed of sand and fine gravel (Figure 21 and 22). In comparison, overbank deposits to the west of the chute-splay area were finer-grained and thinner (Figure 21 and 23). Significant erosion occurred along the bank of the upper basin (Figure 21 and 24), where is has retreated approximately 5 m since September 2015 as a result of inlet expansion and thalweg erosion.

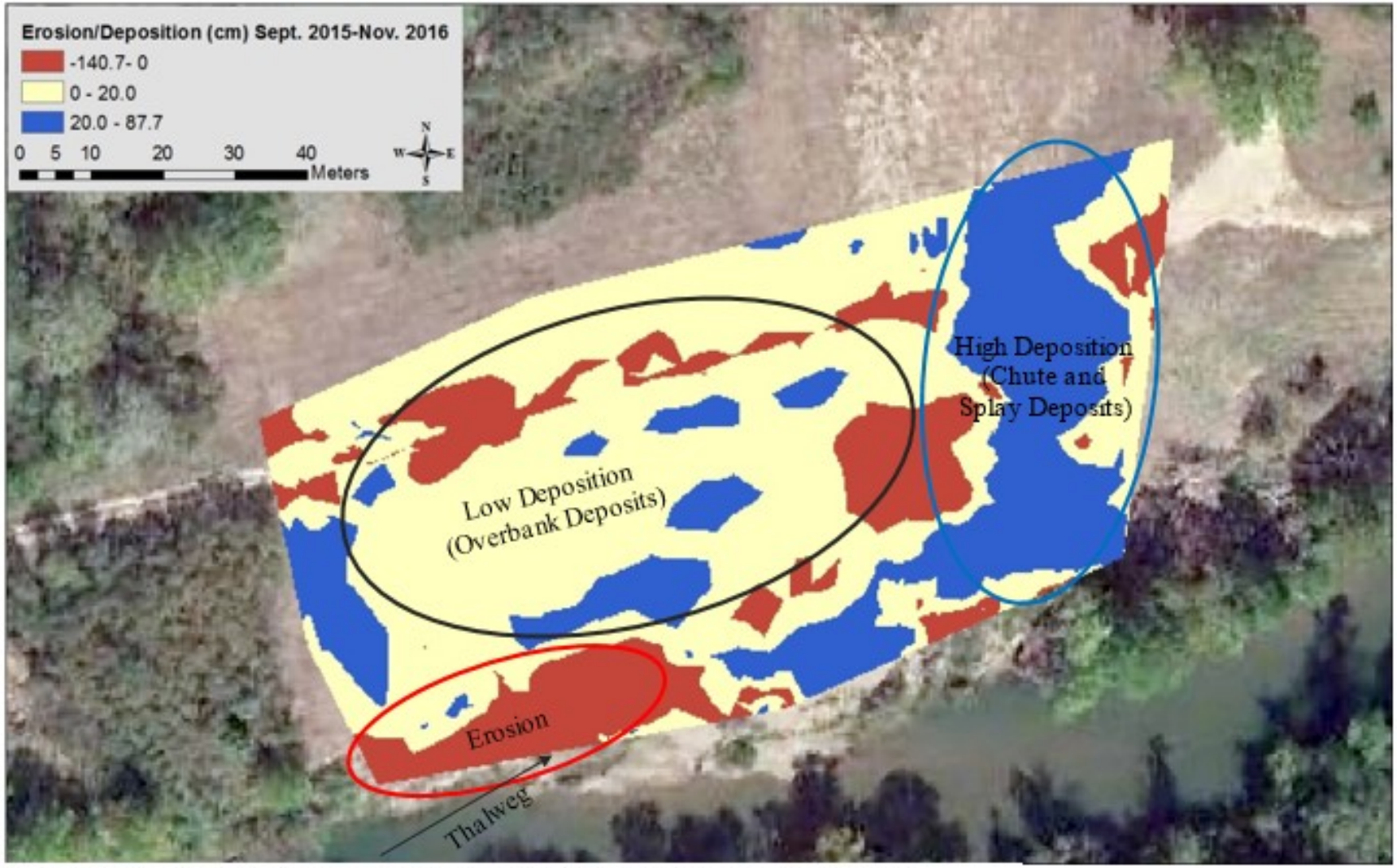

Figure 21. Changes in erosion and deposition from September 2015 to November 2016.

Figure 22. Coarse chute and splay deposits near inlet and chute (9/15/15).

Figure 23. Fine-grained overbank deposits west of splay deposits (12/14/15).

Figure 24. Bank erosion along bank of upper basin (12/14/15).

Sediment deposition following the largest flood event follow similar trends of those that occurred over the entire study period (Figure 25). Sediment deposition between this time (Dec. 14, 2015 – Jan. 21, 2016) ranged from – 59.7 to 84.1 cm with an average of 10.7 cm. The largest amounts of sediment were still deposited along the outside of the chute, while the rest of the basin experienced less sediment deposition. However, there were slightly different patterns of erosion. During the largest flood event, more erosion occurred within the inlet and chute, and bank erosion was measure over a larger area (Figure 25).

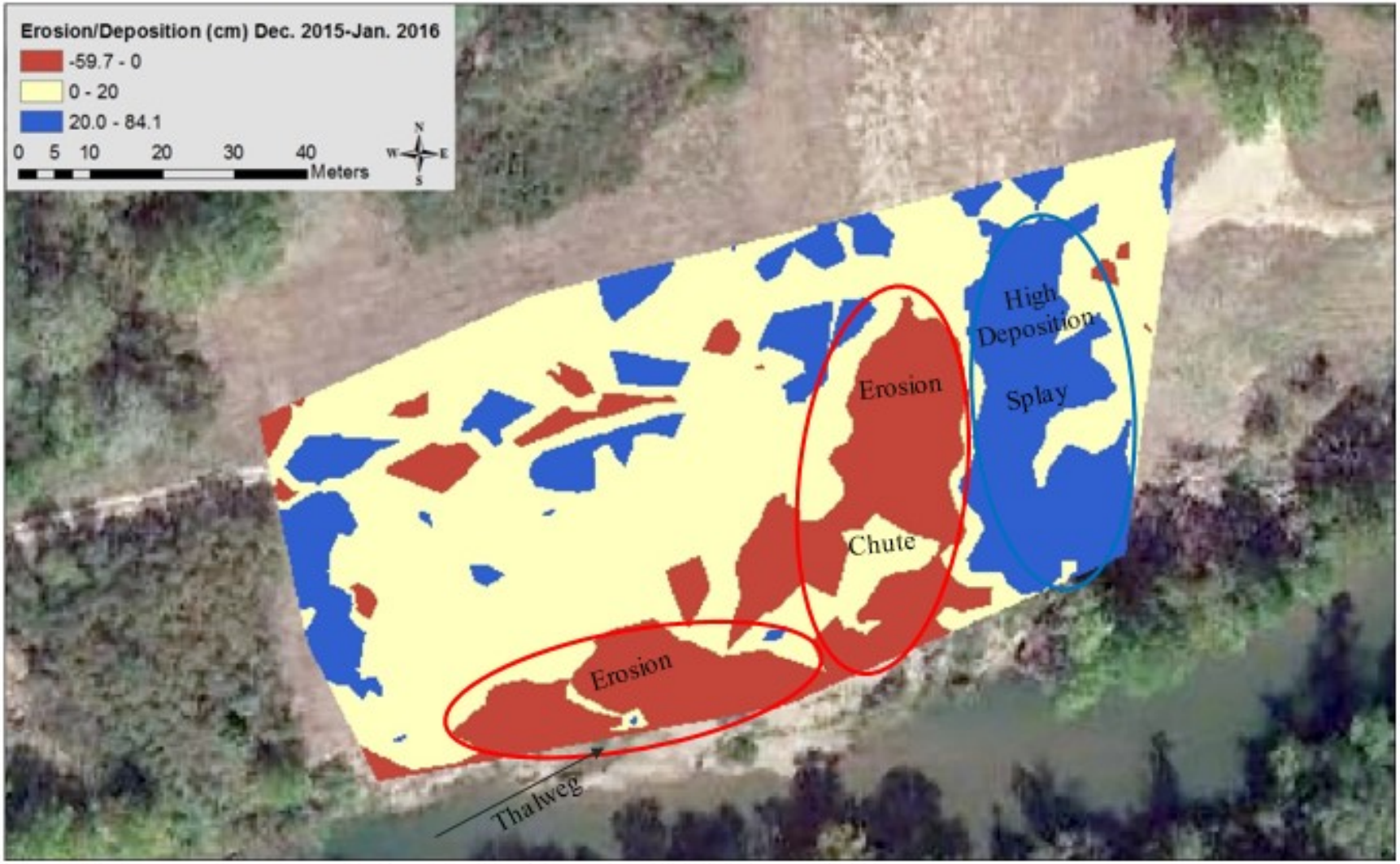

Figure 25. Changes in erosion and deposition from December 2015 to January 2016.

Sediment Storage. The total volume of sediment trapped from September 2015 to November 2016 is approximately 865 m^3 in area of 7,100 m^2. The amount of sediment trapped is not evenly distributed and some areas did not trap any sediment. Additionally, some areas lost sediment due to erosion, such as the inlet and bank of the upper basin. Overall, sediment is being trapped at a higher rates near the inlet and along the outside of the chute, while lower rates of sediment are being trapped in the center of the basin and in areas further away from the basin inlet.

The volume of sediment stored may be larger than expected for an average long-term conditions due to two factors. First, the inlet enlargement by bank erosion shortly (<6 months) after construction was completed may have added to the volume of sediment stored in the upper basin. These banks have experienced significant erosion since September 2015 due to high energy flows entering the inlet and trying to cut-off the inside bend of the channel due to the leftward shift of the thalweg. The erosion of the inlet and bank indicated from the RTK surveys is confirmed by what is observed in the field (Figure 24). Second, a relatively frequent series of nine flooding events filled the basin during this time and therefore the present results may over-represent deposition rates compared to the average number of flooding events expected to occur during a given year.

Deposition Patterns. Over the course of the study period, flooding events of various magnitudes and durations have inundated the upper basin and deposited varying amounts of sediment. However, the overall patterns of deposition seems relatively uniform. The highest rates of sediment deposition are around inlet and along the outside of the chute. During flooding events, water first enters the basin through the inlet with its

greatest carrying capacity and largest sediment load. As water flows through the inlet towards the flood way, flow velocities drop with distance from the inlet and sediment transport capacity decreases. Decrease in flow velocity is also aided by the hillslope to the east that increases roughness, reducing flow velocity and transport capacity. As a result, sand and gravel-sized sediment is deposited first, in the form of splay deposits, and fines away from the inlet. Also, the initial high flow velocities can potentially have the energy necessary to erode the banks and inlet of the upper basin.

The lowest rates of sediment deposition occur in the west areas of the basin and areas north of the road. The west areas of the basin are far from the inlet-chute channel where flow velocities are slower. Further, low rates of fine sediment (<2 mm) deposition suggest relatively low loads of silt and clay entering the upper basin as suspended load. Areas north of the road also experience lower flow velocities than the chute, but tend to deposit coarser grained sediment than the west areas of the upper basin. This is likely due to the main flow and sediment load moving through the chute towards the flood way, as lower-energy water slowly spreads out across the rest of the upper basin. Thus, the areas north of the basin, especially between the road and flood way, also experience higher flow velocities than areas to the west and suggest that the sand and fine gravel bedload is being transported into and to the flood way of the basin system by the chute.

Sediment Trap Monitoring using Concrete Blocks

Sediment Deposition. Sampling blocks were used to quantify deposition within the upper basin and also provide information on changes in particle size and geochemistry related to flooding events. Over the course of the study, sampling blocks

were sampled five times (Table 6). The first of sampling events took place prior to sampling blocks being set, and measured the approximate depth of recent sediment deposition since construction of the upper basin (May 2015-August 2015). The following four sampling events used the sampling blocks and took place following at least one flooding event. There were 13 flood events that occurred over the course of five sampling events. Over this period, individual blocks had total sediment accumulation ranging from 2.5 cm to 60 cm with an overall average sediment depth of 28.8 cm (Figure 26; Table 8). Typically, sediment depths measured on sampling blocks ranged from 5-10 cm, with some depths of 25-40 cm, and with an overall coefficient of variation (CV) of 55% (Figure 27).

Average sediment depths on sampling blocks varied greatly between sampling events. Variations of sediment depths on sampling blocks for each sampling period had large CV values ranging from 76% to 203%. The large variation in sediment deposition is likely attributed to the magnitude and duration of flooding events between sampling periods. The largest CVs are from sampling events that experienced only one or two small magnitude floods that inundated the basin for less than a day. These flooding events may have a limited transport capacity or sediment supply, and may have only inundated certain areas of the basin. Thus, only a few sampling blocks would have significant deposition while the rest of the blocks had little or no deposition.

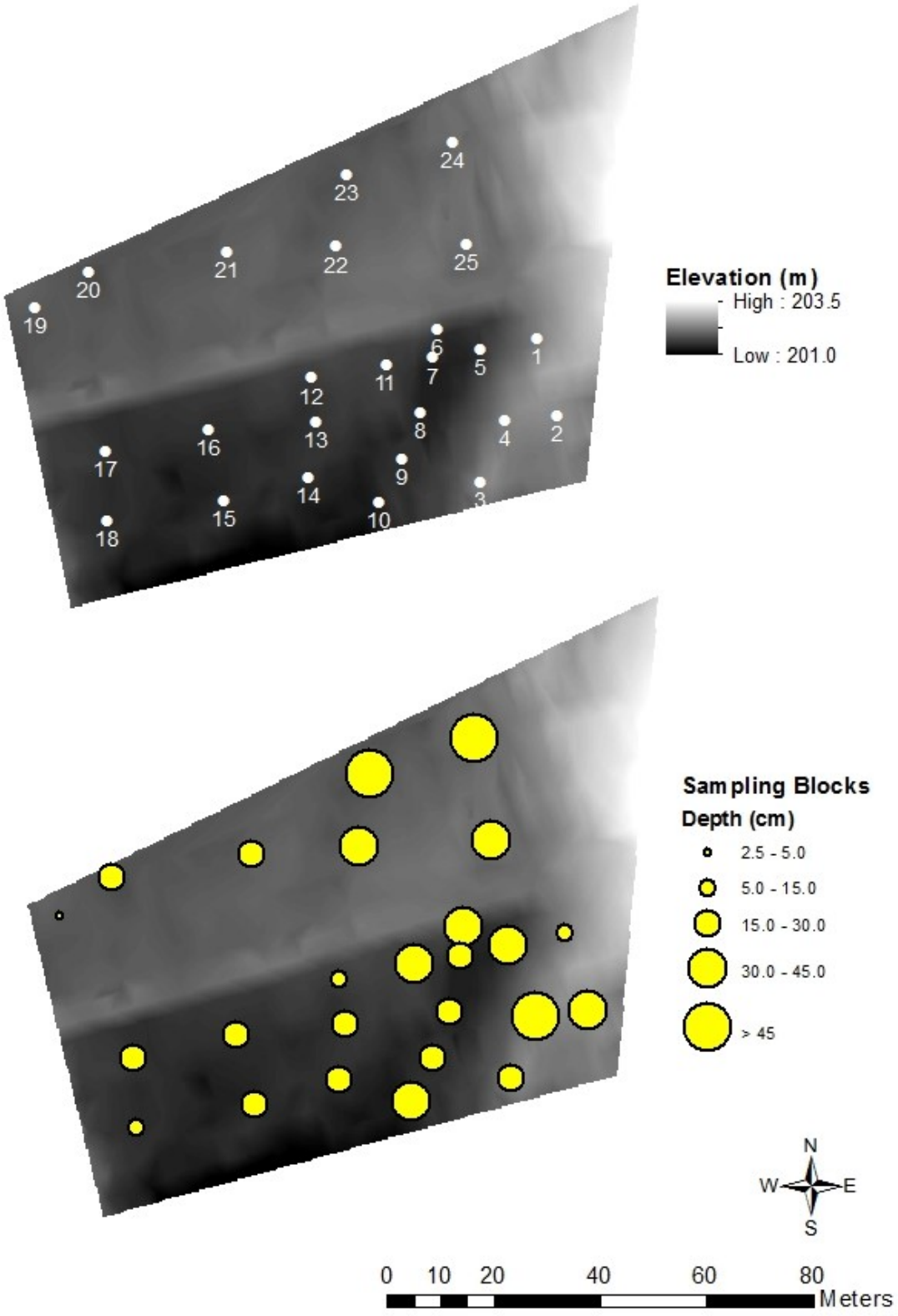

Figure 26. Location of sampling blocks (top) and average depth of sediment on sampling blocks in upper basin (bottom).

Table 8. Sampling block deposition.

Block ID	Measured Depth (cm) 8/4/15	9/17/15	12/14/15	1/21/16	7/8/16	CV (%) 8/4/15 - 7/8/16	Total Depth (cm) 8/4/15 - 7/8/16
SB1	1.00	3.12	1.68	NA	NA	56.0	5.80
SB2	10.50	0.34	0.40	20.00	2.70	124.9	33.94
SB3	4.00	5.70	0.40	0.00	12.60	112.5	22.70
SB4	20.00	40.00	NA	NA	NA	47.1	60.00
SB5	13.80	6.20	0.60	0.00	19.00	105.0	39.60
SB6	13.70	6.86	1.40	10.00	9.60	54.9	41.56
SB7	14.10	3.50	0.90	0.00	5.10	119.1	23.60
SB8	13.50	1.14	0.60	10.00	0.00	123.9	25.24
SB9	9.90	7.30	1.80	0.00	0.80	110.6	19.80
SB10	10.00	4.02	7.40	3.00	17.10	68.0	41.52
SB11	9.00	1.45	1.10	19.00	8.50	93.3	39.05
SB12	0.30	1.05	0.80	8.00	4.70	111.4	14.85
SB13	7.00	1.40	0.70	14.00	6.60	90.1	29.70
SB14	5.00	1.15	1.30	0.00	14.70	136.4	22.15
SB15	0.20	0.60	0.50	6.00	9.90	126.3	17.20
SB16	2.40	0.35	0.30	14.00	3.02	142.3	20.07
SB17	1.80	0.10	0.20	17.00	2.16	169.0	21.26
SB18	2.00	0.10	0.20	2.00	1.90	80.4	6.20
SB19	0.80	0.00	0.00	1.00	0.70	93.8	2.50
SB20	11.90	0.06	0.30	3.50	1.14	146.5	16.90
SB21	3.00	0.48	0.30	10.00	15.60	114.2	29.38
SB22	5.30	0.82	0.20	12.00	12.00	95.1	30.32
SB23	3.30	0.54	0.30	30.00	25.40	122.2	59.54
SB24	11.40	15.60	0.40	12.00	16.40	57.3	55.80
SB25	18.00	0.02	1.20	23.00	0.00	132.1	42.22
n	25	25	24	23	23	25	25
mean	7.68	4.08	0.96	9.33	8.24	105.31	28.84
Stdev.	5.86	8.28	1.46	8.49	7.22	31.58	15.73
CV%	76.3	203.2	152.4	91.0	87.6	30.0	54.6

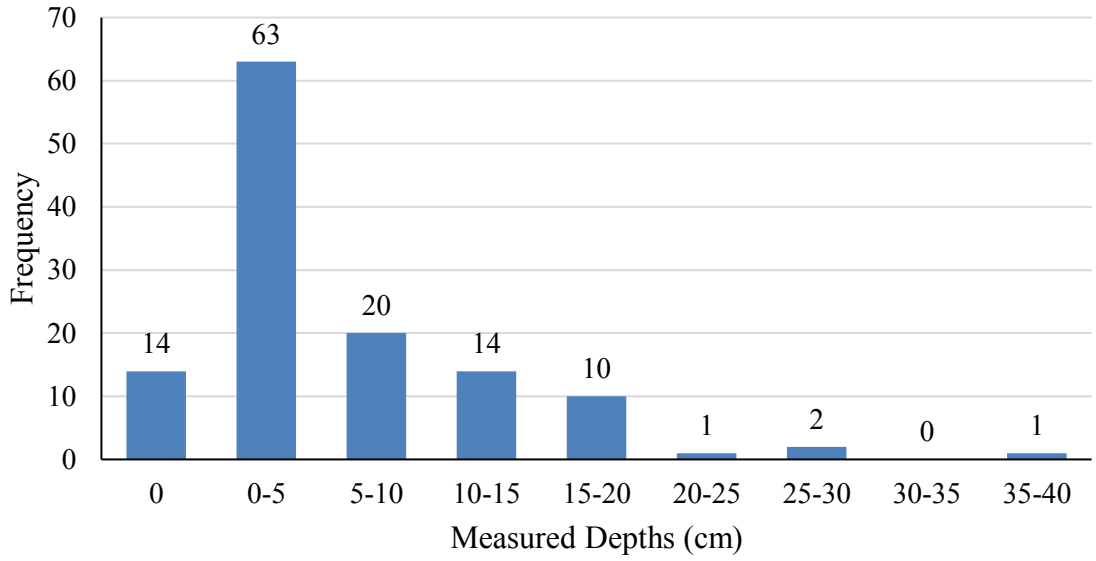

Figure 27. Frequency distribution of sampling block sediment depths.

Sediment Storage. All sampling blocks are located within an area about 6,300 m^2. The total volume of sediment trapped from average sampling block measurements from Aug, 2015 to July 2016 is approximately 1,800 m^3. The volume of sediment trapped in not evenly distributed throughout the upper basin. However, most of the sediment seems to be trapped in similar locations as shown by both sampling block measurements and repeat surveys. A majority of the sediment was deposited on sampling blocks located along the outside of the chute in areas that accumulated sand and fine-gravel splay deposits, and sampling blocks located between the road and floodway. The smallest quantities of sediment where deposited on sampling blocks located in west areas of the upper basin. So even though estimates of sediment storage are quite different between the repeat surveys and sampling block measurements, they both show similar depositional patterns.

Block averages produced a total volume of sediment storage about 2.1 times that from the repeat surveys and are from a smaller area. The main reason for the difference in sediment storage is that the sampling block measurements only yield zero or positive deposition, while the repeat surveys can have negative values. Sampling block measurements also do not take into account the significant bank erosion that has occurred. Thus, sampling blocks are likely to over predict sediment storage. Since repeat surveys do take erosion, the average sediment depths are lower than that if it did not include any erosion. They are also more likely to represent the net volume of sediment trapped since sediment is both being eroded and deposited in the upper basin. Additionally, the density of sampling points is much greater for the RTK (~500 points) compared to the sampling blocks (25). Therefore, repeat surveys have a higher resolution, particularly in areas along the margins of the upper basin with lower deposition rates.

Sediment Size and Contamination

Sediment Size. Sediment samples collected from sampling blocks were evaluated for texture. The grain size of sediment deposited varied throughout the upper basin and between flooding events. The majority (>95%) of sediment being deposited in the upper basin is <2 mm in diameter (Figure 28; Table 9). However, sand and gravel splay deposits were consistently deposited near the inlet and in a splay along the outside of the chute. Samples collected from these deposits typically contained 20 to 40 % >2 mm material with a few samples >50 % of the sediment >2 mm (Table 9). Similar deposits were also found at those locations following the largest flood event, but sand and gravel splay deposits extended north of the road.

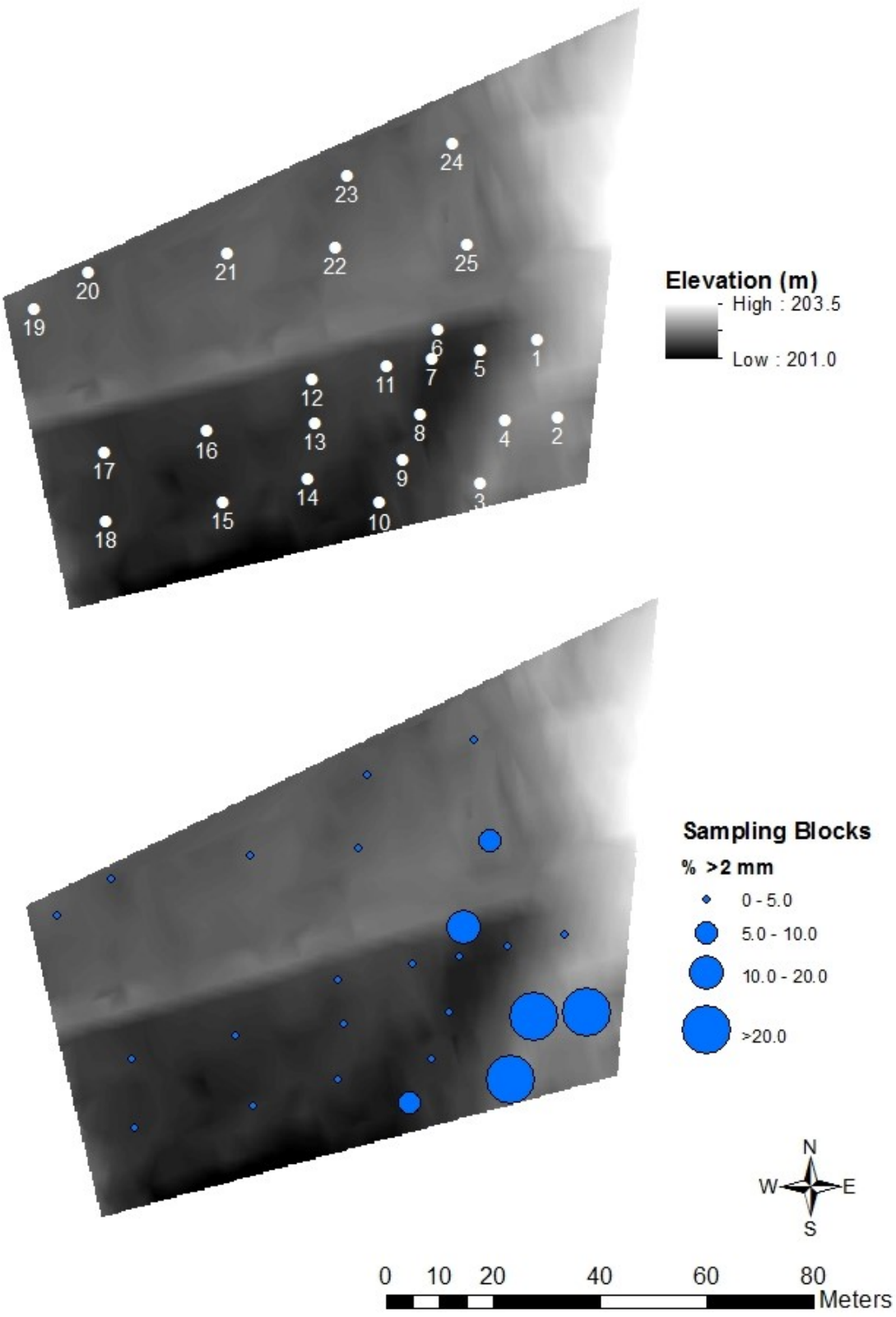

Figure 28. Location of sampling blocks (top) and average percent >2 mm on sampling blocks in upper basin (bottom).

Table 9. Grain-size data from sampling block sediment samples.

Block ID	< 2mm (%) 8/4/15	9/17/15	12/14/15	1/21/16	7/8/16	CV (%) 8/4/15 - 7/8/16	Avg. <2 mm (%) 8/4/15 - 7/8/16
SB1	95.6	100.0	99.2	NA	NA	2.4	98.27
SB2	74.9	91.9	86.7	44.2	49.0	31.3	69.35
SB3	70.1	49.6	57.7	NA	44.0	20.5	55.33
SB4	60.3	74.6	45.1	NA	NA	24.6	59.97
SB5	98.1	93.0	98.2	NA	95.9	2.6	96.30
SB6	98.4	100	80.0	51.8	100	24.3	86.02
SB7	98.8	99.6	93.9	NA	99.5	2.8	97.93
SB8	99.4	100	100	98.6	NA	0.7	99.51
SB9	98.6	99.5	99.8	NA	98.2	0.7	99.00
SB10	96.5	97.0	99.3	99.2	76.9	10.1	93.77
SB11	100	100	96.9	94.5	100	2.5	98.28
SB12	100	100	100	98.1	100	0.9	99.62
SB13	99.8	100	100	91.3	100	3.9	98.22
SB14	99.6	100	100	NA	100	0.2	99.89
SB15	100	100	100	90.5	100	4.3	98.10
SB16	99.6	100	100	99.1	100	0.4	99.74
SB17	99.7	100	100	98.9	100	0.5	99.71
SB18	98.9	100	100	93.5	99.6	2.8	98.40
SB19	98.4	NA	NA	100	100	0.9	99.46
SB20	98.3	100	100	99.8	100	0.8	99.62
SB21	99.7	100	100	100	99.7	0.2	99.88
SB22	99.0	100	100	99.6	100	0.4	99.73
SB23	99.4	100	100	98.9	100	0.5	99.65
SB24	99.5	97.3	99.2	97.8	83.6	7.0	95.46
SB25	98.2	NA	99.2	85.1	NA	8.3	94.18
n	25	23	24	18	21	25	25
mean	95.2	95.8	94.0	91.2	92.7	6.2	93.4
Stdev.	10.4	11.5	14.1	16.3	16.5	9.0	12.5
CV%	10.9	12.0	15.0	17.9	17.8	146.4	13.4

Overbank sediment deposited in west areas of the basin, away from the main flow, tended to be silt or fine sand-sized. The grain size of these deposits was fairly consistent with the percent <2 mm fraction ranging from 90 to 100%. These deposits formed in ponded water within relatively high and thick grass that resulted in lower flow velocities and transport capacities. Also, leaf litter often accumulated in west areas of the upper basin and not around the inlet and chute since flow velocities were high enough to transport leaf litter out of the upper basin. As a result, deposits in the west areas of the basin would often be underneath leaves, intermixed with leaves, or on top of leaves depending on the timing of flooding events and time of year relative to leaf fall (November - December).

Additionally, the grain size of sediment deposited in the west areas varied depending on the magnitude of flood events. Larger flood events were able to transport and deposit coarser sediment to areas further from the inlet compared to smaller flood events. The grain size of sediment deposited near the inlet and in a splay along the outside of the chute, however, rarely differed as a result of various magnitude floods. Instead, sand and gravel was consistently deposited by both small and large magnitude floods.

Distribution of Sediment. Sediment deposition in the upper basin was often a combination of both vertical/overbank deposits and lateral/channel deposits. Sediment deposits in the west areas of the basin that have slowly accumulated sediment are similar to vertical accretion deposits. On the other hand, sediment deposited around the inlet and chute was coarser and represents portions of the bed load of the river and are similar to

lateral accretion deposits. This mixture of sediment deposits has created an uneven topography across the upper basin that is re-worked during each flooding event. Overall, there was not a strong relationship between average <2 mm fraction and sampling blocks distance from the inlet (Figure 29). A majority of samples have 80-100 % <2 mm fractions regardless of sampling block distance from the inlet, aside from samples collected from sampling blocks 2, 3, and 4 that have much smaller <2 mm fractions. These blocks are located along the outside of the chute where sand and gravel splay deposits have accumulated. This relationship suggests that distances from the inlet <100 m have little effect on grain size distribution. Instead variations in grain size may be more effected by local variations in transport capacity and surrounding topography that influence flow directions and the degree to which either bed load or suspended load is delivering the sediment.

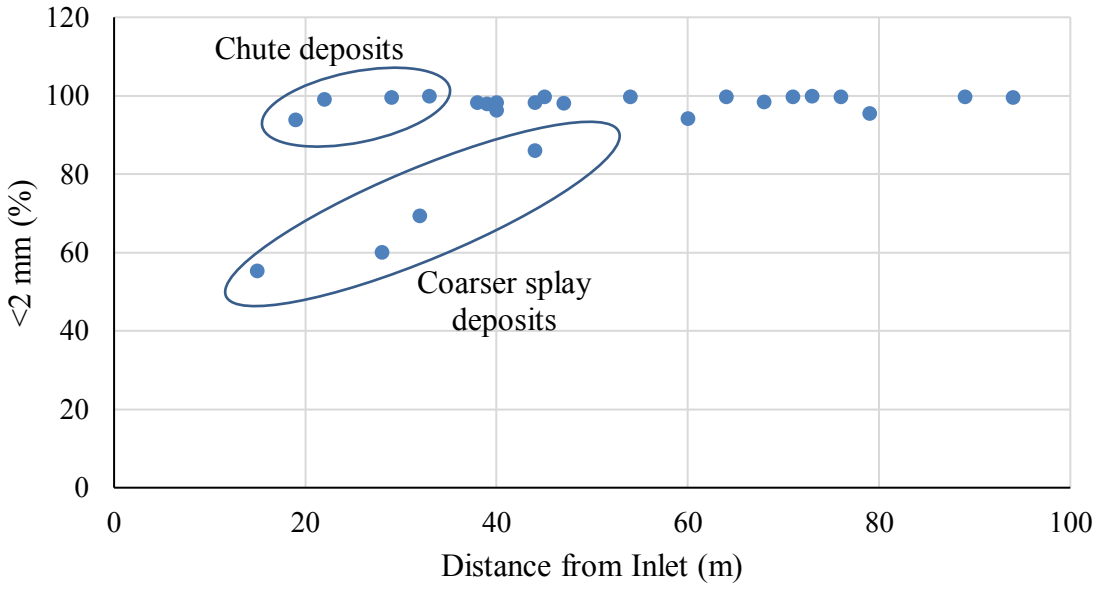

Figure 29. Relationship between distance from the inlet and percent sediment <2 mm.

Metal Concentrations in Sediment. Of the 143 individual samples collected from sampling blocks, Pb concentrations range from 479 to 2,315 ppm with an average concentration of 1,142 ppm. Concentrations of Zn range from 567 to 4,745 ppm with an average concentration of 1,223 ppm. Higher Zn concentrations suggest inputs of contaminates originated from Leadwood and Desloge tailings piles, as expected (Table 3). Concentrations of Ca ranged from 14,318 to 160,715 ppm with an average of 59,202 ppm.

The distribution of Pb concentrations is bi-modal with peaks at 900 ppm and 1,400 ppm Pb (Figure 30). Typically, the samples associated with the first peak are from samples found in splay deposits produced by bed transport, while those in the second peak were collected in the west areas of the upper basin produced by suspended sediment transport. The distribution of Zn concentrations is normal with a peak at 1,200 ppm Zn (Figure 31). The concentrations of Pb and Zn found in samples are significantly higher than the aquatic PEC for Pb (128 ppm) and Zn (459 ppm) established by MacDonald et al. (2000). Concentrations of Pb are also above the threshold limit of 400 ppm for residential soil in accordance with U.S. EPA Region 9 "Regional Screening Levels (RSL) for Chemical Contaminants at Superfund Sites" reported at http://www.epa.gov/region09/superfund/prg/index.html.

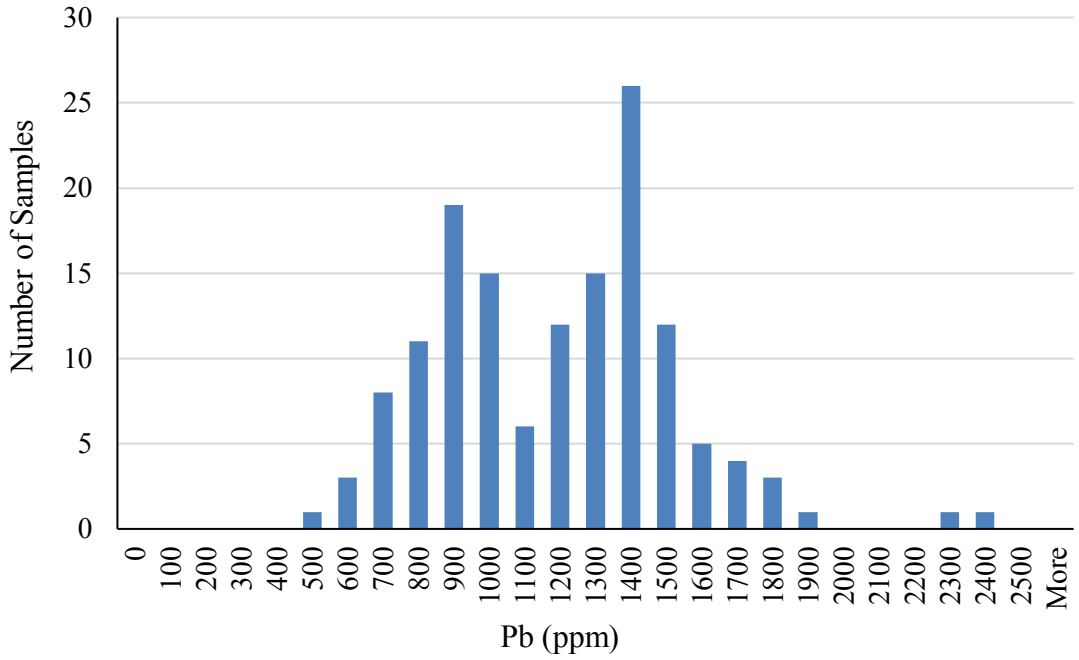

Figure 30. Distribution of Pb concentrations.

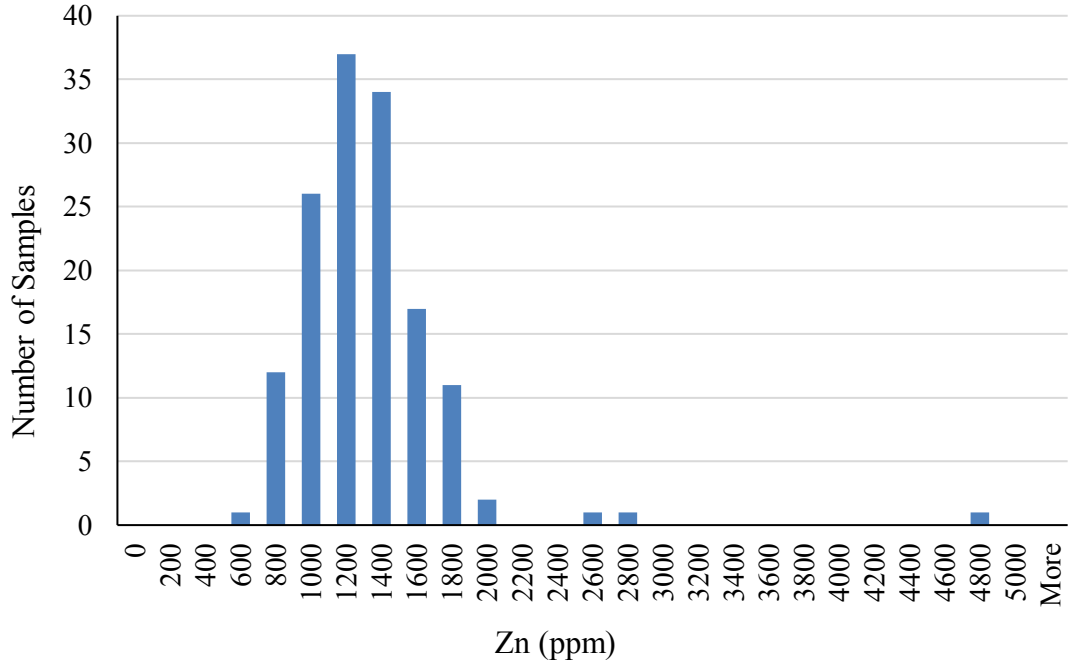

Figure 31. Distribution of Zn concentrations.

Average concentrations of Pb, Zn, and Ca, along with Pb/Zn ratios, for each sampling event are summarized in Figures 32 and 33. Average concentrations of Pb in samples collected each sampling event ranges from 913 to 1,279 ppm, while average concentrations of Zn ranges from 1,188 to 1,410 ppm (Figure 32). The coefficient of variation for Pb in samples collected each sampling event ranges from 17.0 to 36.9 % and averages 18.4% over the entire study period, indicating a relatively low variability of Pb concentrations in basin sediments. More variability was found for Zn concentrations in samples between sampling events with coefficient of variations ranging from 10.6 to 77.4%. However the average concentrations over the entire study period showed little variation (16.5%).

Similar to concentrations of Zn, Ca concentrations were the more variable between sampling events, however, Ca concentrations were more variable over the entire sampling period (Figure 33). The coefficient of variation for Ca ranges from 40.9 to 69.5% with an average of 37.7%. Ratios of Pb and Zn over the entire study period range from 1.0 to 1.3 with an average of 1.1, suggesting inputs of contaminates from Leadwood or Desloge tailings piles (Table 3; Figure 33). These concentration of Pb and Zn differ from those found in tailings stored at the National and Federal tailings piles where average Zn concentrations are lower (<450 ppm) and Pb/Zn ratios are higher (>3.0). Additionally, the Pb/Zn ratio over the entire study period suggest roughly equal inputs of Desloge and Leadwood mine tailings.

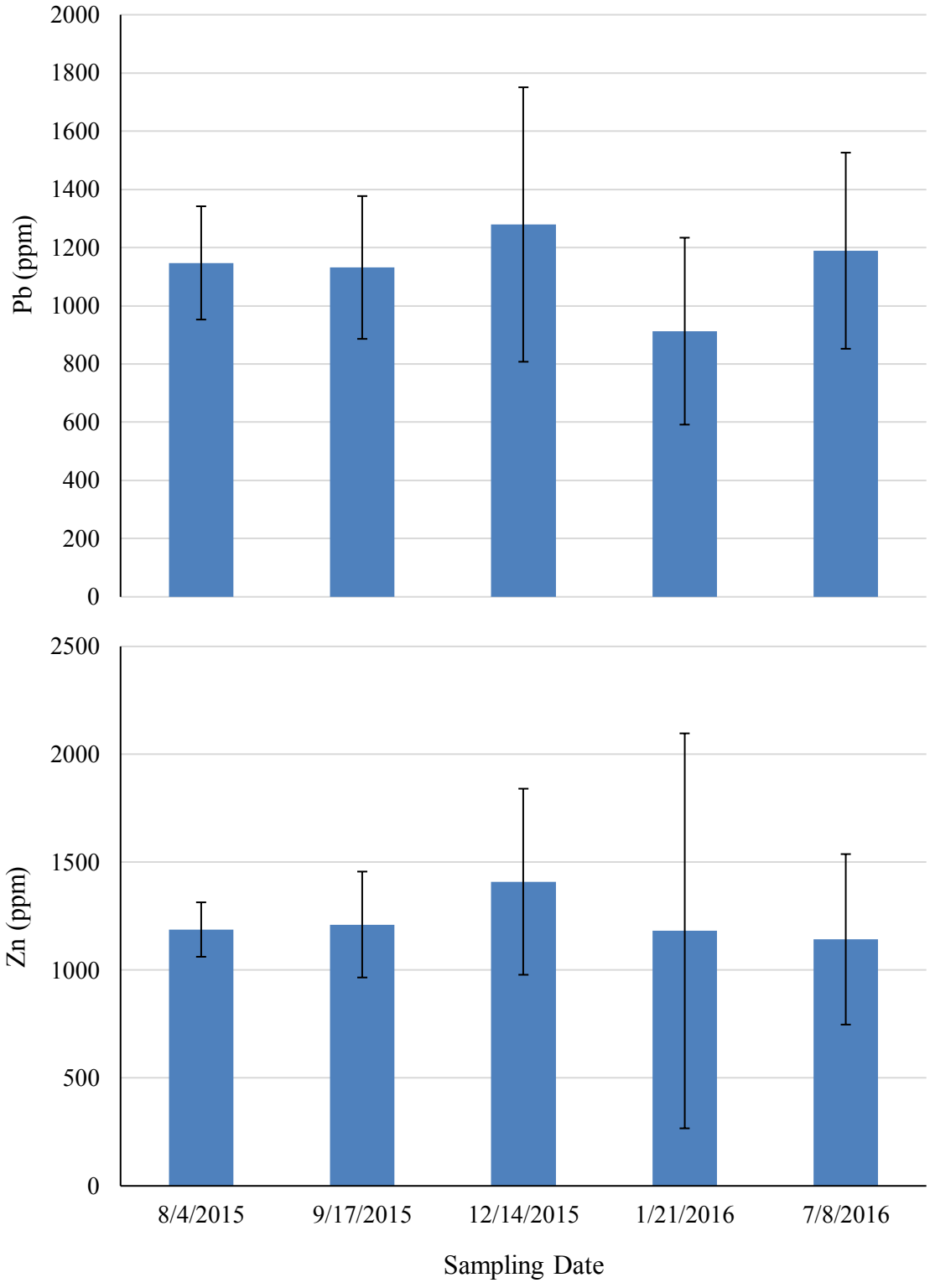

Figure 32. Average concentrations of Pb (top) and Zn (bottom) in block samples collected each sampling period with ± one standard deviation.

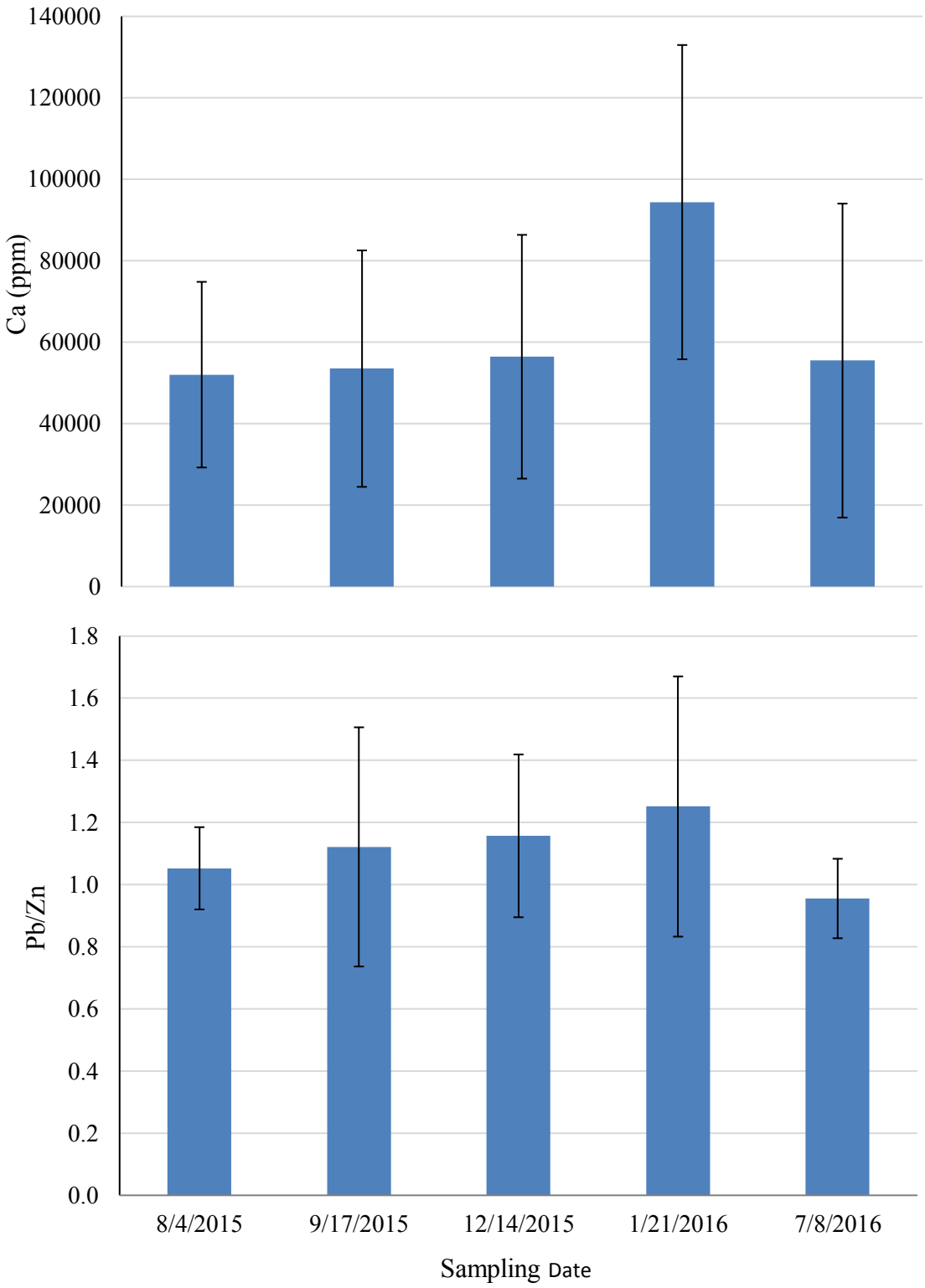

Figure 33. Average concentrations of Ca (top) and Pb/Zn ratios (bottom) of block samples collected each sampling period with ± one standard deviation.

Distribution of Contamination. Overall, sediment Pb concentrations tend to be lower near the inlet and increase with distance away from the inlet in the upper basin (Figure 34). Average Pb concentrations from individual sampling blocks over the entire study period range from 639 to 1,435 ppm with an average of 1,116 ppm (Table 10). The highest concentrations of Pb tend to be in samples collected from sampling blocks 11-18 and 21-23 that have average concentrations greater than 1,200 ppm.

Concentrations of Zn tend to follow similar trends as Pb concentrations with the greatest concentrations being from the same samples, although the overall pattern appears more random (Figure 35). Average Zn concentrations from individual blocks over the entire study period range from 905 to 1,818 ppm with an average of 1,231 (Table 11). Variations of average Pb and Zn over the entire study period are small with coefficients of variation of 18.4% and 16.5% respectively. This suggests that the river sediment load entering the basin system contains relatively consistent levels of Pb and Zn and that both mining and natural sediment supplies are well mixed.

To determine the mass of Pb and Zn stored in deposited sediment and at what rates, metal storage and mass deposition rates of sediment <2 mm were estimated from individual sampling block samples that had minimal amounts of sediment >2 mm (<5%). The mass of Pb stored on individual blocks ranges from 0.27 to 8.59 g. The mass of Zn stored on individual blocks ranges from 0.30 to 9.20 g. The mass deposition rates of Pb and Zn associated with the mass of metal stored ranges from 0.003 to 0.089 g/cm^2/yr for Pb and from 0.003 to 0.95 g/cm^2/yr for Zn. The mass of Pb and Zn stored in those deposits does not represent the total mass of Pb and Zn stored throughout the upper basin

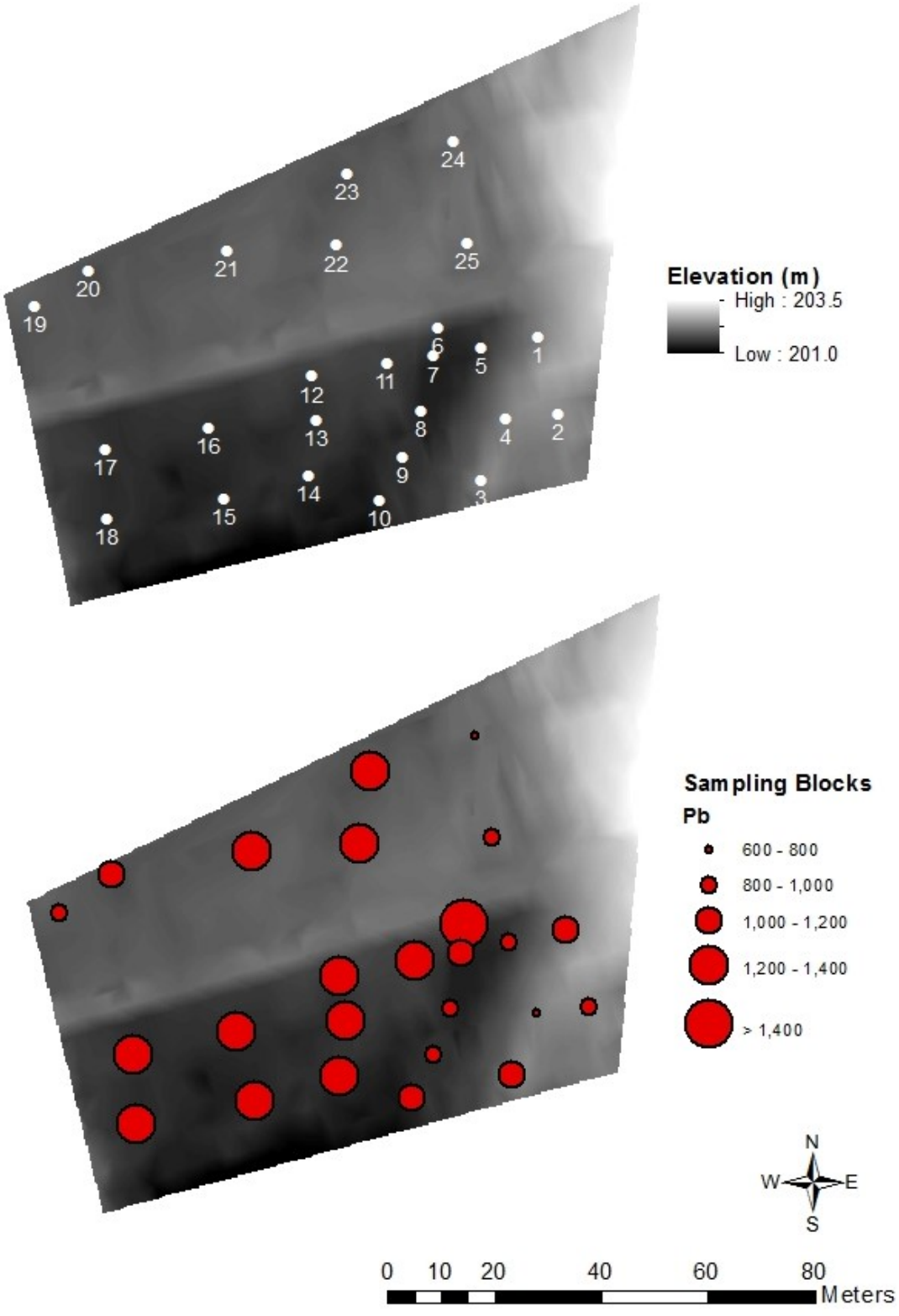

Figure 34. Location of sampling blocks (top) and average Pb concentration of sampling block deposits in the upper basin (bottom).

Table 10. Sampling block Pb concentrations.

Block ID	XRF Pb (ppm) 8/4/15	9/17/15	12/14/15	1/21/16	7/8/16	CV (%) 8/4/15 - 7/8/16	Avg. Pb (ppm) 8/4/15 - 7/8/16
SB1	1134	677	905	NA	NA	25.2	1033
SB2	1050	1167	821	1415	887	22.2	981
SB3	1416	896	819	NA	942.5	26.5	1018
SB4	678	725	514	NA	NA	17.3	639
SB5	1159	931	914	NA	676	21.4	920
SB6	1030	1306	1732	829	2276	40.4	1435
SB7	1129	1054	1183	NA	1374.5	11.6	1185
SB8	1019	808	1168	479	NA	34.4	869
SB9	1107	964	630	NA	739	25.1	860
SB10	1089	853	732	1865	1246	38.3	1157
SB11	1064	1390	1747	1023	1243	22.7	1293
SB12	1342	1352	1629	537	1343	33.2	1241
SB13	1087	1316	2315	759	1417	42.2	1379
SB14	1174	1331	1782	NA	1148	21.6	1261
SB15	1420	1290	1652	870	1403	21.7	1282
SB16	1194	1239	1682	645	1252	30.7	1236
SB17	1318	1247	1621	1051	1087	18.0	1265
SB18	1484	1354	1369	991	1265	14.4	1293
SB19	928	NA	NA	797	1100	16.1	942
SB20	922	1254	1357	999	1093	15.9	1125
SB21	1346	1283	1499	929	1394	16.8	1290
SB22	1232	1430	1532	654	1228	28.0	1215
SB23	1382	1387	1573	883	1146	20.9	1274
SB24	1151	774	600	736	715	26.3	795
SB25	828	NA	925	970	NA	8.0	908
n	25	23	24	18	21	25	25
mean	1147	1132	1279	913	1189	24.0	1116
Stdev.	195	245	471	321	337	8.8	205
CV%	17.0	21.7	36.9	35.2	28.3	36.8	18.4

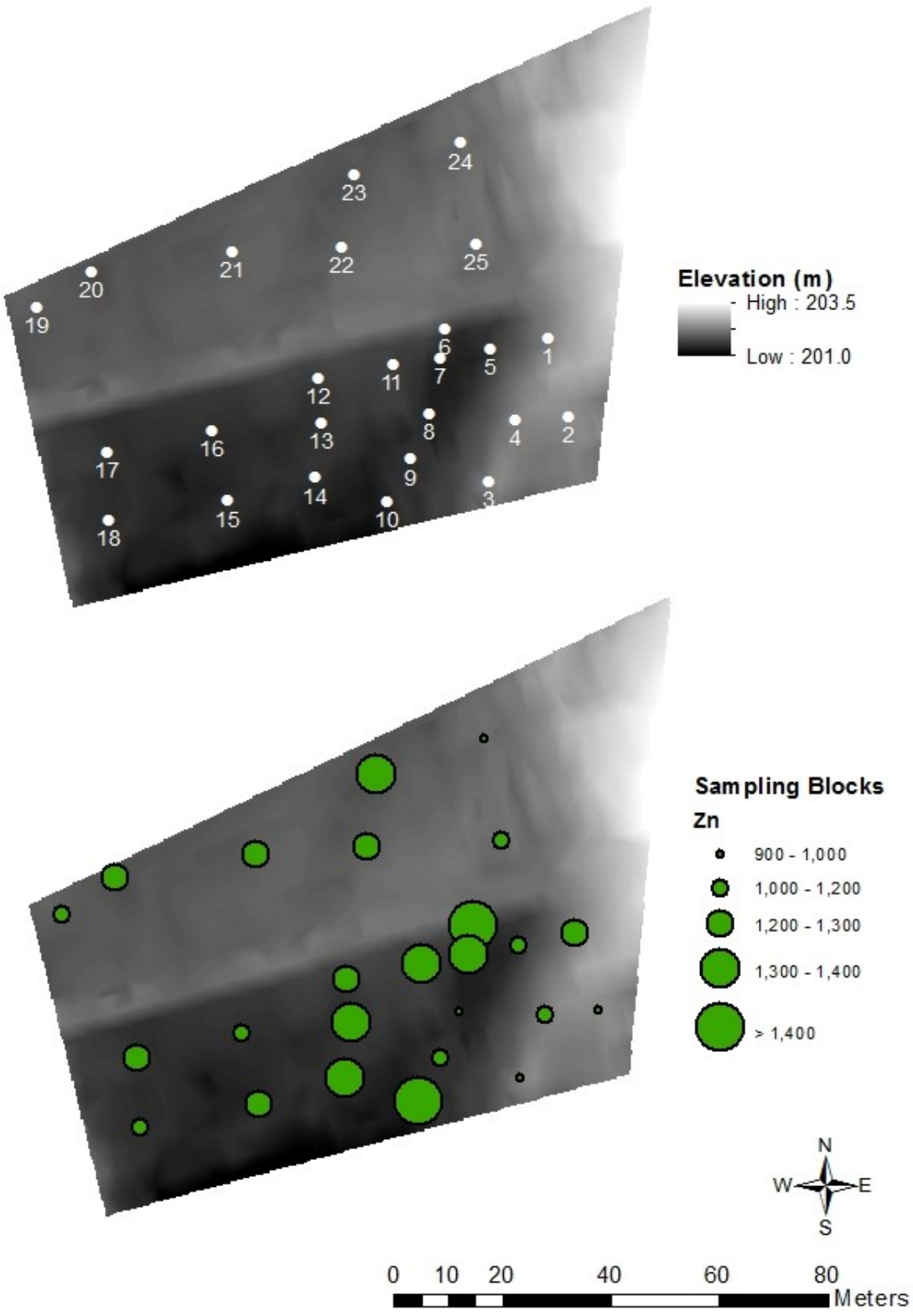

Figure 35. Location of sampling blocks (top) and average Zn concentration of sampling block deposits in the upper basin (bottom).

Table 11. Sampling block Zn concentrations.

Block ID	XRF Zn (ppm) 8/4/15	9/17/15	12/14/15	1/21/16	7/8/16	CV (%) 8/4/15 – 7/8/16	Avg. Zn (ppm) 8/4/15 - 7/8/16
SB1	1150	707	1798	NA	NA	45.0	1218
SB2	1105	1242	778	927	815	20.2	973
SB3	1220	806	1079	NA	752	23.1	964
SB4	854	1815	773	NA	NA	50.5	1147
SB5	1255	1190	1303	NA	890	16.0	1160
SB6	1143	1439	1855	1043	2466	36.7	1589
SB7	1123	1175	1726	NA	1449	20.3	1368
SB8	1072	955	1249	633	NA	26.5	977
SB9	1082	1705	930	NA	567	44.3	1071
SB10	1233	1255	929	4745	928	90.4	1818
SB11	1172	1319	1697	1258	1241	15.5	1337
SB12	1233	1304	1537	801	1208	21.9	1217
SB13	1089	1133	2605	645	1342	54.3	1363
SB14	1242	1213	1730	NA	1248	18.3	1358
SB15	1304	1162	1624	765	1393	25.5	1250
SB16	1109	1111	1668	906	1183	23.7	1195
SB17	1257	1091	1623	1094	944	21.7	1202
SB18	1440	1177	1200	868	1155	17.4	1168
SB19	1153	NA	NA	1066	935	10.4	1051
SB20	1316	1101	1494	1145	965	17.0	1204
SB21	1225	1110	1473	1043	1448	15.4	1260
SB22	1228	1518	1402	987	1279	15.6	1283
SB23	1472	1182	1539	1516	1115	14.7	1365
SB24	1176	1148	747	779	675	26.3	905
SB25	1050	NA	1071	1053	NA	1.1	1058
n	25	23	24	18	21	25	25
mean	1188	1211	1410	1182	1143	26.9	1220
Stdev.	126	245	431	915	395	18.4	201
CV%	10.6	20.3	30.6	77.4	34.6	68.3	16.5

since Pb and Zn is also stored in sediment >2 mm. However, it does help obtain a general idea of the rate at which Pb and Zn is being stored.

Grain Size-Metal Relationship. To check for the possibility that mining chat tailings might contain significant levels of Pb and Zn, the 2-16 mm fraction for selected samples was evaluated. The 2-16 mm fraction of 12 samples were analyzed for Pb and Zn. Of the 12 samples, Pb concentrations ranged from 606 to 3,072 ppm with an average of 1,714 ppm. Only two of those samples had a lower concentrations of Pb in the 2-16 mm fraction compared to the <2 mm fraction (Table 12 and 13; Figure 36). Additionally, the Pb concentration in the 2-16 mm sediment from the sample containing the lowest <2 mm fraction (40%) had the highest concentration (3,072 ppm Pb) among all samples (n = 165). Concentrations of Zn range from 634 to 1,752 ppm with an average of 1,042 ppm. Concentrations of Zn in 2-16 mm fraction did not consistently have higher Zn concentrations in <2 mm fraction, such as the case with Pb concentrations. However, there were still only 4 samples with lower Zn concentrations in the 2-16 mm fraction compared to the <2 mm fraction (Figure 36).

These findings indicate that in coarse deposits, the 2-16 mm fraction can provide significant storage of Pb and Zn. Samples with significant (>10%) coarse sediment (2-16 mm) were used to compare differences in Pb and Zn storage between fine (<2 mm) and coarse sediment (Table 12 and 13). Coarse sediment deposited in the upper basin can account for 29 to 87% of Pb stored and 26 to 72% of Zn stored in lateral accretion and splay deposits. Overall, these differences show that coarse sediment can account for large percentages of Pb and Zn storage and indicate the importance of coarse grained sediment as a source of Pb and Zn contamination in the Big River.

Table 12. Storage of Pb in sediment 2-16 mm and <2 mm.

Block	ID (BR JV)	Date	2-16 mm (%)	<2 mm (%)	Pb (ppm) 2-16 mm	Pb (ppm) <2 mm	Pb 2-16 : <2	Total Pb Storage (g)	Pb 2-16 mm (%)	Pb <2 mm (%)
2	92	1/21/2016	55.75	44.24	1,251	1,415	0.88	3.8	62.6	37.4
3	114	7/8/2016	59.22	40.78	3,072	964	3.19	4.5	87.4	12.6
4	6	8/4/2015	39.71	60.29	999	678	1.47	2.3	59.3	40.7
6	93	1/21/2016	48.24	51.76	2,719	829	3.28	2.7	82.1	17.9
10	121	7/8/2016	23.09	76.91	1,563	1,243	1.26	2.9	36.2	63.8
24	143	7/8/2016	16.45	83.55	1,847	715	2.58	2.0	43.3	56.7
25	111	1/21/2016	14.88	85.12	1,480	970	1.53	3.0	28.6	71.4

Table 13. Storage of Zn in sediment 2-16 mm and <2 mm.

Block	ID (BR JV)	Date	2-16 mm (%)	<2 mm (%)	Zn (ppm) 2-16 mm	Zn (ppm) <2 mm	Zn 2-16 : <2	Total Zn Storage (g)	Zn 2-16 mm (%)	Zn <2 mm (%)
2	92	1/21/2016	55.75	44.24	744	927	0.80	2.3	60.3	39.7
3	114	7/8/2016	59.22	40.78	924	777	1.19	1.6	72.1	27.9
4	6	8/4/2015	39.71	60.29	1,177	854	1.38	2.8	57.7	42.3
6	93	1/21/2016	48.24	51.76	947	1,043	0.91	1.4	55.9	44.1
10	121	7/8/2016	23.09	76.91	976	1,241	0.79	2.5	26.2	73.8
24	143	7/8/2016	16.45	83.55	1,122	675	1.66	1.6	32.9	67.1
25	111	1/21/2016	14.88	85.12	1,752	1,053	1.66	3.4	30.4	69.6

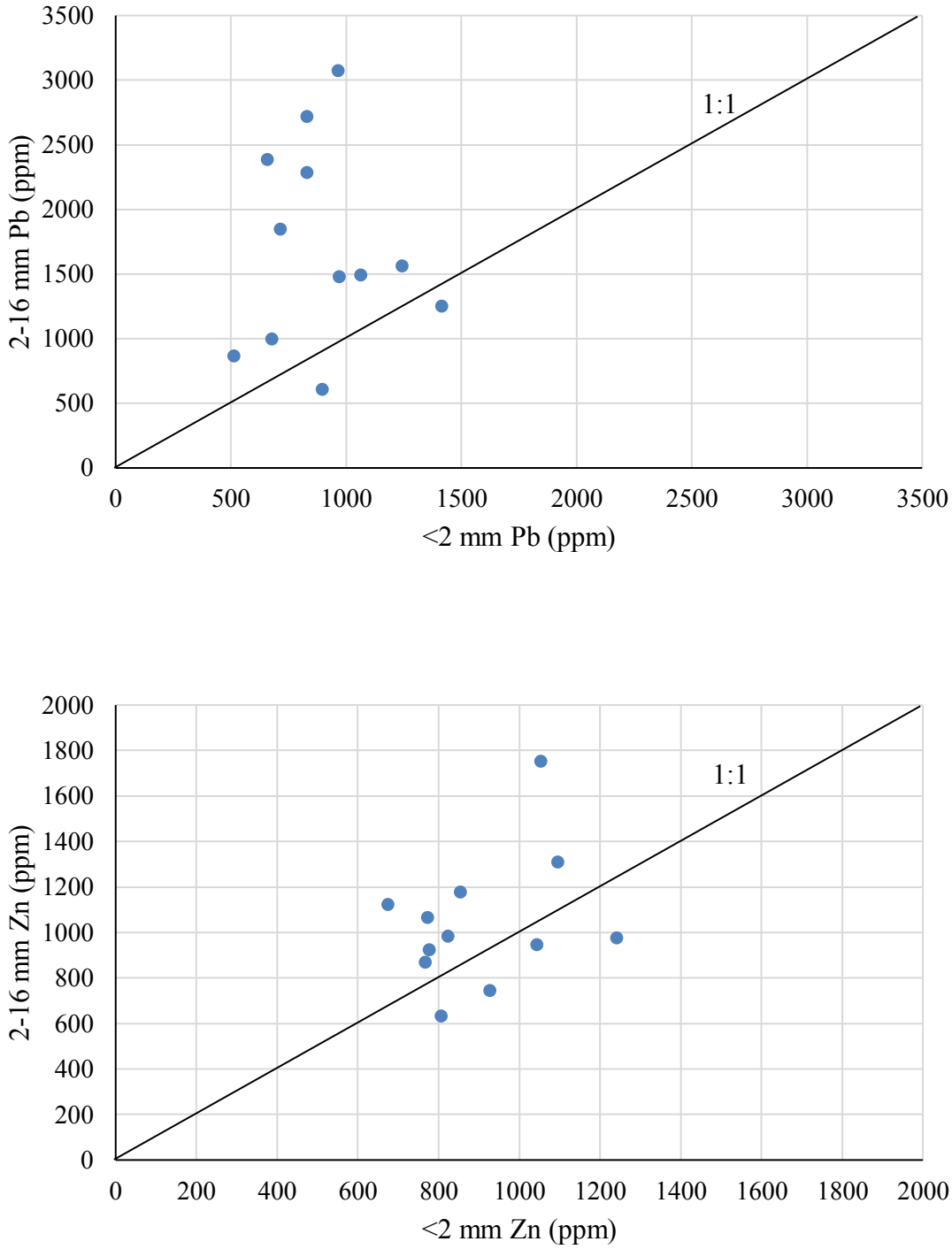

Figure 36. Relationship between concentrations of Pb (top) and Zn (bottom) in sediment 2-16 mm and <2 mm.

Flood Influence on Sediment Deposition

Flood events exert a dominant control over sediment deposition on floodplains (Benedetti, 2003; Nardi et al., 2006; Wohl, 2014). The action of flowing water during flooding events mediates geomorphic processes the transfer sediment and develop floodplains (Curtis et al., 2013; Hupp et al., 2015). In the past it was generally believed that rare extreme flood events were the most important in depositing sediment to develop landforms, such as floodplains (Asselman and Middelkoop, 1998). However, Wolman and Miller (1960) stated a more accurate sense of the overall effectiveness of geomorphic processes should not only include rare extreme flood events, but also events of moderate magnitudes that occur more frequently.

Flood Magnitude. The peak gage height of the largest flood event between each sampling period was compared to the average depth of sediment deposited on sampling blocks. There was a moderately strong relationship between the two with more sediment deposited after larger magnitude floods (Figure 37). The largest magnitude flood had the highest average sediment depth and the smallest magnitude flood had the lowest average sediment depth. A stronger relationship is found between the cumulative peak gage height of flood events between sampling periods and the average depth of sediment deposited on sampling blocks (Figure 38). The cumulative peak gage height helps account for smaller magnitude floods that may have occurred between sampling events with multiple flood events. Differences in average sediment depth between similar magnitude floods may influenced by the frequency or duration of floods between sampling periods.

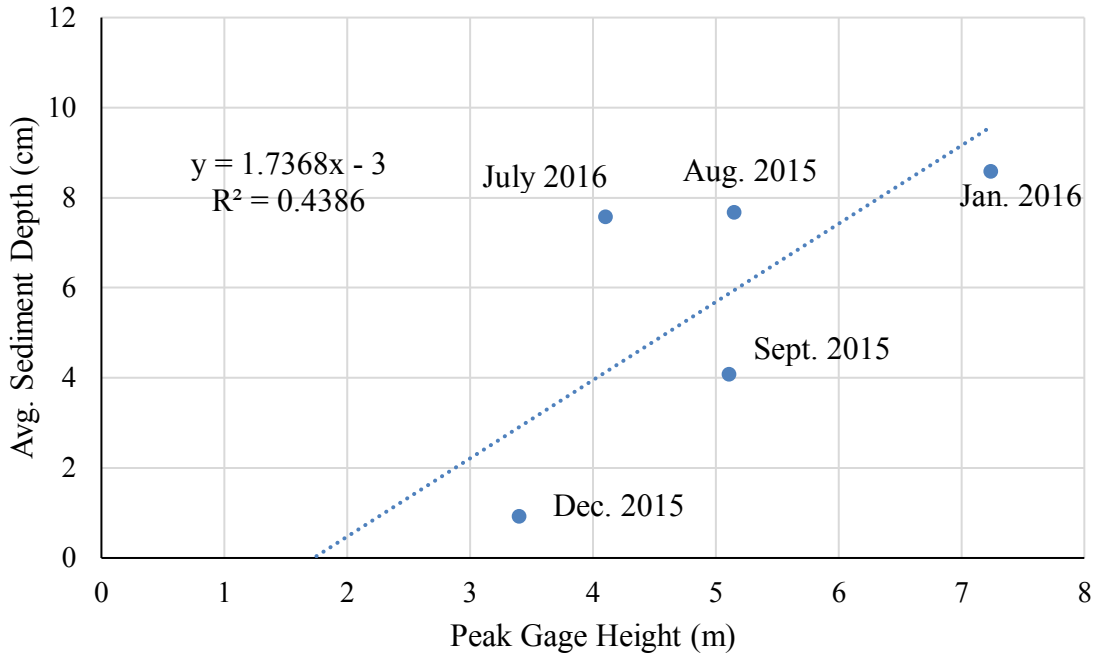

Figure 37. Relationship between peak gage height and average sediment depth.

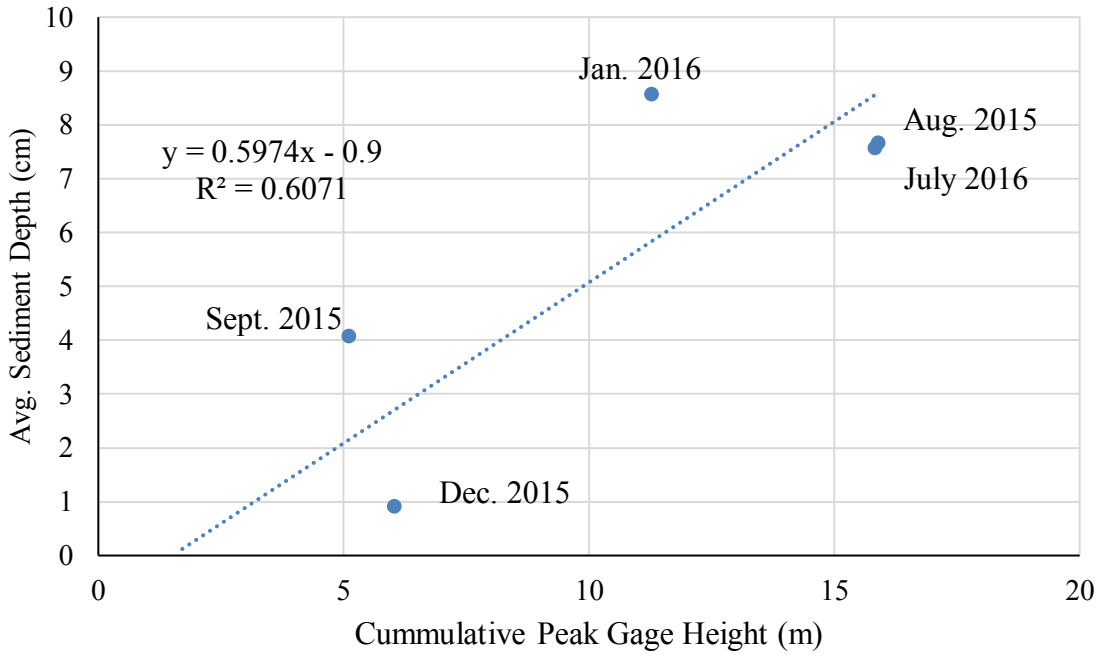

Figure 38. Relationship between cumulative peak gage height and average sediment depth.

Flood Frequency. The frequency of flooding events controls the number of opportunities for sediment to be deposited in the basin system. Although, the relationship between the number of floods and average sediment depth for each sampling period is not significant, more floods generally deposited more sediment (Figure 39). The differences in sediment depths for sampling periods with the same number of floods can be explained by the magnitude of the flooding events. The December 2015 sampling event had the same number of floods as the January 2016 sampling event, however, the peak gage height for the January 2016 event was double that of the two floods for the December 2015 event. This suggests that flood magnitude has a stronger influence on sediment deposition and that flood frequency has little effect, if any, on sediment deposition.

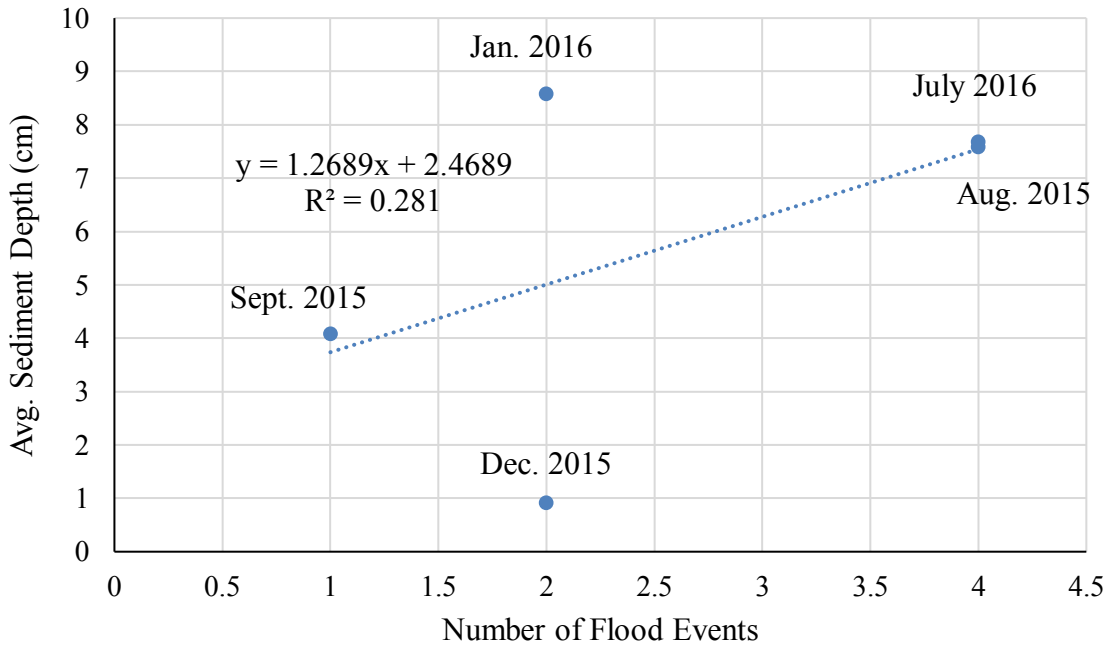

Figure 39. Relationship between number of flood events and average sediment depth.

Flood Period Duration. The duration of flooding events had the strongest influence on average sediment depths (Figure 40). Generally, more sediment was deposited on sampling blocks the longer the basin was inundated. The biggest difference in average sediment depths for sampling events that had similar inundation lengths could be due to the magnitude of flooding events. The flooding events that deposited sediment measured during the December 2015 sampling event had a lower peak gage height compared to the flooding events that deposited sediment for the September 2015 sampling event (Figure 37). This is further supported by the flood record over the study period that suggests that inundation times are strongly related to cumulative peak gage heights (Figure 41).

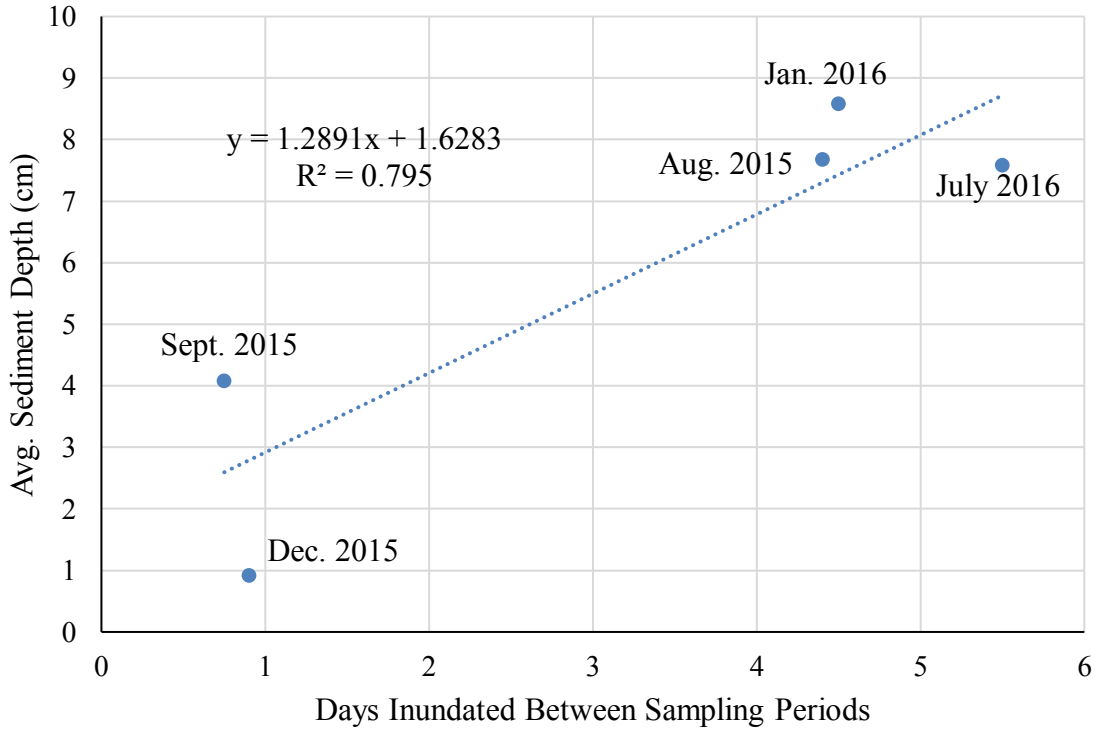

Figure 40. Relationship between days basin was inundated and average sediment depth.

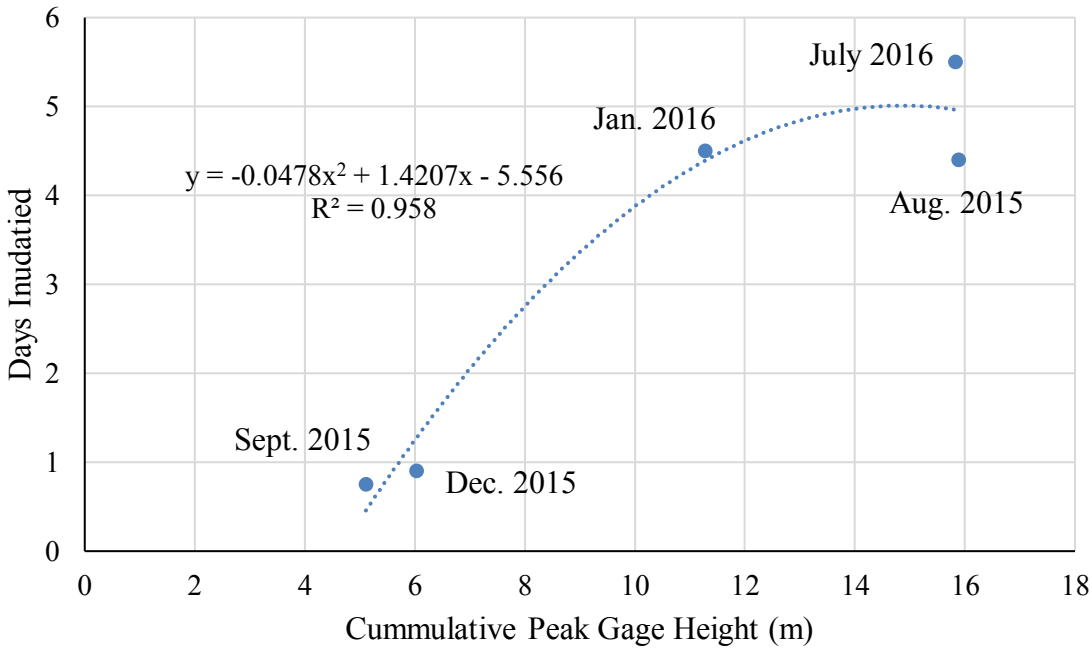

Figure 41. Relationship between cumulative peak gage stage at Desloge and days the basin was inundated.

Flood and Sedimentation Factors. Historical mining in the Old Lead Belt has allowed large quantities of heavy metal-rich sediment to enter local streams through erosion, runoff, and retention pond and dam failure. Fluvial processes have since reworked contaminated sediment and distributed it downstream (Meneau, 1997). Presently, there are still large quantities of contaminated sediment stored in channel and bar deposits that provide a potential source of contamination to downstream segments (Owen et al., 2012). There is also large quantities of contaminated sediment stored in floodplains (Pavlowsky et al., 2010).

Modifications to the floodplain and bank during construction of the basin system has affected the influence of flood events on sediment deposition. Lowering the elevation of banks in order to create an inlet to the upper basin has increased connectivity with the channel that allowed sediment from the bed load and suspended load to be transported

into the upper basin. Lowering and grading of the floodplain created areas in the upper basin and lower basin where water tended to pond and allow suspended sediment to settle out. It also created a sand and fine-gravel splay deposition area in the upper basin near the inlet and chute. Erosion of the bank and expansion of the inlet have contributed an additional supply of sediment to the upper basin. Together these modifications have increased sediment supply to the basin system, thus increasing sediment deposition.

Differences in sediment deposition throughout the upper basin can be contributed to one or more of the following factors: flood magnitude, frequency, or duration (Benedetti, 2003; Baborowski et al., 2007; Curtis et al., 2013). Generally, an increase in any of those factors could increase deposition rates (Asselman and Middelkoop, 1998; Lecce and Pavlowsky, 2001; Curtis et al., 2013). Flood and sedimentation data suggest that cumulative peak gage height (flood magnitude) and flood durations have the strongest influence on sediment deposition, while flood frequency has little to no influence on sediment deposition. However, fluctuations in flood factors and complex topography may contribute irregular rates and patterns of sediment deposition (Lecce and Pavlowsky, 2004; Dennis et al, 2009; Sear et al., 2010). Also, the small sample size that spans a relatively short period makes it difficult to determine the exact influence of those factors on sediment deposition in the basin system. A better relationship could be determined with a larger number of sampling events.

Even though it is a small sample size, mangers could use the relationship between cumulative peak gage heights and duration of inundation of the basin system to roughly estimate the volume of sediment available for dredging. This was relationship was used to estimate the volume of sediment deposited during flooding events over the study

period (Table 14). The cumulative peak gage height between sampling events was used to estimate the duration the basin was inundated, which then used the linear regression from Figure 40 to estimate the average sediment depth. That average depth was multiplied by the surface area of the sampling block boundary to produce an estimated volume of sediment trapped. Overall, this produced an estimated 1,815 m^3 of sediment trapped in the upper basin over the entire study period, which is almost identical the volume estimated from direct sampling block measurements.

Table 14. Estimated sediment storage during the study period using flood characteristics.

Sampling Event	Cumulative Peak Gage Height (m)	Estimated Days Inundated	Estimated Avg. Sediment Depth (cm)	Estimated Sediment Storage (m^3)
Aug. 2015	15.89	4.9	8.0	505
Sept. 2015	5.11	0.5	2.2	140
Dec. 2015	6.03	1.3	3.3	206
Jan. 2016	11.28	4.4	7.3	459
July. 2016	15.83	5.0	8.0	505

Longitudinal Basin Trends

Sediment Depth. Sediment depths recorded through the entire sediment basin system represent deposition from construction (April 2015) to November 21, 2016. Sediment depths range from 1 to 56 cm with an average depth of 27 cm (Figure 42; Table 15). Generally, larger sediment depths were recorded closer to the inlet and decreased with distance from the inlet, although the relationship is not strong (Figure 43). This decrease typically occurs due to decreases in transport capacity and sediment supply as flow velocities decrease with increasing distance from the inlet. However, several samples collected in the flood way and lower basin had sediment depths over 30 cm. Variations in sediment depths is large with a CV of 61.7% and may be affected by non-random sampling and variations in post-construction topography, such as depressions or ruts that may have filled in locally.

Sediment Size. The majority (>95%) of sediment deposited throughout the flood way and lower basin is <2 mm in diameter (Table 15). Variations of <2 mm in these samples is small with a CV of 14.4%. Generally, the percent of sediment >2 mm decreases with increasing distance from the inlet (Figure 43). Samples with sediment larger than 2 mm in lower basin may be due to scouring and incision of the flood way introducing coarse grained material or may have been inherited as a result of construction of the basin system. This would help explain why some samples located farther from the inlet contain more coarse material (2-16 mm) than others at similar locations.

Figure 42. Depth of sediment throughout the entire basin system since construction.

Table 15. Sediment data of samples collected throughout the basin system.

ID	Depth (cm)	>2 mm (%)	<2 mm (%)	Pb (ppm)	Zn (ppm)	Pb/Zn ratio
V1	30	41.8	58.2	880	1,511	0.6
V2	23	0.0	100	1,513	1,517	1.0
V3	40	0.0	100	1,488	1,468	1.0
V4	44	13.0	87.0	831	990	0.8
V5	22	16.9	83.1	830	823	1.0
V6	51	46.8	53.2	1,265	765	1.7
V7	56	10.6	89.4	1,063	1,095	1.0
V8	33	12.9	87.1	840	875	1.0
V9	40	0	100	1,618	1,343	1.2
V10	25	7.0	93.0	971	1,165	0.8
V11	28	5.7	94.3	657	612	1.1
V12	5	0	100	1,739	1,792	1.0
V13	47	6.1	93.9	758	871	0.9
V14	5	2.6	97.4	1,586	1,549	1.0
V15	4	20.6	79.4	1,308	1,238	1.1
V16	40	0.7	99.3	1,130	1,260	0.9
V17	32	0.2	99.8	532	610	0.9
V18	1	0	100	1,507	1,225	1.2
V19	15	0	100	888	916	1.0
V20	10	0	100	1,626	1,333	1.2
V21	7	0	100	1,611	1,255	1.3
V22	35	3.3	96.7	1,135	654	1.7
n	22	22	22	22	22	22
mean	27	8.6	91.4	1172	1130.3	1.1
Stdev.	17	13.1	13.1	369	335	0.3
CV%	61.7	153.6	14.4	31.5	29.6	24.5

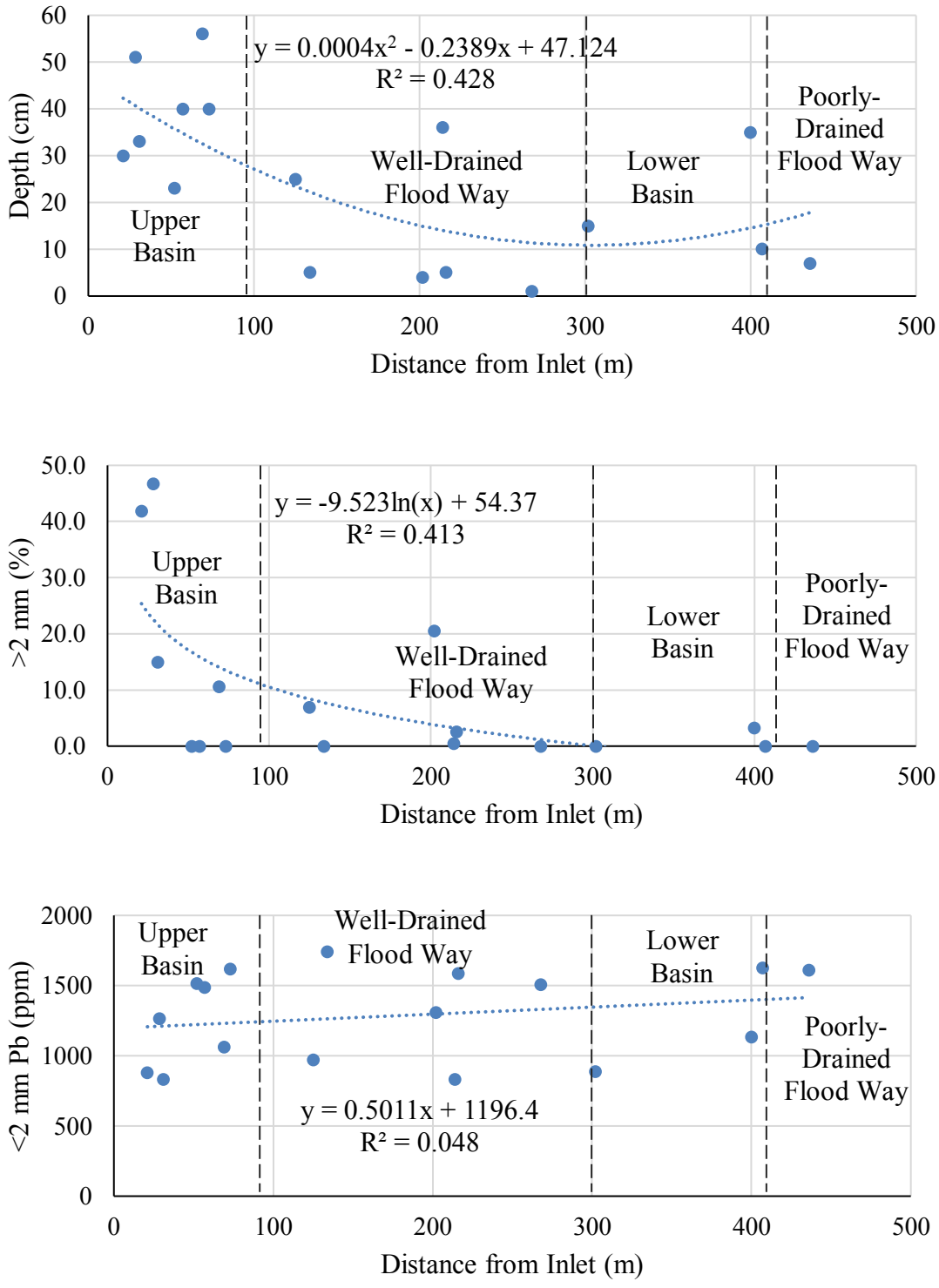

Figure 43. Relationship between inlet distance and depth (top), texture (middle), and Pb concentrations (bottom).

Sediment samples collected in the upper basin vary from 53% to 100% <2 mm. This variation in the upper basin is similar to sampling block trends with coarser material being deposited near the inlet and along the outside of the chute as sand and gravel splay deposits. This pattern of grain size distribution suggest that flows through the basin system usually have enough energy to transport and deposit coarse grained material in the upper basin, but not throughout the rest of basin system. This could be due to decreases in transport capacity and sediment supply as distance from the inlet increases and differences in inundation frequencies for different areas of the basin system.

Contamination. Of the 22 samples collected from the upper to lower basin, Pb concentrations range from 532 ppm to 1,739 ppm with an average concentration of 1,172 ppm (Table 15). Concentrations of Zn ranged from 610 ppm to 1,792 ppm with an average of 1,130 ppm. High concentration of Pb (>1,500 ppm) and Zn (>1,200 ppm) are found throughout the entire basin system (Figures 43, 44 and 45). Huggins (2016) also found similar concentrations of Pb and Zn in floodplain soils at the site (pre-construction) with an average Pb concentration of 1,257 ppm and average Zn concentration of 1,118 ppm. The ratio of Pb and Zn ranges from 0.6 to 1.7 with an average ratio of 1.1, suggesting inputs of mining waste from the Leadwood and Desloge tailings piles and possible Elvins tailings pile (Table 3). Overall, concentration of Pb and Zn and Pb/Zn ratios are comparable to the concentrations of sampling block samples and suggest that highly contaminated sediment is deposited throughout the entire basin system.

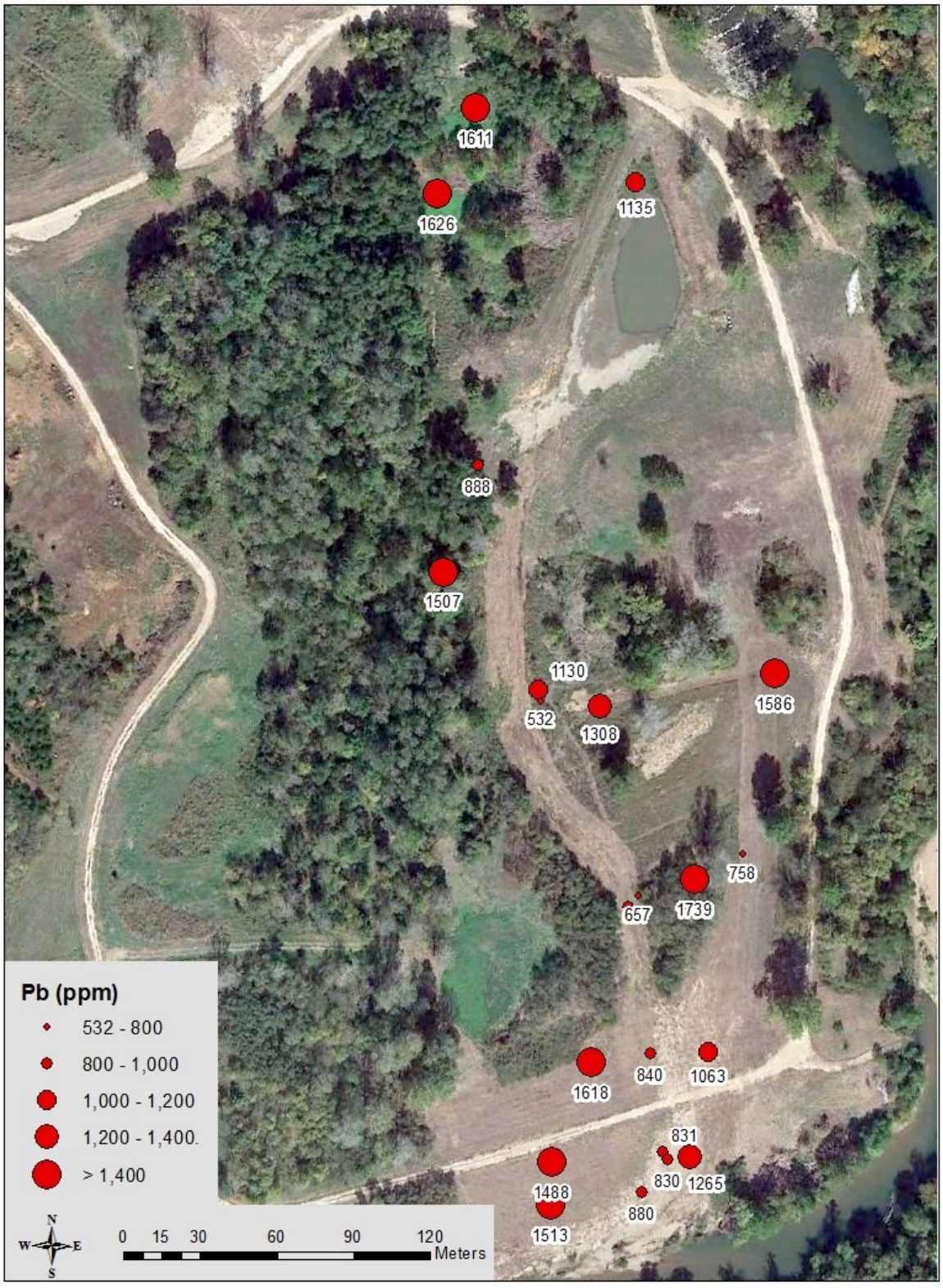

Figure 44. Concentrations of Pb in samples collected throughout the basin system.

Figure 45. Concentrations of Zn in samples collected throughout the basin system.

Storage. Together, the upper basin, well-drained flood way, lower basin, and poorly-drained flood way cover an area of approximately 22,000 m^2 (Figure 46; Table 16). The volume of contaminated sediment stored in the upper basin (865 m^3) has already been estimated from repeat surveys. The volume of contaminated sediment stored in the rest of basin system is roughly 3,800 m^3. However, similar to sampling block measurements, the average sediment depths used to calculate sediment storage in these areas only measured zero or positive depths and are limited in number, thus, sediment storage may be overestimated or not accurately represent storage over the entire area.

Most areas of the basin system account for 13-25% of sediment stored, beside the poorly-drained flood way that only accounts for a small percentage (4.5%) of sediment stored (Table 16). This suggests that sediment is being stored throughout the entire basin system and not solely in the upper basin, which is important to know when determining areas to dredge. Overall, the total volume of sediment trapped in the basin system is only a very small percent (0.1%) of the estimated 3,700,000 m^3 of contaminated sediment stored in the channel of the Big River and 170,000 m^3 of contaminated sediment stored in the channel of the Flat River.

Figure 46. Basin system sediment storage areas.

Table 16. Summary of sediment storage in basin system.

Location	ID	Area (m^2)	Avg. Depth (m)	Vol. Stored (m^3)	Storage (%)
RTK Upper Basin Boundary	1	7,100	0.122	865	18.4
North Upper Basin	2	2,100	0.430	903	19.2
East Well-Drained Flood Way	3	2,400	0.260	624	13.2
Well-Drained Flood Way	4	2,900	0.313	908	19.3
Lower Basin	5	4,800	0.250	1,200	25.5
Poorly-Drained Flood Way	6	2,500	0.085	213	4.5
Total	6	21,800	0.243 (Avg.)	4,712	100

Controls on Longitudinal Deposition Patterns. Typically, the depth of floodplain deposits tend to decrease across the floodplain with distance from the channel as a function of roughness and decreasing suspended sediment concentrations (Piegay et al., 2008; Wohl, 2014). However, due to fluctuations of flood characteristics that control the amount of sediment transported and deposited, patterns of floodplain sedimentation are variable (Dennis et al, 2009; Sear et al., 2010). Also, complex topography and variable geometry of floodplains contribute to irregular rates and patterns of sediment deposition that result from the combination of diffusion, convection, and variations in the time and depth of inundation (Lecce and Pavlowsky, 2004).

Even though the sedimentation basin system is not a typical or "natural" floodplain, the same processes control the longitudinal patterns of sedimentation and contamination. Generally, cumulative peak stage and duration the basin is inundated

controls the amount of sediment transported and deposited, and patterns of sedimentation (Figure 38 and 40). Larger magnitude floods tend to inundate the basin system for longer periods and have a larger transport competence and capacity that allows more time for more sediment to be deposited (Figure 41). They also tend to deposit larger quantities of coarse material as splays or chute bars compared to smaller magnitude floods. Thus, areas that were more frequently inundated like the upper basin, generally had larger sediment depths and coarser sediment deposits compared to the rest of the basin system (Figure 42; Table 15). The upper basin is also closer to the channel thalweg of the Big River which may be directing coarse material into the primary inlet.

Irregular deposition patterns and amount of sediment deposited over the entire basin system is also controlled by topography and roughness. Differences in topography and roughness at certain areas or features in the basin system promote either deposition or erosion due to differences in flow velocities. Typically, sediment deposition is quite small on basin slopes located alongside of the main flow areas due to higher elevations that experience lower flow velocities and are less frequently inundated. On the other hand, areas in the floodway that experience increased flow velocities and increased transport rates due to local increases in slope, like at sampling sites V10 and V11 where little sediment was deposited (Figure 42). While sampling sites V16 and V17, which are located in relatively flat areas of the flood way where flow velocities decrease and promote deposition, had greater sediment deposition (Figure 42).

Study Period Deposition Rates

Sediment deposition was not uniform over the upper basin. Instead, there are certain locations within the upper basin that experience net erosion, such as the bank, and areas with both higher and lower deposition rates compared to the entire upper basin (Table 17; Figure 47). Since there are distinct differences in the amount and texture of sediment deposited, the upper basin was divided into high deposition and low deposition areas (Figure 47). Annual deposition rates were calculated for those areas in addition to the upper basin as a whole.

The annual deposition rate for the entire upper basin was estimated to be 10.3 cm/yr (Table 17). The high deposition splay area has an average depth of 26.0 cm and annual deposition rate of 22.0 cm/yr. The low deposition west area has an average depth of 6.2 cm and annual deposition rate of 5.2 cm/yr. Differences in average sediment depths and deposition rates can be attributed to more erosion occurring over a larger area in the low deposition area compared to the high deposition area. Also, smaller, more uniform depths of sediment are found in the west area with very few places where sediment deposition is >40 cm.

Table 17. Deposition rates for areas of the upper basin.

Location	Length of record (days)	Avg. Depth (cm)	Rate (cm/yr)
Upper Basin	432	12.2	10.3
Sampling Blocks (Avg.)	434	28.0	23.6
High Deposition Area	432	26.0	22.0
Low Deposition Area	432	6.2	5.2

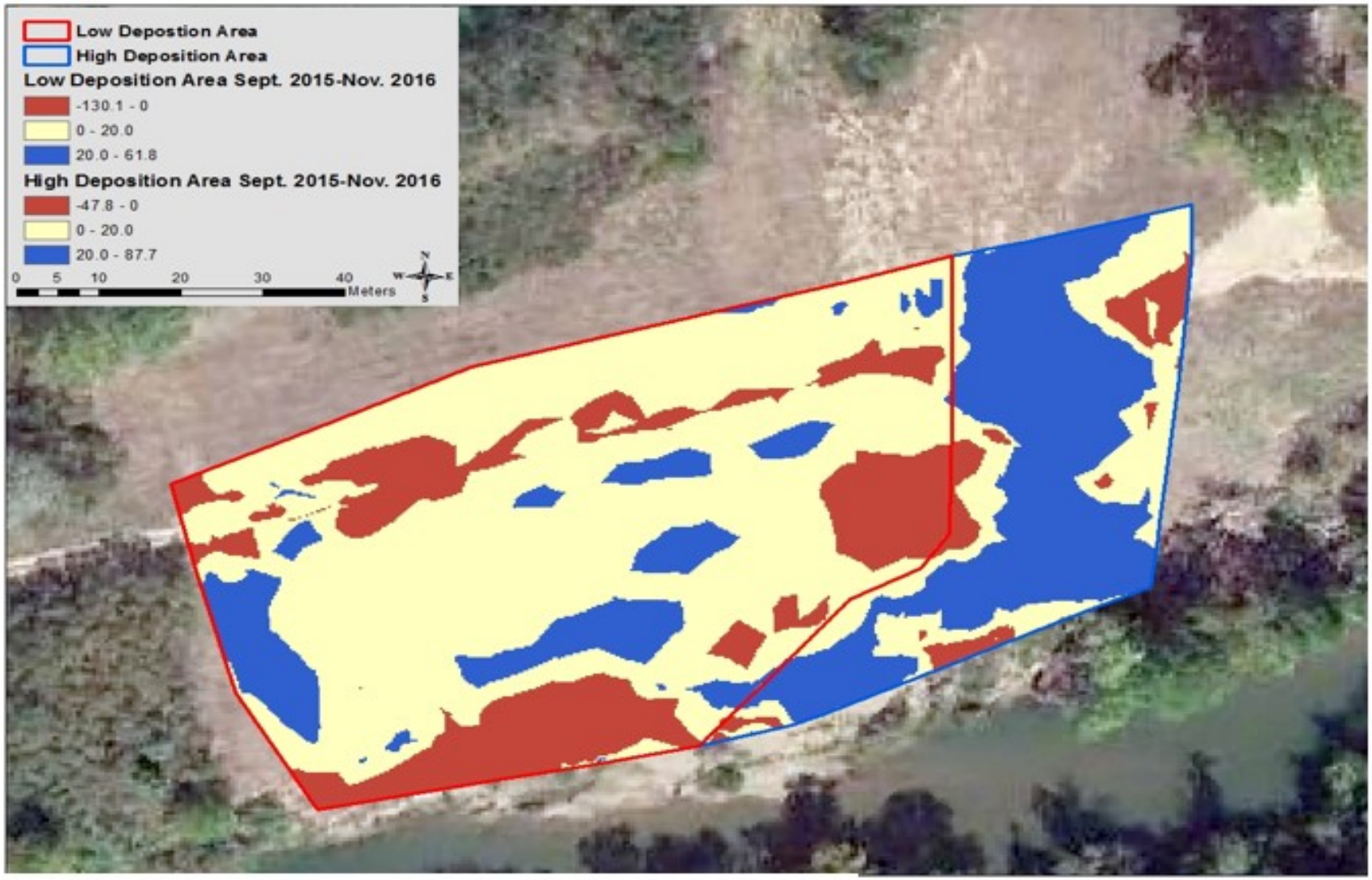

Figure 47. Erosion and deposition in high and low deposition areas.

Annual deposition rates were also calculated from sampling block data. Sampling blocks measures deposition that occurred over the course of 434 days (May 1, 2015 – July 8, 2016). The annual deposition rate estimated from induvial sampling block depths ranged from 2.1 to 50.5 cm/yr with an average of 23.6 cm/yr (Table 17). It is important to note that only deposition rates calculated from repeat surveys take erosion into account when determining the average depth of sediment deposition, which help explain the higher average sediment depths for sampling blocks that produce higher sedimentation rates. Also, the frequency and magnitude of flooding events varied over the sampling block period and survey period, and deposited varying amounts of sediment.

Most deposition rates estimated for the upper basin are greater than contemporary deposition rates estimated for natural floodplains, which range from 0.3 mm/yr to 1.0 cm/yr (Table 2). The only exception is a deposition rate of 10 cm/yr estimated by Florsheim and Mount (2002). However, that deposition rate was estimated for a floodplain where the levee was intentionally breached to increase connectivity with the channel and enhance sediment deposition. That deposition rate is more likely to compare to deposition rates estimated for the upper basin due to the fact that both floodplains were modified to enhance sediment deposition by lowering bank height at the primary inlet.

Contemporary deposition rates estimated for the upper basin are also greater than long-term deposition rates estimated from cores collected at the study site prior to construction of the basin system (Table 18; Figure 48). The long-term deposition rates ranged from 0.1 to 2.5 cm/yr with an average of 0.8 cm/yr. The average long-term deposition rate at the site is less than half of the lowest deposition rate estimated for an individual sampling block and about five times less than the deposition rate estimated for

the low deposition zone. The large differences in deposition rates between natural floodplains and pre-construction study site, help confirm enhanced sediment deposition in the upper basin

Table 18. Long-term deposition rates at the BRLRS site.

Core	Top Elevation (m asl)	Total Length (cm)	Post-196 Depth (cm)	Rate (cm/yr)
9	203.32	140	55	1.1
11	202.23	144	125	2.5
12	202.03	175	25	0.5
13	202.66	216	5	0.1
17	203.66	110	5	0.1
Avg.	202.78	157	43	0.8

Figure 48. Location of cores collected in 2014.

Basin Mitigation Effectiveness

The sedimentation basin system was constructed to allow increased water and sediment to enter the basin during high flows compared to a natural floodplain. Since construction of the basin in April 2015, there has been enhanced sediment deposition in the upper basin. Sediment in the upper basin is being deposited at greater rates compared to pre-construction deposition rates. The increase in sediment deposition is due to increased connectivity with the channel and the high frequency, magnitude, and duration of flooding events that occurred over the study period. This suggests that during the study period the basin system is operating as intended.

Overall, the basin system is trapping mining contaminated sediment. Sediment samples collected throughout the entire basin system contained high concentrations of Pb and Zn (>1,000 ppm). Also, both highly contaminated fine tailings and chat are being trapped in the basin system. As expected due to the location of the inlet above Flat River, the Pb/Zn ratio suggests the source of contaminated sediment is likely upstream on the Big River from mines at Desloge and Leadwood and not from the Flat River.

Even though the rates of sediment deposition are relatively high and sediment being trapped is highly contaminated, it may not be significant compared to the amount of contaminated sediment stored in Big River. Pavlowsky et al. (2010) estimated that there is about 3,700,000 m^3 of contaminated sediment is stored in the channel and about 86,800,000 m^3 is stored in floodplains. Hill (2016) estimated 170,000 m^3 of contaminated sediment is stored as channel and bar deposits in the Flat River. Given that total basin storage per year is about 4,700 m^3, contaminated sediment trapped in the basin system represent a very small percent (0.005%) of the total volume of contaminated sediment in

the Big River and Flat River. Assuming the rate of deposition remains the same, it would take roughly 820 years to just trap all the contaminated sediment stored in the channel of the Big River and Flat River, not including floodplain storage. Averages of two sites upstream of the study site on the Big River at Leadwood and Desloge results in an estimated contaminated channel sediment storage volume of 432,000 m^3 (Pavlowsky et al., 2010). When just this storage is considered, only 1.1% of the contaminated sediment was trapped over the study period and would take roughly 90 years to trap all the contaminated sediment stored in the channel of the Big River upstream of the study site.

However, this study covered an odd period when floods were five times more common than an average year. Thus, the deposition rate reported here may be higher than expected and will probably be lower in future years, depending on flood frequency and stage. Nonetheless, it is not reasonable to expect the basin system to trap all the contaminated sediment within the Big River, however, it underscores the long-term severity of contamination in the watershed and how difficult it is to remediate.

CHAPTER 6 – SUMMARY AND CONCLUSIONS

Historical mining in the Old Lead Belt created a serious contamination within the Big River watershed by introducing large quantities of metal-rich sediment to local streams. While it is known that sediment in the Big River is contaminated, little is known about the patterns and rates of contaminated sediment deposition on floodplains, especially those that have been modified for remediation purposes. This studied evaluated the influence of flood characteristics and floodplain topography on contemporary deposition patterns and rates in a sedimentation basin system constructed within a floodplain along the Big River that was designed to trapped contaminated during flood events and reduce Pb exposure downstream.

Sediment traps were used to sample sediment deposited during flooding events and to measure sediment deposition. GIS analysis was also used to calculate sediment deposition and sediment storage from repeat topographic survey data, and to analyze the patterns and rates of sedimentation throughout the basin system. From Sept. 17, 2016 to Nov. 22, 2016 sediment deposition ranged from -140.2 to 87.8 cm with an average of 12.2 cm (negative values indicates erosion). Areas of erosion are associated with the expansion of the primary inlet may be the result of a shifting thalweg towards the left bank. The surveys covered approximately 7,100 m^2 where approximately 865 m^3 of sediment has been stored. A majority of the sediment is being stored as splay deposits near the inlet and chute, leading toward the basin channel. This pattern of sediment storage can be observed from both sampling block data and topographic surveys. There is approximately 4,700 m^3 of sediment stored throughout the basin system (22,000 m^2) with

a majority of the sediment deposited <2 mm in diameter. These deposits contain high concentrations of Pb and Zn (>1,000 ppm). High concentrations of Pb and Zn were also found in sediment 2-16 mm in diameter.

Deposition rates in the upper basin estimated from topographic surveys ranged from 5.2 to 22.0 cm/yr with an average deposition rate of 10.3 cm/yr. Average deposition rate estimated from sampling block data was 23.6 cm/yr. These deposition rates are greater than those of natural floodplains in the U.S and Europe, and of long-term rates estimated for floodplains at the study site before construction of remediation structures. Even though sediment is currently being deposited at a faster rate and sediment trapped in the basin system is contaminated, the volume of contaminated sediment trapped may be insignificant compared to the total volume of sediment stored in the Big River watershed.

Key Findings

The key findings of this study include:

1) Flooding events have occurred more frequently than a normal year. It is expected that an average of 1-3 flooding events occur a year. However, there were 15 flooding events over the course of a year and half. NOAA predicts an increase in intense rainfall events in the Ozark region in the future which suggest this trend in flooding events will continue (Kennedy, 2014; Mallakpour and Villarini, 2015).

2) The upper basin is accumulating sediment at greater rates than natural floodplains, which typically are no more than a few centimeters per year (Piegay et al., 2008; Wohl, 2014). However, deposition rates for the upper basin average 10.3 cm/yr. These deposition rates are also greater than long-term floodplain deposition rates at the study site which range from 0.1 to 2.5 cm/yr.

3) The duration of inundation of the upper basin had the strongest influence on sediment deposition ($r^2 = 0.80$). More sediment was deposited the longer the basin was inundated. The duration was largely controlled by cumulative peak

stage, which also had a moderately strong influence ($r^2 = 0.61$) on sediment deposition. The frequency of flooding had little to no effect on sediment deposition. Overall, sediment deposition in the upper basin can be simply estimated using the cumulative peak stage of all floods between sampling events.

4) There was relatively weak ($r^2 = 0.43$) relationship between sediment depths and distance from the inlet. Typically, floodplain deposits tend to decrease across the floodplain with distance from the channel as a function of roughness and decreasing suspended sediment concentrations (Piegay et al., 2008; Wohl, 2014). However, due to fluctuations in magnitude and duration of flooding events that control the amount of sediment deposited and variations in post-construction topography, patterns and rates of sediment deposition throughout the basin system is varied. Mixtures of overbank and splay deposition may have also clouded this trend.

5) Sediment deposited in the basin system is highly contaminated from historical mining activity. The EPA threshold for Pb in soils where children are present is 400 ppm. The aquatic PEC for Pb established by MacDonald et al. (2000) is 128 ppm. Concentrations of Pb average 1,142 ppm, indicating a significant threat to human and riparian ecosystem health.

6) Generally, the finest sediment and tailings particles tend to contain the highest concentrations of heavy metals (Smith and Schumacher, 1993). However, concentrations of Pb and Zn > 1,000 ppm were found in both coarse (2-16 mm) and fine (<2 mm) sediments. Coarse sediment found in splay deposits can account for 29 to 87% of Pb stored and 26 to 72% of Zn stored, indicating that chat tailings can provide a significant source of Pb and Zn in Big River channel sediment.

7) The sedimentation basin system is only trapping a very small percent (1.1%) of the contaminated sediment stored in the channel of the Big River upstream of the study site. Over a little more than a year, approximately 4,700 m^3 of sediment was trapped in the basin system compared to the 432,000 m^3 of sediment stored in the channel of the Big River upstream of the study site as estimated by Pavlowsky et al. (2010).

Future Work

This study provided a detailed analysis of sediment deposition rates and patterns within the basin system and the factors that influence sediment deposition. However, it is important to discuss the future work that needs to be conducted to better understand the current flood regime and associated deposition rates. The flood record over the study period shows flooding events occurring more frequently and at larger magnitudes than the average expected for a given year. Contemporary sedimentation rates under this recent flood record were estimated to be much greater than that of natural floodplains. This is due to a combination of the basin system being constructed to enhance deposition and an increase in flood frequency and magnitude. Sediment deposition from flooding events were studied over a relatively short period so it is uncertain whether this trend in deposition and flooding events will continue. However, NOAA and others predict a trend in increased intense rainfall events in the Ozark region (Kennedy, 2014; Mallakpour and Villarini, 2015). Therefore, it is important to continue monitoring flooding events and sediment deposition over a longer period.

It is also important to assess the design of the basin system and discuss potential improvements that could be useful to similar remediation structures. This is one of the first basin systems designed as a long-term remediation effort of Pb contamination due to historical mining activities. Results of this study suggest that the basin system is effectively trapping significant amounts of sediment and that sediment contains high concentrations of Pb and Zn. However, the amount of contaminated sediment trapped represents only a small fraction of the total amount of contaminated sediment stored in the Big River watershed. Also, the bank along the upper basin has gone through episodes

of erosion during the study period due to large magnitude floods, which may affect long-term stability of the bank. The effect of primary inlet expansion due to erosion on basin function is not clear. Thus, it may be beneficial for future similar basin systems to be designed to handle larger, more frequent flooding events. Additionally, it is difficult to monitor and observe the basin system during flooding events. While there was a USGS gaging station in close proximity to the study site, it is difficult understand flow rates and patterns through the basin system as a result of various magnitude flooding events. So, it might be useful to implement some type of stage monitoring equipment throughout the basin system. Exploring these ideas may improve the results of this study by better understanding the influences of local flood regime and topography on sedimentation and also improve future remediation projects using similar structures.

REFERENCES

Acreman, M.C., Riddington, R., Booker, D.J., 2003, Hydrological impacts of floodplain restoration: a case study of the River Cherwell, UK: Hydrology and Earth System Sciences, v. 7, p. 75-85.

Adamski, J.C., Peterson, J.C., Freiwald, D.A., and Davis, J.V., 1995, Environmental and hydrologic setting of the Ozark Plateau study unit, Arkansas, Kansas, Missouri, and Oklahoma: U.S. Geological Survey Water-Resources Investigations Report 94-4022.

Asselman, N.E.M., and Middelkoop, H., 1998, Temporal variability of contemporary floodplain sedimentation in the Rhine-Meuse Delta, The Netherlands: Earth Surface Processes and Landforms, v. 23, p. 595-609.

Baborowski, M., Buttner, O., Morgenstern, P., Kruger, F., Lobe, I., Rupp, H., and Tumpling, W.V., 2007, Spatial and temporal variability of sediment depositionon artificial-lawn traps in a floodplain of the River Elbe: Environmental Pollution, v. 148, p. 770-778.

Baptist, M.J., Penning, W.E., Duel, H., Smits, A.J.M., Geerling, G.W., Van Der Lee, G.E.M., Van Alphen, J.S.L., 2004, Assessment of the effects of cyclic floodplain rejuvenation on flood levels and biodiversity along the Rhine River: River Research and Applications, v. 20, p. 285-297.

Benedetti, M.M., 2003, Controls on overbank deposition in the Upper Mississippi River: Geomorphology, v. 56, p. 271-290.

Bridge, J.S., 2003, Rivers and floodplains: forms, processes, and sedimentary record: Oxford, Blackwell, 491 p.

Bunte, K., Abt, S.R., 2001, Sampling surface and subsurface particle-size distributions in wadeable gravel- and cobble-bed streams for analyses in sediment transport, hydraulics, and streambed monitoring: General Technical Report RMRS-GTR-74, U.S. Department of Agriculture, U.S. Forest Service, Rocky Mountain Research Station, 428 p.

Castro, J.M., Jackson, P.L., 2001, Bankfull discharge recurrence intervals and regional hydraulic geometry relationships: patterns in the Pacific Northwest, USA: Journal of American Water Resources Association, v. 37, p. 1249-1262.

Charlton, R., 2008, Fundamentals of Fluvial Geomorphology: New York, Routledge, 234 p.

Ciszewski, D., and Malik, I., 2004, The use of heavy metal concentrations and dendrochronology in the reconstruction of sediment accumulation, Mala Panew River Valley, southern Poland: Geomorphology, v. 58, p. 161-174.

Ciszewski, D., Kubsik, U., and Aleksander-Kwaterczak, U., 2012, Long-term dispersal of heavy metals in catchment affected by historic lead and zinc mining: Physical and Biochemical Processes, v. 12, p. 1445-1462.

Ciszewski, D., Grygar, T.M., 2016, A review of flood-related storage and remobilization of heavy metal pollutants in river systems: Water, Air, and Soil Pollution, v. 227, p. 1-19.

Curtis, J.A., Flint, L.E., and Hupp, C.R., 2013, Estimating floodplain sedimentation in the Laguna de Santa Rosa, Sonoma County, CA: Wetlands, v. 33, p. 29-45

Day, G., Dietrich, W.E., Rowland, J.C., and Marshall, A., 2008, The depositional web on the floodplain of the Fly River, Papua New Guinea: Journal of Geophysical Research, v.113, p. 1-19.

Dennis, I.A., Coulthard, T.J., Brewer, P., and Macklin, M.G., 2009, The role of floodplains in attenuating contaminated sediment fluxes in formerly mined drainage basins: Earth Surface Processes and Landforms, v. 34, p. 453-466.

Dunne, T., Leopold, L.B., 1978, Water in Environmental Planning: New York, W.H. Freeman, 819 p.

Dunne, T., Alto, R.E., 2013, Large river floodplains, *in* Shroder, J., Wohl, E., eds., Treatise on Floodplains: San Diego, California, Academic Press, p. 645-675.

Elliott, T., 1974, Interdistributary bay sequences and their genesis: Sedimentology, v. 21, p. 611-622.

Environmental Protection Agency (EPA), 1998, Field portable x-ray fluorescence spectrometry for the determination of elemental concentrations in soil and sediment: Report for Method 6200, revised 2007.

Faulkner, D.L., McIntyre, S., 1996, Persisting sediment yields and sediment delivery changes: Water Resources Bulletin, v. 32, p. 817-829.

Featherstone, W.E., Stewart, M.P., 2001, Combined analysis of real-time kinematic GPS equipment and its users for height determination: Journal of Surveying Engineering, v. 127, p. 31-51.

Florsheim, J.L., Mount, J.F., 2002, Restoration of floodplain topography by sand-splay complex formation in response to intentional levee breaches, Lower Consumnes River, California: Geomorphology, v. 44, p. 67-94.

Flynn, K.M., Kirby, W.H., Hummel, P.R., 2006, User's Manual for Program PeakFQ Annual Flood-Frequency Analysis Using Bulletin 17B Guidelines: U.S. Geological Survey, 42 p.

Forstner, U., and Salomons, W., 2010, Sediment research, management and policy: Journal of Soils and Sediments, v. 10, p. 1440-1452.

Gale, N.L., Adams, C.D., Wixson, B.G., Loftin, K.A., and Huang, Y-W, 2002, Lead concentrations in fish and river sediments in the Old Lead Belt of Missouri: Environmental Science and Technology, v. 26, p 4262-4268.

Gale, N.L., Adams, C.D., Wixson, B.G., Loftin, K.A., and Huang, Y-W., 2004, Lead, zinc, copper, and cadmium in fish and sediments from the Big River and Flat River Creek of Missouri's Old Lead Belt: Environmental Geochemistry and Health, v. 26, p. 37-49.

Gomez, B., Mertes, L.A., Phillips, J.D., Magilligan, F.J., and James, L.A., 1995, Sedimentcharacterstics of an extreme flood: 1993 upper Mississippi River valley: Geology, v. 23, p. 963-966.

Gregg, J.M., and Shelton, K.L., 1989, Minor-and trace-element distributions in the Bonneterre Dolomite (Cambrian), southeast Missouri: Evidence for possible multi-basin fluid sourcesand pathways during lead-zinc mineralization: Geological Society of America Bulletin, v. 101, p. 221-230.

Harrison, L.R., Dunne, T., Fisher, Fisher, G.B., 2015, Hydraulic and geomorphic processes in an overbank flood along a meandering, gravel-bed river: implications for chute formation: Earth Surface Processes and Landforms, v. 40, p. 1239-1253.

He, Q., and Walling, D.E., 1996, Use of fallout Pb-210 measurements to investigate longer-term rates and patterns of overbank sediment deposition on the floodplains of lowland rivers: Earth Surface Processes and Landforms, v. 21, p. 141-154

Hensel, P.F., Day, J.W., and Pont, D., 1999, Wetland vertical accretion and soil elevation change in the Rhone river delta, France: The importance of riverine flooding: Journal of Coastal Research, v. 15, p. 668-681.

Hiemann, D.C., Roell, M.J., 2000, Sediment loads and accumulation in a small riparian wetland system in northern Missouri: Wetlands, v. 20, p. 219-231.

Hill, R., 2016, Channel sediment and mining-lead storage in Flat River Creek, Old Lead Belt, Missouri [Master's Thesis]: Missouri State University, 160 p.

Hooke, J.M., 1995, River channel adjustment to meander cutoffs on the river Bollin and river Dane, northwest England: Geomorphology, v. 14, p. 235-253.

Horowitz, A.J., 1991, A Primer on Sediment-Trace Element Chemistry, 2nd Ed.: U.S. Geological Survey Open-File Report 91-76, 136 p.

Howard, A.D., 1996, Modelling Channel Evolution and Floodplain Morphology: Floodplain Processes: Chichester, UK, John Wiley and Sons, p. 15-62.

Huggins, D.B., 2016, Spatial distribution and geomorphic factors of lead contamination on floodplains affected by historical mining, Big River, S.E. Missouri [Master's Thesis]: Missouri State University, 141 p.

Hung, N.N., Delgado, J.M., Gunter, A., Merz, B., Bardossy, A., and Apel, H., 2013, Sedimentation in the floodplain of the Mekong Delta, Vietnam Part II: deposition and erosion: Hydrologic Processes, v. 28, p. 3145-3160.

Hupp, C.R., 2000, Hydrology, geomorphology, and vegetation of Coastal Plain rivers in the southeastern United States: Hydrological Processes, v. 14, p. 2991-3010.

Hupp, C.R., Schenk, E.R., Kroes, D.E., Willard, D.A., Townsed, P.A., and Peet, R.K., 2015, Patterns of floodplain sediment deposition along the regulated lower RoanokeRiver, North Carolina: Annual, decadal, centennial scales: Geomorphology, v. 228, p. 660-680.

Jeffries, R., Darby, S.E., and Sear, D.A., 2003, The influence of vegetation and organic debris on flood-plain sediment dynamics: Case study of a low-order stream in the New Forest, England: Geomorphology, v. 51, p. 61-80.

Kennedy, C., 2014, Heavy downpours more intense, frequent in a warmer world: https://www.climate.gov/news-features/featured-images/heavy-downpours-more-intense-frequent-warmer-world (accessed February 2017).

Kleiss, B.A., 1996, Sediment retention in a bottomland hardwood wetland in eastern, Arkansas: Wetlands, v. 16, p. 321-333.

Kooistra, L., Lueven, R.S.E.W., Neinhuis, P.H., Wehrens, R., and Buydens, L.M.C., 2001, Aprocedure for incorporation spatial variability in ecological risk assessment ofDutch River floodplains: Environmental Management, v. 28, p. 359-373.

Kruit, C., 1955, Sediments of the Rhone delta: grain size and microfauna [Ph.D. Thesis]: University of Groningen, 141 p.

Lambert, C.P., and Walling, D.E., 1987, Floodplain sedimentation: a preliminary investigation of contemporary deposition within the lower reaches of the River Culm, Devon, UK: Physical Geography, v. 69, p. 393-404.

Lecce, S.A., and Pavlowsky, R.T., 1997, Storage of mining-related zinc in floodplain sediments, Blue River, Wisconsin: Physical Geography, v. 18, p. 424-439.

Lecce, S.A., and Pavlowsky, R.T., 2001, Use of mining-contaminated sediment tracers to investigate the timing and rates of historical flood plain sedimentation: Geomorphology, v. 38, p. 85-108.

Lecce, S.A., and Pavlowsky, R.T., 2004, Spatial and temporal variation in grain-size characteristics of historical flood plain deposits, Blue River, Wisconsin, USA: Geomorphology, vol. 61, p. 361-371.

Lecce, S.A., and Pavlowsky, R.T., 2014, Floodplain storage of sediment contaminated by mercury and copper from historic gold mining at Gold Hill, North Carolina, USA: Geomorphology, v. 206, p. 122-132.

Lecce, S.A., Pease, P.P., Gares, P.A., 2004, Floodplain sedimentation during an extreme flood: the 1999 flood on the Tar River, eastern North Carolina: Physical Geography, v. 25, p. 334-346.

Leff, J.A., 2014, Big River lead remediation structures Environmental Protection Agency (EPA) Mr. Vaughn Counts' property St. Francois County, Missouri: US Army Corps of Engineers

Leopold, L.B., Wolman, M.G., Miller, J.P., 1964, Fluvial Processes in Geomorphology: California, W.H. Freeman, 522 p.

MacDonald, D.D., Ingersol, C.G., and Berger, T.A., 2000, Development and evaluation of consensus-based sediment quality guidelines for freshwater ecosystems: Environmental Contamination and Toxicology, v. 39, p. 20-31.

Macklin, M.G., Brewer, P.A., Hudson-Edwards, K.A., Bird, G., Coulthard, T.J., Dennis, I.A., Lechler, P.J., Miller, J.R., and Turner, J.N., 2006, A geomorphological approach to the management of rivers contaminated by metal mining: Geomorphology, v. 79, p. 423-447.

Mallakpour, I., Villarini, G., 2015, The changing nature of flooding across the central United States: Nature, v. 5, p. 1-5.

Marron, D.C., 1992, Floodplain storage of mine tailings in the Belle Fourche River system: A sediment budget approach: Earth Surface Processes and Landforms, v. 17, p. 675-685.

Martin, C.W., 2015, Trace metal storage in recent floodplain sediments along the Dill River, central, Germany: Geomorphology, v. 235, p. 52-62.

Martin, D.J., Pavlowsky, R.T., and Harden, C.P., 2016, Reach-scale characterization of large woody debris in a low-gradient, Midwestern U.S.A. river system: Geomorphology, v. 262, p. 91-100.

McGowen, J.H., Garner, L.E., 1970, Physiographic features and stratification types of coarse-grained point bars-modern and ancient examples: Sedimentology, v. 14, p. 77-111.

Meneau, K.J., 1997, Big River Watershed Inventory and Assessment. Missouri Department of Conservation: http://mdc.mo.gov/fish/wastershed/big/contents (accessed November 2015).

Middlekoop, H., 2002, Reconstructing floodplain sedimentation rates from heavy metal profiles by inverse modeling: Hydrologic Processes, v. 16, p. 46-64.

Miller, J.R., 1997, The role of fluvial geomorphic processes in the dispersal of heavy metals from mine sites: Journal of Geochemical Exploration, v. 58, p. 101-118.

Missouri Department of Natural Resources (MDNR), 2001, Biological assessment and fine sediment study: Flat River (Flat River Creek), St. Francois County, Missouri, Prepared by the Water Quality Monitoring Section, Environmental Services Program, Air and Land Protection Division of the Missouri Department of Natural Resources.

Missouri Department of Natural Resources (MDNR), 2003, Biological assessment and fine sediment study: Big River (lower): Irondale to Washington State Park, St. Francois, Washington, and Jefferson Counties, Missouri, Prepared by the Water Quality Monitoring Unit, Environmental Services Program, Air and Land Protection Division of the Missouri Department of Natural Resources.

Missouri Department of Natural Resources (MDNR), 2007, The estimated volume of mine-related benthic sediment in the Big River at two point bars in St. Francois State Park using ground penetrating radar and x-ray fluorescence, Prepared by the Water Quality Monitoring Unit, Environmental Services Program, and Field Services Division of the Missouri Department of Natural Resources.

Mosby, D.E., Weber, J.S., and Klahr, F., 2009, Final phase 1 damage assessment plan for thesoutheast Missouri lead mind district: Big River Mine Tailings Superfund Site, St. Francois County, and Viburnum Trend sites, Reynolds and Iron counties: http://dnr.mo.gov/env/wpp/tmdl/info/2074-2080-2168-big-r-info.pdf (accessed Janurary 2016).

Mulligan, C., Yong, R., and Gibbs, B., 2001, Remediation technologies for metal-contaminated soils and groundwater: an evaluation: Engineering Geology, v. 60, p. 193-207.

Nardi, F., Vivoni, E.R., and Grimaldi, S., 2006, Investigating a floodplain scaling relation using a hydrogeomorphic delineation method: Water Resources Research, v. 42, p. 1-15.

Nanson, G.C., and Croke J.C., 1992, A genetic classification of floodplains: Geomorphology, v. 4, p. 459-486.

Newfields, 2007, Volume of sediment in Big River, Flat River Creek, and Owl Creek-St. Francois County mined Areas, Missouri: Focused Remedial Investigation of Mined Areas in St. Francois County, Missouri.

National Water Information System (NWIS), 2017, USGS 07017260 Big River below Desloge, MO: https://nwis.waterdata.usgs.gov/mo/nwis/uv?site_no=07017260 (accessed January 2017).

Olde Venterink, H., Vermaat, J.E., Pronk, M., Weigman, F., van der Lee, G. can den Hoorn, M.W., Higler, L., and Verhoeven, J., 2006, Importance of sediment depositionand denitrification for nutrient retention in floodplain wetlands: Applied Vegetation Science, v. 9, p. 163-174.

Owen, M.R., Pavlowsky, R.T., and Womble, P.J., 2011, Historical disturbance and contemporary floodplain development along an Ozark river, southwest Missouri: Physical Geography, v. 32, p. 423-444.

Owen, M.R., Pavlowsky, R.T., and Martin, D.J., 2012, Big River borrow pit monitoring project-Final Report.

Ozarks Environmental and Water Resources Institute (OEWRI), 2006, Standard Operating Procedure for: Chain of Custody: OzarksEnvironmental and Water Resources Institute, Missouri State University.

Pavlowsky, R.T., Owen, M.R., and Martin, D.J., 2010, Contaminated sediment geochemistry, distribution and storage in channel deposits of the Big River in St. Francois, Washington, and Jefferson counties, Missouri – Final Report.

Pavlowksy, R.T., and Owen, M.R., 2016, Quality Assurance Project Plan (QAPP) for Big River Lead Remediation Structure (BRLRS) Monitoring Project: Completed for: Jason Gunter, Remedial Project Manager U.S Environmental Protection Agency, Region, VII, Ozarks Environmental and Water Resources Institute at Missouri State University, OEWRI QAPP-16-001.

Peng, J., Song, Y., Yuan, P., Cui, X., and Qui, G., 2009, The remediation of heavy metals contaminated sediment: Journal of Hazardous Materials, v. 161, p. 633-640.

Phillips, J.D., Marden, M., Gomez, B., 2007, Residence time of alluvium in aggrading fluvial systems: Earth Surface Processes and Landforms, v. 32, p. 307-316.

Piégay, H., Hupp, C.R., Citterio, A., Dufour, S., Moulin, B., and Walling, D.E., 2008, Spatial and temporal variability in sedimentation rates associated with cutoff channel infill deposits: Ain River, France: Water Resources Research, v. 44, p. 1-18.

Pierce, A.R., King, S.L., 2008, Spatial dynamics of overbank sedimentation in floodplain systems: Geomorphology, v. 100, p. 256-268.

Rafferty, M.D., 1980, The Ozarks: Land and Life: University of Oklahoma Press, Norman, 282 p.

Roberts, A.D., Mosby, D.E., Weber, J.S., Besser, J., Hundley, J., McMurray, S., and Faiman, S., 2009. An assessment of freshwater mussel (Bivalvia Margaritiferidae and Unionidae) populations and heavy metal sediment contamination in the Big River, Missouri. Report prepared for the U.S. Department of Interior, Washington, D.C.

Schenk, E.R., Hupp, C.R., 2010, Floodplain sediment trapping, hydraulic connectivity, and vegetation along restored reaches of the Kissimmee River, Florida, *in* Proceedings, 2nd Joint Federal Interagency Conference: Las Vegas, Nevada.

Sear, D.A., Millington, C.E., Kitts, D.R., and Jeffries, R., 2010, Logjam controls on channel: floodplain interactions in wooded catchments and their role in the formation of multi-channel patterns: Geomorphology, v. 116, p. 305-319.

Simon, A., Dickerson, W., Heins, A., 2004, Suspended-sediment transport rates at the 1.5-year recurrence interval for ecoregions of the United States: transport conditions at the bankfull and effective discharge?: Geomorphology, v. 58, p. 243-262.

Smith, B.J., Schumacher, J.G., 1993, Surface-water and sediment quality in the Old Lead Belt, southeastern Missouri-1988-89: U.S. Geological Survey Water-Resources Investigations Report 93-4012.

United States Department of Agriculture (USDA), 1981, Soil Survey of St. Francois County, Missouri: National Cooperative Soil Survey.

United States Department of Agriculture (USDA), 2000, Soil Survey of Jefferson County, Missouri: National Cooperative Soil Survey

United States Department of Agriculture (USDA), 2002, Horsecreek Series: https://soilseries.sc.egov.usda.gov/OSD_Docs/H/HORSECREEK.html (accessed November 2015).

Walling, D.E., and Bradley, S.B., 1989, Rates and patterns of contemporary floodplain sedimentation: a case study of the River Culm, Devon, UK: GeoJournal, v. 19, p. 53-62.

Walling, D.E., He, Q., 1994, Rates of overbank sedimentation on the flood plains of several British rivers during the past 100 years: Proceedings of the Canberra Symposium, p. 203-210.

Walling, D.E., He, Q., 1997, Use of fallout Cs^{137} in investigations of overbank sediment deposition on river floodplains: Catena, v. 29, p. 263-282.

Walling, D.E., Owens, P.N., Carter, J., Leeks, G.J., Lewis, S., Meharg, A.A., and Wright, J., 2003, Storage of sediment-associated nutrients and contaminants in river channel and floodplain systems: Applied Geochemistry, v. 18, p. 195-220.

Walling, D.E., Quine, T.A., He, Q., 1992, Investigating contemporary rates of floodplain sedimentation, *in* Carling, P.A., Petts, G.E., eds, Lowland Floodplain Rivers: Geomorphology Perspectives: Chichester, UK, John Wiley & Sons, p. 164-184.

Wang, Q., Kim, D., Dionysiou, D.D., Sorial, G.A., Timberlake, D., 2004, Sources and remediation for mercury contamination in aquatic systems-a literature review: Environmental Pollution, v. 131, p. 323-336.

Weaver, J.C., Feaster, T.D., Gotvald, A.J., 2009, Magnitude and frequency of rural floods in the Southeastern United States, through 2006 – Volume 2, North Carolina: U.S Geological Survey Scientific Investigations Report 2009-5158.

Wohl, E., 2014, Rivers in the Landscape: Science and Management: Chichester, UK, John Wiley & Sons, 318 p.

Wolman, M.G., Leopold, L.B., 1957, River flood plains: Some observations on their formation: Geological Survey Professional Paper 282-C.

Wolman, M.G., Miller, J.P., 1960, Magnitude and frequency of forces in geomorphic processes: The Journal of Geology, v. 68, p. 54-74.

Young, B.M., 2011, Historical channel change and mining-contaminated sediment remobilization in the lower Big River, eastern Missouri [Master's Thesis]: Missouri State University, 144 p.

Zwolinski, Z., 1992, Sedimentology and geomorphology of overbank flows on meandering river floodplains: Geomorphology, v. 4, p. 367-379.

APPENDICES

Appendix A – Photo Log

Upper basin with road cutting through looking upstream (11/21/16).

Upper basin bank looking downstream (9/17/15).

Basin inlet looking upstream (12/14/15).

Upper basin chute and splay deposits (7/8/16).

Finer-grained splay deposits north of the road in upper basin (12/14/15).

West ponding area in upper basin (12/14/15).

Sampling block 25 with erosion around block (9/17/15).

Basin inlet during early flood stages (12/14/15).

Erosion of inlet around large woody debris (12/14/15).

Well-drained flood way at upper basin boundary (12/14/15).

Headcut within well-drained flood way looking back towards the upper basin (12/14/15).

Lower basin wet all year long (12/14/15).

Newberry-type rocked riffle (1/21/16).

Lower inlet in lower basin (12/14/15).

Poorly-drained flood way (12/14/15).

Debris jam blocking primary outlet (12/14/15).

Primary outlet to Big River from culverts (12/14/15).

Concrete spillway (11/21/16).

Appendix B – Sediment Sample Grain Size Distribution

Sample ID	>16 mm (%)	8-16 mm (%)	4-8 mm (%)	2-4 mm (%)	<2 mm (%)
BR JV 1	-	-	1.2	2.4	96.4
BR JV 2	-	1.9	1.9	1.3	94.9
BR JV 3	-	1.5	4.5	10.5	83.5
BR JV 4	4.3	6.2	11.7	11.5	66.3
BR JV 5	2.1	5.9	9.8	12.1	70.1
BR JV 6	4.9	6.9	13.0	15.0	60.3
BR JV 7	-	-	0.5	0.5	99.0
BR JV 8	-	-	1.1	1.6	97.3
BR JV 9	-	-	-	0.5	99.5
BR JV 10	-	0.5	0.7	1.6	97.3
BR JV 11	-	-	-	-	100
BR JV 12	-	-	1.5	1.0	97.5
BR JV 13	-	-	-	-	100
BR JV 14	-	-	0.6	0.6	98.9
BR JV 15	-	-	-	-	100
BR JV 16	-	-	1.0	1.9	97.1
BR JV 17	-	-	-	1.5	98.5
BR JV 18	-	0.6	1.7	3.4	94.4
BR JV 19	-	-	-	-	100
BR JV 20	-	-	-	-	100
BR JV 21	-	-	-	-	100
BR JV 22	-	-	-	-	100
BR JV 23	-	-	0.2	0.2	99.6
BR JV 24	-	-	-	-	100
BR JV 25	-	0.3	0.3	0.3	99.1
BR JV 26	-	-	-	-	100
BR JV 27	-	-	-	0.4	99.6
BR JV 28	-	-	-	0.3	99.7
BR JV 29	-	-	0.5	0.5	98.9
BR JV 30	-	0.3	1.0	0.3	98.4
BR JV 31	-	-	0.8	-	99.2
BR JV 32	2.3	0.2	0.1	0.1	97.4
BR JV 33	-	-	0.4	-	99.6
BR JV 34	-	-	-	-	100
BR JV 35	-	-	1.0	1.0	98.1
BR JV 36	-	-	-	-	100
BR JV 37	-	1.3	-	-	98.7

Appendix B Sediment Sample Grain Size Distribution

Sample ID	>16 mm (%)	8-16 mm (%)	4-8 mm (%)	2-4 mm (%)	<2 mm (%)
BR JV 38	-	-	-	-	100
BR JV 39	-	-	0.5	0.5	99.1
BR JV 40	-	-	1.4	0.5	98.2
BR JV 41	-	-	-	-	100
BR JV 42	-	0.6	2.5	5.0	91.9
BR JV 43	23.9	10.4	7.9	8.2	49.6
BR JV 44	2.8	5.1	6.9	10.7	74.5
BR JV 45	-	1.4	2.7	2.9	93.0
BR JV 46	-	-	-	-	100
BR JV 47	-	-	-	-	100
BR JV 48	-	-	0.2	0.2	99.6
BR JV 49	-	-	-	-	100
BR JV 50	-	-	0.3	0.3	99.5
BR JV 51	-	0.7	0.4	1.1	97.8
BR JV 52	-	-	0.6	3.1	96.2
BR JV 53	-	-	-	-	100
BR JV 54	-	-	-	-	100
BR JV 55	-	-	-	-	100
BR JV 56	-	-	-	-	100
BR JV 57	-	-	-	-	100
BR JV 58	-	-	-	-	100
BR JV 59	-	-	-	-	100
BR JV 60	-	-	-	-	100
BR JV 61	-	-	-	-	100
BR JV 62	-	-	-	-	100
BR JV 63	-	-	-	-	100
BR JV 64	-	-	-	-	100
BR JV 65	-	-	-	-	100
BR JV 66	-	-	0.2	1.4	98.4
BR JV 67	-	-	1.2	2.6	96.2
BR JV 68	-	-	0.5	0.3	99.2
BR JV 69	6.2	-	3.7	3.3	86.7
BR JV 70	8.2	13.9	10.6	9.6	57.7
BR JV 71	15.8	12.6	13.6	13.0	45.1
BR JV 72	-	-	0.5	1.4	98.2
BR JV 73	-	-	-	-	100
BR JV 74	-	-	-	0.7	99.3
BR JV 75	-	-	-	-	100

Appendix B Sediment Sample Grain Size Distribution

Sample ID	>16 mm (%)	8-16 mm (%)	4-8 mm (%)	2-4 mm (%)	<2 mm (%)
BR JV 76	-	-	-	0.2	99.8
BR JV 77	-	-	0.2	0.5	99.3
BR JV 78	-	-	-	-	100
BR JV 79	-	-	-	-	100
BR JV 80	-	-	-	-	100
BR JV 81	-	-	-	-	100
BR JV 82	-	-	-	-	100
BR JV 83	-	-	-	-	100
BR JV 84	-	-	-	-	100
BR JV 85	-	-	-	-	100
BR JV 86	-	-	-	1.6	98.4
BR JV 87	-	-	-	-	100
BR JV 88	-	-	-	-	100
BR JV 89	-	-	-	-	100
BR JV 90	-	-	-	0.8	99.2
BR JV 91	-	-	0.3	0.8	99.0
BR JV 92	18.0	9.0	14.8	13.9	44.2
BR JV 93	23.4	7.2	8.4	9.3	51.8
BR JV 94	-	-	0.5	0.9	98.6
BR JV 95	-	-	-	0.8	99.2
BR JV 96	-	-	1.6	3.9	94.5
BR JV 97	-	-	0.4	1.5	98.1
BR JV 98	-	2.7	2.7	3.4	91.3
BR JV 99	1.9	1.0	2.6	4.0	90.5
BR JV 100	-	-	0.4	0.4	99.1
BR JV 101	-	-	-	0.4	99.6
BR JV 102	-	0.9	0.9	-	98.1
BR JV 103	-	-	2.0	4.5	93.5
BR JV 104	-	-	-	-	100
BR JV 105	-	-	-	0.4	99.6
BR JV 106	-	-	-	-	100
BR JV 107	-	-	-	-	100
BR JV 108	-	-	-	0.4	99.6
BR JV 109	-	-	-	1.1	98.9
BR JV 110	-	0.5	0.5	1.2	97.8
BR JV 111	3.8	0.7	3.8	6.5	85.1
BR JV 112	-	11.4	17.7	21.5	49.5
BR JV 113	-	10.7	19.2	21.6	48.5

Appendix B Sediment Sample Grain Size Distribution

Sample ID	>16 mm (%)	8-16 mm (%)	4-8 mm (%)	2-4 mm (%)	<2 mm (%)
BR JV 114	23.4	9.6	13.1	13.2	40.8
BR JV 115	14.9	9.8	13.8	14.3	47.2
BR JV 116	-	0.2	1.0	2.9	95.9
BR JV 117	-	-	-	-	100
BR JV 118	-	-	-	0.7	99.3
BR JV 119	-	-	-	0.4	99.6
BR JV 120	-	-	0.1	1.6	98.2
BR JV 121	-	1.3	4.9	16.8	76.9
BR JV 122	-	-	-	-	100
BR JV 123	-	-	-	-	100
BR JV 124	-	-	-	-	100
BR JV 125	-	-	-	-	100
BR JV 126	-	-	-	-	100
BR JV 127	-	-	-	-	100
BR JV 128	-	-	-	-	100
BR JV 129	-	-	-	-	100
BR JV 130	-	-	-	-	100
BR JV 131	-	-	-	0.4	99.6
BR JV 132	-	-	-	-	100
BR JV 133	-	-	-	-	100
BR JV 134	-	-	-	-	100
BR JV 135	-	-	-	-	100
BR JV 136	-	-	-	-	100
BR JV 137	-	-	-	0.5	99.5
BR JV 138	-	-	-	0.5	99.5
BR JV 139	-	-	-	-	100
BR JV 140	-	-	-	-	100
BR JV 141	-	-	-	-	100
BR JV 142	-	-	-	-	100
BR JV 143	-	1.3	5.4	9.7	83.6
BR JV 144	-	6.9	17.7	17.3	58.2
BR JV 145	-	-	-	-	100
BR JV 146	-	-	-	-	100
BR JV 147	4.3	0.9	4.0	7.5	83.2
BR JV 148	-	0.6	4.4	11.9	83.1
BR JV 149	11.7	4.9	14.1	22.3	47.0
BR JV 150	1.6	1.4	2.3	6.8	88.0
BR JV 151	-	1.5	2.9	8.5	87.1

Appendix B Sediment Sample Grain Size Distribution

Sample ID	>16 mm (%)	8-16 mm (%)	4-8 mm (%)	2-4 mm (%)	<2 mm (%)
BR JV 152	-	-	-	-	100
BR JV 153	-	0.7	2.3	3.9	93.0
BR JV 154	-	0.2	1.5	4.0	94.3
BR JV 155	-	-	-	-	100
BR JV 156	-	-	2.3	3.8	93.9
BR JV 157	-	1.5	0.5	0.5	97.4
BR JV 158	5.3	3.7	9.5	6.3	75.3
BR JV 159	-	-	-	0.7	99.3
BR JV 160	-	-	-	0.2	99.8
BR JV 161	-	-	-	-	100
BR JV 162	-	-	-	-	100
BR JV 163	-	-	-	-	100
BR JV 164	-	-	-	-	100
BR JV 165	21.4	1.4	0.6	0.6	76.0

Appendix C – Sediment Sample Geochemistry

Sample ID	Pb ppm	Zn ppm	Ca ppm
BR JV 1	1,363	1,247	34,558
BR JV 2	906	1,052	85,491
BR JV 3	1,399	1,332	32,452
BR JV 4	702	877	94,724
BR JV 5	1,416	1,220	51,052
BR JV 6	678	854	123,634
BR JV 7	1,527	1,467	36,431
BR JV 8	792	1,043	99,032
BR JV 9	1,285	1,442	32,629
BR JV 10	776	843	84,859
BR JV 11	1,390	1,311	34,342
BR JV 12	869	935	113,175
BR JV 13	1,190	1,151	29,819
BR JV 14	849	993	83,195
BR JV 15	1,396	1,337	27,652
BR JV 16	818	826	98,213
BR JV 17	1,411	1,385	37,540
BR JV 18	768	1,081	91,337
BR JV 19	1,282	1,418	36,596
BR JV 20	846	925	53,798
BR JV 21	1,342	1,233	32,819
BR JV 22	1,306	1,212	33,481
BR JV 23	868	966	49,899
BR JV 24	1,440	1,290	31,342
BR JV 25	909	1,194	52,856
BR JV 26	1,420	1,304	44,592
BR JV 27	1,194	1,109	29,543
BR JV 28	1,318	1,257	22,073
BR JV 29	1,484	1,440	29,903
BR JV 30	928	1,153	38,600
BR JV 31	1,014	934	17,663
BR JV 32	830	1,697	77,342
BR JV 33	1,346	1,225	22,568
BR JV 34	1,324	1,229	34,553
BR JV 35	1,141	1,227	38,564
BR JV 36	1,523	1,767	27,364
BR JV 37	1,241	1,176	34,906

Appendix C Sediment Sample Geochemistry

Sample ID	Pb ppm	Zn ppm	Ca ppm
BR JV 38	1,378	1,356	29,322
BR JV 39	924	995	92,222
BR JV 40	828	1,050	93,191
BR JV 41	677	707	82,403
BR JV 42	1,167	1,242	40,081
BR JV 43	896	806	89,851
BR JV 44	724	1,815	104,983
BR JV 45	931	1,190	90,204
BR JV 46	1,508	1,464	49,621
BR JV 47	1,103	1,414	57,186
BR JV 48	1,054	1,175	71,305
BR JV 49	808	955	81,753
BR JV 50	964	1,705	104,600
BR JV 51	859	1,103	90,795
BR JV 52	847	1,406	74,937
BR JV 53	1,390	1,319	40,860
BR JV 54	1,352	1,304	34,121
BR JV 55	1,316	1,133	34,891
BR JV 56	1,331	1,213	37,197
BR JV 57	1,359	1,255	38,582
BR JV 58	1,221	1,068	46,303
BR JV 59	1,239	1,111	19,310
BR JV 60	1,246	1,091	20,856
BR JV 61	1,354	1,177	26,633
BR JV 62	1,254	1,101	26,495
BR JV 63	1,283	1,110	18,893
BR JV 64	1,430	1,518	35,239
BR JV 65	1,387	1,182	23,604
BR JV 66	693	1,054	66,253
BR JV 67	854	1,241	71,219
BR JV 68	905	1,798	60,823
BR JV 69	821	778	75,417
BR JV 70	819	1,079	67,246
BR JV 71	514	773	78,570
BR JV 72	914	1,303	57,656
BR JV 73	1,732	1,855	56,819
BR JV 74	1,183	1,726	63,266
BR JV 75	1,168	1,249	57,128

Appendix C Sediment Sample Geochemistry

Sample ID	Pb ppm	Zn ppm	Ca ppm
BR JV 76	630	930	101,373
BR JV 77	732	929	108,932
BR JV 78	1,747	1,697	33,247
BR JV 79	1,629	1,537	35,902
BR JV 80	2,315	2,605	45,329
BR JV 81	1,782	1,730	42,220
BR JV 82	1,652	1,624	24,526
BR JV 83	1,682	1,668	24,802
BR JV 84	1,621	1,623	26,023
BR JV 85	1,369	1,200	32,647
BR JV 86	1,357	1,494	26,916
BR JV 87	1,499	1,473	24,605
BR JV 88	1,532	1,402	41,001
BR JV 89	1,573	1,539	35,736
BR JV 90	600	747	123,924
BR JV 91	925	1,071	110,206
BR JV 92	1,415	927	143,927
BR JV 93	829	1,043	160,715
BR JV 94	479	633	19,473
BR JV 95	1,865	4,745	37,270
BR JV 96	1,023	1,258	105,439
BR JV 97	537	801	95,940
BR JV 98	759	645	138,500
BR JV 99	870	765	139,561
BR JV 100	645	906	81,628
BR JV 101	811	1,054	95,410
BR JV 102	1,290	1,134	26,208
BR JV 103	991	868	89,684
BR JV 104	797	1,066	86,614
BR JV 105	859	931	83,067
BR JV 106	1,138	1,358	41,968
BR JV 107	929	1,043	73,889
BR JV 108	654	987	93,502
BR JV 109	883	1,516	63,074
BR JV 110	736	779	120,338
BR JV 111	970	1,053	126,086
BR JV 112	657	767	102,236
BR JV 113	1,117	862	98,102

Appendix C Sediment Sample Geochemistry

Sample ID	Pb ppm	Zn ppm	Ca ppm
BR JV 114	964	777	117,408
BR JV 115	921	726	134,590
BR JV 116	676	890	94,728
BR JV 117	2,276	2,466	40,017
BR JV 118	1,287	1,408	56,099
BR JV 119	1,462	1,489	46,247
BR JV 120	739	567	123,017
BR JV 121	1,246	928	119,217
BR JV 122	1,243	1,241	42,624
BR JV 123	1,348	1,222	28,203
BR JV 124	1,337	1,194	29,610
BR JV 125	1,417	1,342	31,761
BR JV 126	1,148	1,248	62,273
BR JV 127	1,403	1,393	28,805
BR JV 128	1,303	1,296	22,226
BR JV 129	1,201	1,069	21,039
BR JV 130	1,087	944	15,336
BR JV 131	1,265	1,155	21,427
BR JV 132	1,100	935	20,432
BR JV 133	1,038	909	14,318
BR JV 134	1,148	1,020	16,287
BR JV 135	1,399	1,313	24,464
BR JV 136	1,392	1,263	53,920
BR JV 137	1,471	1,682	30,921
BR JV 138	1,313	1,533	34,285
BR JV 139	1,277	1,182	35,002
BR JV 140	1,178	1,375	29,596
BR JV 141	1,322	1,148	35,486
BR JV 142	970	1,081	63,540
BR JV 143	715	675	104,609
BR JV 144	880	1,511	86,361
BR JV 145	1,513	1,517	35,925
BR JV 146	1,488	1,468	36,290
BR JV 147	831	990	103,636
BR JV 148	830	823	77,618
BR JV 149	1,265	765	149,200
BR JV 150	1,063	1,095	55,617
BR JV 151	840	875	104,713

Appendix C Sediment Sample Geochemistry

Sample ID	Pb ppm	Zn ppm	Ca ppm
BR JV 152	1,618	1,343	31,576
BR JV 153	971	1,165	64,659
BR JV 154	657	612	158,141
BR JV 155	1,739	1,792	47,291
BR JV 156	758	871	84,717
BR JV 157	1,586	1,549	45,519
BR JV 158	1,308	1,238	45,831
BR JV 159	1,130	1,260	60,231
BR JV 160	532	610	75,020
BR JV 161	1,507	1,225	30,501
BR JV 162	888	916	47,923
BR JV 163	1,626	1,333	35,210
BR JV 164	1,611	1,255	23,425
BR JV 165	1,135	654	16,933